SWEDARCTIC Arctic Ocean 2016

Expedition Report edited by: Katarina Gårdfeldt & Åsa Lindgren

Photo: Åsa Lindgren

POLARFORSKNINGS SEKRETARIATET
SWEDISH POLAR RESEARCH SECRETARIAT

An expedition report

Oden Arctic Ocean 2016

Expedition dates: Longyearbyen, 20160808 – 20160920

List of Content

1. Introduction and background

The Swedish Polar Research Secretariat is a governmental agency that promotes and coordinates Swedish polar research. The main platform used for marine polar expeditions is the icebreaker Oden, owned and operated by the Swedish Maritime Administration. An agreement between Swedish Polar Research Secretariat and Swedish Maritime Administration has been established for the use of Oden for research purposes, when Oden is not used as an icebreaking capacity in the Baltic. Oden is equipped with research laboratories including a sea water intake system, multibeam sonar with a sub bottom profiler and the science equipment out on deck can be modified for each expedition depending on the science requirements.

A Memorandum of Understanding on Science and Technology Cooperation was signed between Canada and Sweden in 2010 and in December 2015, a Cooperation Arrangement outlining enhanced collaboration in Arctic marine geoscience was signed between the Swedish Polar Research Secretariat and the Geological Survey of Canada, the Earth Science Sector. The Cooperation Arrangement is a five year agreement with The Swedish Polar Research Secretariat to support cooperation in marine geoscience and innovation activities in the Arctic.

The Geological Survey of Canada, Earth Science Sector (ESS), and the Canadian Hydrographic Service, Fisheries and Oceans Canada are responsible for data collection to support Canada's claim for an extended continental shelf according to the United Nations Convention on the Law Of the Sea (UNCLOS) protocol. To obtain these data, ESS requested ice breaking and research support from Oden, to work alongside the Canadian icebreaker CCGS Louis S. St-Laurent. This opened the opportunity for a two-ship cruise focusing on marine geology in the Arctic Ocean in the summer 2016.

The 2016 survey was the last major survey for Canada's UNCLOS program and targeted new areas where geoscience data was collected in order to strengthen Canada's UNCLOS submission. Priorities for CCGS Louis S. St-Laurent were seismic reflection, seismic refraction (sonobuoy deployments), multibeam bathymetry and deployment of seismometers either via helicopter or ship.

Priorities for IB Oden was ice breaking support for CCGS Louis S. St-Laurent, multibeam and subbottom profiles, seismic reflection, deployment of seismometers via helicopter/ship and dredging/coring sampling. In addition there was a Swedish research program onboard Oden, included in the SWEDARCTIC program. Altogether, there were 12 work packages (WP) onboard Oden, shown in Table 1.1. The monitoring projects were initiated by the Swedish Polar Research Secretariat as pilot projects to test the possibility to establish long-term monitoring onboard Oden. In February 2016, the Swedish Polar Research Secretariat became a partner in SamCot (Sustainable Arctic Marine and Coastal Technology) and as a part of this cooperation three scientists from the Norwegian University of Science and Technology (NTNU) were invited to the expedition. Prior to the expedition, all participants were invited to a workshop in Helsingborg with a special aim

to present the focus of each Work Package and to identify synergies and cross linkages between the Canadian UNCLOS and the Swedish research programmes respectively.

Associated with five of the work packages are ten Early Career Scientists (ECS) that has been selected after an open call for applications in the regime of the Swedish Polar Research Secretariat. The aim with the ECS programme is to offer early career scientists a comprehensive education in marine field methods and to support future polar researchers.

Table 1.1 The work packages onboard Oden during the expedition Arctic Ocean 2016.

	WP name	**WP Co-leader**	**WP leader onboard**	**Type of project**
SR	Seismic Reflection Profiling	Thomas Funck	Thomas Funck	Canadian contract
DS	Dredge samples	Thomas Funck	Thomas Funck	Canadian contract
GDL	Gravimeter Data Logging	Gordon Oakey	Gordon Oakey	Canadian contract
GM	Geophysical Mapping & Water Column Imaging	Martin Jakobsson	Kevin Jerram	Canadian contract
SC	Sediment coring & properties	Martin Jakobsson	Carina Johansson	Canadian contract
PO	Physical oceanography (CTD)	Katarina Gårdfeldt	Katarina Gårdfeldt	SWEDARCTIC
TGB	Trace Gas Biogeochemistry	Patrick Crill	-	SWEDARCTIC monitoring
MAB	Meteorology, atmospheric boundary layer and surface fluxes	Michael Tjernström	Ian Brooks	SWEDARCTIC monitoring
IM	Ice management	Sveinung Löseth	Runa A. Skarbø	SWEDARCTIC NTNU cooperation
HM	Heavy metals and micro plastics –Water, Air and Ice & snow	Katarina Gårdfeldt	Katarina Gårdfeldt	SWEDARCTIC Roadmap/ monitoring
IT	Ice thickness	Per Holmlund	-	SWEDARCTIC monitoring
PoSta	Polar on Stage/The Big White and Art & Science	Åsa Johannisson	Åsa Johannisson	SWEDARCTIC Artist Programme

Table 1.2 Science participants with the affiliations during the expedition. *shorebased

Anders Dahlin	SR/DS	ahdahlin@hotmail.com
Andreas Skifter Madsen	SR/DS	andreasmadsen@live.dk
Anna Fitch	MAB	anna.fitch@smhi.se
Axel Meiton	Science technichian	axel.meiton@polar.se
Bengt Berglund	Helicopter technician	aircraftservice@hotmail.com
Brett Thornton*	TGB	Brett.thornton@geo.su.se
Carina Johansson	SC	carina.johansson@geo.su.se
Christian Smith	GM	chr.smith999@gmail.com
Christian Stranne*	GM	Christian.stranne@geo.su.se
Dale Ruben	Marine Mammal Obs	Daleirsruben85@hotmail.com
Darren Hiltz	GM	darren.hiltz@dfo-mpo.gc.ca
Dave Sinnott	GM	dave.sinnott@dfo-mpo.gc.ca
Draupnir Einarsson	SC	draupnir.einarsson@geo.su.se
Evgenia Bazhenova	GM	evgenia.bazhenova@gmail.com
Gary Sonnichsen	Liaison Officer	gary.sonnichsen@canada.ca
Gordon Oakey	DS/GDL	gordon.oakey@canada.ca
Grace Shephard	SC	g.e.shephard@geo.uio.no
Hans-Martin Heyn	IM	martin.heyn@ntnu.no
Ian Brooks	MAB	i.brooks@see.leeds.ac.uk
John Prytherch	MAB	J.Prytherch@leeds.ac.uk
John R.Hopper	SR/DS/GDL	jrh@geus.dk
Jon Bjørnø	IM	jonbjor@stud.ntnu.no
Katarina Gårdfeldt	HM/PO	katarina.gardfeldt@chalmers.se
Kevin Jerram	GM	kjerram@ccom.unh.edu
La Daana Kanhai	HM/PO	ladaanakada@yahoo.com
Lara F. Perez	GM	lfp@geus.dk
Lars Lehnert	Science technichian	lars.lehnert@polar.se
Lars Rasmussen	SR/DS	geolr@geo.au.dk
Lasse Nygaard Eriksen	SR/DS	lasse-nygaard@hotmail.com
Luz Maria Mejia Ramirez	SC	luzmamera2@yahoo.com
Markus Karasti	SC	m.karasti@gmail.com
Martin Jakobsson*	SC/GM	Martin.jakobsson@geo.su.se
Michael Tjernström*	MAB	michaelt@misu.su.se
Michelle Nerentorp	HM/PO	michelle.nerentorp@chalmers.se
Nicke Juuso	Meteorologist	nicke.juuso@gmail.com
Per Holmlund*	IT	Per.holmlund@geo.su.se
Per Salo	Science technichian	per.salo@polar.se
Patrick Crill*	TGB	Patrick.crill@geo.su.se
Per Trinhammer	SR/DS	trinhammer@geo.au.dk
Piotr Kupiszewski	MAB	piotr.kupiszewski@gmail.com
Robert Holden	Science technichian	robert.holden@polar.se
Runa A. Skarbø	IM	runa.skarbo@ntnu.no
Sofi Jonsson	HM/PO	sofi.jonsson@uconn.edu
Stefan Bratell	Medical Doctor	stefanbratell@hotmail.com
Steffen Wiers	SC	steffen.wiers@geo.uu.se
Ted Juliussen	Helicopter pilot	ted@airpilot.no
Thomas Funck	SR/DS	tf@geus.dk
Tommy Kessler	SR/DS	tommy.kessler@chem.au.dk
Trine Andreasen	SR/DS	trunsea@gmail.com
Åsa Johannisson	PoSta	asa@asajohannisson.se
Åsa Lindgren	Liaison Officer	asa.lindgren@polar.se

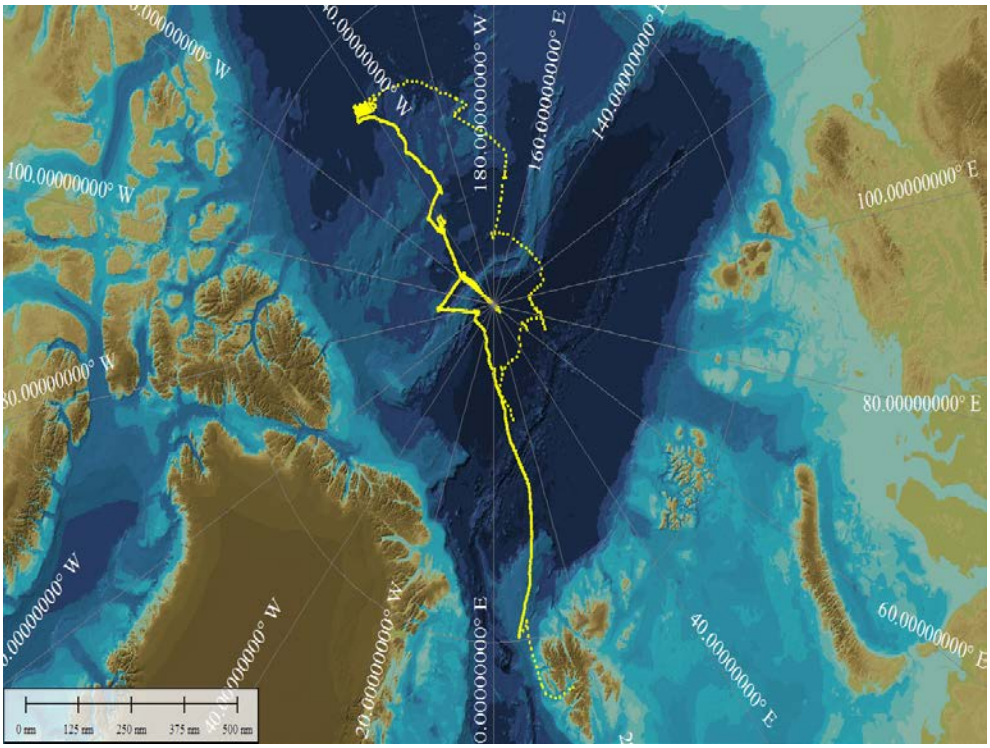

Figure 1.1 Cruise track Oden Arctic Ocean 2016. Dotted lines are indicating routes when Oden was travelling alone. Oden and LSSL met at the ice edge August 10 and separated September 2.

Figure 1.2 The two ships were alongside for some hours September 2 and a group photo of all the expedition participants from both icebreakers was taken. Photo: Lars Lehnert

2. Work Package: Seismic Reflection and Refraction Survey (SR)

Thomas Funck[1], John R. Hopper[1], Per Trinhammer[2], Lars Rasmussen[2], Tommy Kessler[2], Anders Dahlin[2], Andreas Skifter Madsen[2], Lasse Nygaard Eriksen[2], Trine Andreasen[2]

[1] Geological Survey of Denmark and Greenland (GEUS), [2] Department of Geoscience, Aarhus University

2.1 Summary

The seismic work was part of Canada's UNCLOS (United Nations Convention on the Law of the Sea) program to map the extended continental shelf in the Arctic Ocean. The seismic work was divided into two phases, with the two ships operating together during the first phase and separately during the second. The first phase ran from August 11 until September 2, 2016 and was carried out with an airgun array on CCGS Louis S. St-Laurent for a seismic source while Oden deployed seismic receivers (18 sonobuoys and 6 Taurus ice stations). Additional receivers were deployed from CCGS Louis S. St-Laurent and both vessels recorded the data transmitted from all active sonobuoys. Coincident seismic reflection data were obtained by towing a streamer behind CCGS Louis S. St-Laurent while Oden sailed ahead to break ice. Five seismic lines were acquired: two crossing the Lomonosov Ridge, one along the Marvin Spur, and two from the Makarov Basin and onto the Alpha Ridge.

During the second phase of the program, Oden acquired seismic data on her own in Amundsen Basin. Prior to data acquisition, Oden first broke a track through the ice and then returned along the track to collect seismic data. Reflection data were recorded on a 200-m-long streamer towed behind the Oden, while wide-angle seismic reflection/refraction data were recorded by 14 sonobuoys and two Taurus ice stations. A total of 197 km of seismic reflection data were acquired along four seismic lines. The seismic reflection records are of high quality and provide information on the sedimentary structure down to the basement. The sonobuoys recorded refractions from both the sedimentary layers and the crust up to offsets of >20 km.

Seismic lines acquired during the first phase were primarily designed to answer questions on the large-scale tectonic development and opening history of the Arctic Ocean and to better describe the crustal structure of the ridges and spurs found in the basins. In terms of UNCLOS, this information will improve the general understanding of the geological setting of the extended continental shelf along Canada's Arctic margin and will help to classify the submarine ridges and elevations. During the second phase of the expedition, seismic data were collected to determine the sediment thickness in Amundsen Basin to document Gardiner points for the delineation of the outer limits of the continental shelf.

2.2 Background

Canada ratified UNCLOS in 2003 and the Arctic Ocean 2016 expedition is the last planned survey to map Canada's extended continental shelf in the Arctic Ocean. Canada used the polar-class icebreaker CCGS Louis S. St-Laurent in seven seismic programs running from 2007 through 2015. In each of these expeditions, the seismic operation was supported by another icebreaker (either USCGC Healy or CCGS Terry Fox) that had to break a lead ahead of CCGS Louis S. St-Laurent. In this year's expedition, CCGS Louis S. St-Laurent worked together with Oden and this was the first experiment with seismic equipment installed on both vessels. GEUS and Aarhus University developed a seismic system specifically designed for Arctic work on board Oden that was used on five previous expeditions between 2007 and 2015.

With two vessels capable of acquiring seismic data, significant flexibility was added to the program by allowing both two-ship and single-ship experiments depending on ice conditions and logistical requirements. During the first phase of the expedition, both vessels operated together and Oden broke ice for CCGS Louis S. St-Laurent. Later, the ships separated to acquire seismic data in different areas. Both ships were equipped with helicopters and this added capacity to deploy seismic stations ahead of the shooting vessel. This was of particular importance as the first five profiles were designed as seismic refraction lines for which reversed seismic data are essential.

2.3 Seismic Reflection Equipment

The seismic reflection data along lines LSL1601 through LSL1605 were acquired on CCGS Louis S. St-Laurent and no details on that acquisition system are reported here. For profiles OD1601 through OD1604, the seismic equipment from GEUS/Aarhus University was used. The system consists of standard seismic equipment modified for data acquisition under extreme ice conditions. The most important elements of the seismic equipment are a digital streamer and recording system produced by Geometrics and an airgun array.

The seismic source consisted of a 1040 cu. in. linear airgun cluster comprised of two Sercel 520 cu. in. G-guns (Fig. 2.1). The firing interval was 14 s randomized to ± 0.4 s and the firing pressure was 190 bar. The pressurized air was produced by two Hamworthy 185E_MK2 70mm Series Air Compressors and two Bauer K23 High Pressure Compressor units. A trigger pulse generated by the navigation software NaviPac was sent to the gun trigger unit (Macha TGS-8) that synchronized and triggered the guns. The trigger pulse was also sent to the Geometrics GeoEel SPSU (streamer power supply unit) to start recording at the same time. A time-break signal was sent to the TGS-8 trigger unit from each G-gun for synchronization of the guns. A depth transducer (Fig. 2.2) was mounted on the gun cluster to monitor the tow depth of the array.

Data were recorded in SEG-D format (8058 revision 1) on a PC running Geometrics GeoEel controller software CNT-2. The controller was connected to the SPSU via Ethernet and received the digitized data from the 32 channels of the streamer as well as from eight auxiliary channels. Data from the five sonobuoy radio receivers were recorded

on auxiliary channels 1 through 5 while the PPS pulse from the GPS was logged on auxiliary channel 6. To avoid cross talk, the PPS pulse was reduced by a factor of 10. Data were recorded simultaneously on the internal RAID drive and an external SSD drive.

Figure 2.1 Sercel 1040 cu.in. linear airgun cluster. Photo: Per Trinhammer.

Figure 2.2 Geometrics GeoEel streamer on aft deck of Oden. Photo: Per Trinhammer.

The navigation software NaviPac sent an event trigger every 14 s, randomized by ± 0.4 s, and a string to COM port 1 on the Geometrics GeoEel PC. The string contained year, Julian day, time, event number, position of the gun cluster (x and y), gun depth and water depth from the centre beam of the Kongsberg EM 120 multibeam system. This

information was transferred to the SEG-D header. To avoid coherent stacking of multiple energy the shot time was randomized by ±400 ms. A separate GPS receiver (Thales ZX sensor) was used for calculating the position of the seismic reflection equipment. This was done by the NaviPac software from EIVA A/S. The GPS has a built-in beacon and WAAS receivers for differential corrections. However, the survey area was outside the coverage area of both systems and the GPS was used without differential corrections. NaviPac received antenna coordinates from the GPS and ship's motion information from Furuno gyro to calculate the location of the seismic equipment. A summary of all acquisition parameters is given in Table 2.1.

2.4 Sonobuoys and Ice Stations

A total of 32 sonobuoys were deployed from *Oden*. The sonobuoys (Fig. 2.3) were type AN/SSQ-53D(3) from ULTRA Electronics but adapted by ULTRA to to record frequencies down to 1 Hz to meet the requirements of seismic work. Some buoys were also modified by the manufacturer to delay scuttling (8 hours is the factory default).

Table 2.1 Acquisition parameters for seismic reflection lines OD1601 through OD1604.

Source	2 Sercel G-guns
Chamber volume	2 x 520 cu. Inch
Gun pressure	190 bar
Mechanical delay	Automatically adjusted to 300 ms
Nominal tow depth	14 m
Streamer	Geometrics GeoEel
Length of tow cable	30 m
Length of stretch section	53 m
No of active sections	4
Length of active sections	200 m
No of groups in each section	8
Total no of groups	32
Group interval	6.25 m
No of hydrophones in each group	8
Depth sensors	in each section
Nominal tow depth	12 m
Acquisition system	Geometrics GeoEel controller
Sample rate	1 ms
Low-cut filter	Out
High-cut filter	Anti-alias (405 Hz)
Gain setting	0 dB
No of recording channels	32
No of auxiliary channels	8
Shot interval	14 s ± 400 ms (randomized)
Record length	13 s

The sonobuoys were deployed from the aft deck of *Oden* or by helicopter. For the deployment from the ship, the method developed during the LOMROG II cruise in 2009 was used when the ship was in heavy ice. A 10-m-long rope was attached to the parachute of the buoy. The buoy was then deployed from the far end of the afterdeck on port side, holding the rope until the buoy expanded itself. The parachute and the rope were then pulled back on board. In lighter ice conditions, the buoys were thrown into the water from the port side. Two different methods were used for the helicopter deployments. One method was to drop the sonobuoy from the helicopter at an altitude of about 10 m by opening the sliding door on the left side of the helicopter. Alternatively, a safe landing place on a larger ice floe was chosen with access to open water. The buoy was then attached to a rope to prevent currents from moving the buoy below the ice prior to activation. Fig. 2.4 shows a sonobuoy after deployment.

Figure 2.3 Sonobuoy type AN/SSQ-53D(3) from ULTRA Electronics. The left part of the image shows the sonobuoy in the hermetically sealed buoy launch container. In the centre, the buoy is shown after removal of the storage container. The right part of the picture provides a view on the sonobuoy with the top cap (lanyard) removed, where the parachute is stored. The buoy is deployed in this state. Photo: Thomas Funck.

Figure 2.4 Sonobuoy at station SO-21-01. The orange float contains the antenna that is transmitting the hydrophone data back to the receiving system on Oden. Photo: Thomas Funck.

For the reception of the radio signals transmitted from the sonobuoys, two antennas were used (Fig. 2.5). A Moonraker MD HB-G3/HS dipole antenna was mounted on top of the bridge on the port side. In addition, two Yagi R2-10L antennas were stacked on top of each other pointing to the aft of the ship. The antennas had a height between 27 and 29 m above sea level. While the dipole antenna is omnidirectional, the Yagi antenna is directional.

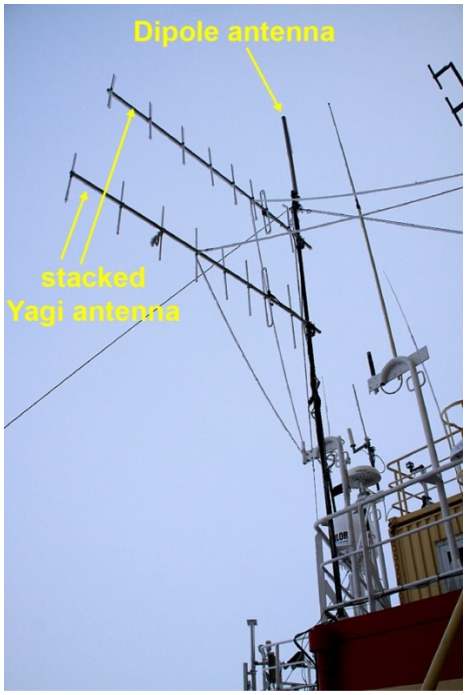

Figure 2.5. Dipole antenna MD HB-G3/HS and Yagi antenna R2-10L mounted on top of the bridge of Oden on the port side. Photo: Thomas Funck.

The signal from the antennas was fed to the five Winradios in the recording container on the fourth deck. The Moonraker dipole antenna was connected to a notch filter to eliminate the ship's AIS frequencies (161.975 and 162.025 MHz); while the signal from the Yagi antenna was not filtered. The output of the Winradios was split to be recorded both on the Geometrics recording system and on a Taurus digital seismometer manufactured by Nanometrics. While the Taurus seismometer allowed for continuous recording, the Geometrics system required the same record length that was used for the simultaneous acquisition of the seismic reflection data.

In addition to the sonobuoys, a total of eight Taurus ice stations (Fig.2.6) were deployed from Oden using the ship's helicopter. The data were recorded by a Taurus seismometer produced by Nanometrics using a sampling rate of 4 ms. Three sensors were connected to the seismometer: two SQ08-P1 hydrophones and one 2-Hz geophone (Model L-4 seismometer, Mark Products Inc.). Each of the hydrophones was connected to the seismometer by a 20-m-long cable.

The Taurus seismometer and the battery pack for the power supply were put in a black cooler box to keep the instrument as warm as possible during the deployment period. The GPS antenna needed for the timing of the Taurus was integrated into the lid of the cooler box. After the helicopter landed on the ice, the cooler box was placed between 2 and 5 m away from the edge of the floe. Any snow cover was removed and the geophone was placed directly on the sea ice using some water to freeze it firmly into position. The two hydrophones were put into the water using the full length of the cables. For locating the Taurus ice station, each deployment site was equipped with an ETS-1500 (CarteNav Solutions Inc.) Iridium satellite tracker.

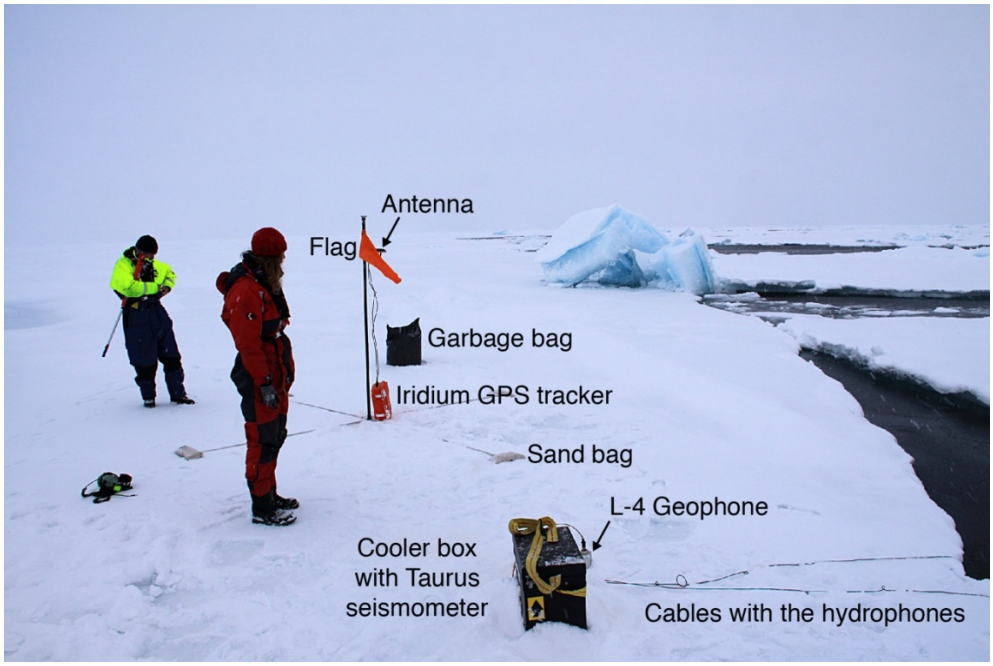

Figure 2.6. Taurus ice station at site TO-01-01 deployed along seismic line LSL1601. Photo: Thomas Funck.

2.5 Line Locations and Operation

During the first phase of the program when both ships worked together, Oden broke a track for CCGS Louis S. St-Laurent, which towed the airgun array and streamer. Both ships deployed sonobuoys: from Oden by helicopter ahead of the planned track line and CCGS Louis S. St-Laurent from the stern of the ship. In addition, Taurus ice stations were deployed by helicopter. Both vessels used their respective receiver system to monitor and record the signals of the sonobuoys. Fig. 2.7 shows the location of the sonobuoys and ice stations deployed from Oden for the seismic lines shot by CCGS Louis S. St-Laurent. Marine mammal observers were present during the seismic data acquisition to mitigate any risk to marine mammals. Neither whales nor polar bears were observed during the acquisition. A detailed listing of the sonobuoys and ice stations deployed is given in Tables 2.2 and 2.3. Two of the ice stations could not be recovered due to time constraints and had to be left on the ice.

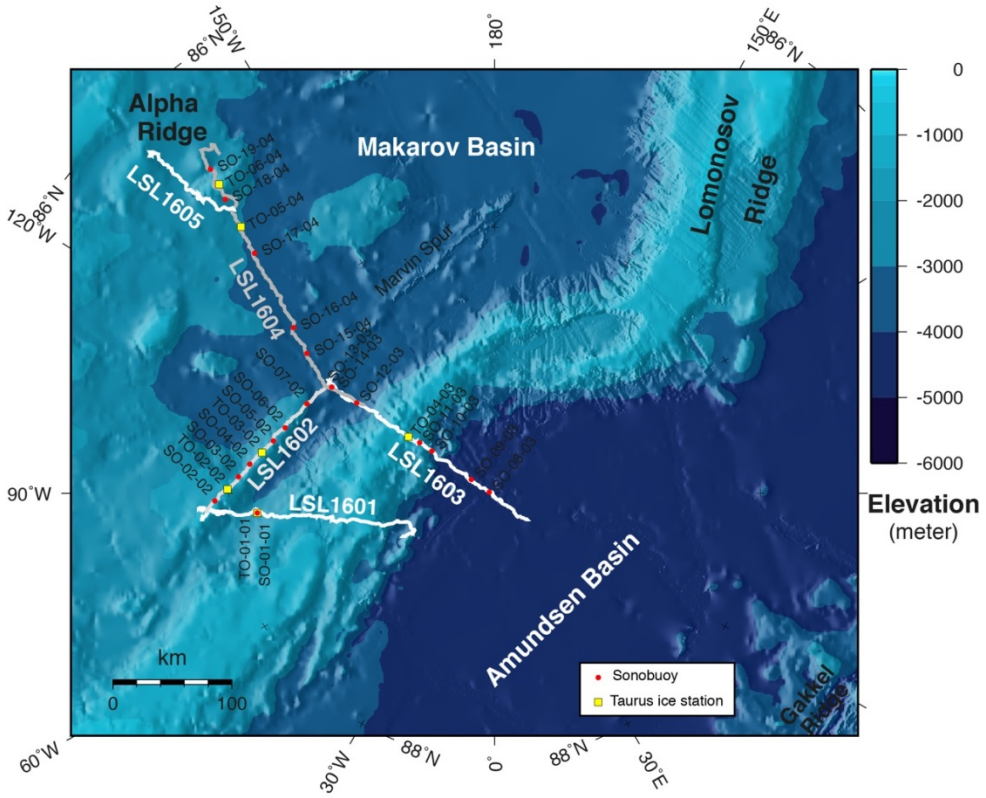

Figure 2.7 Bathymetric map (IBCAO 3.0, Jakobsson et al. 2012) with the location of the sonobuoys and Taurus ice stations deployed from Oden. White and grey lines show the track of Oden during the shooting of lines LSL1601 through LSL1605 from CCGS Louis S. St-Laurent. Note that there is an overlap between lines LSL1603 and LSL1604.

Table 2.2 Deployment of sonobuoys from Oden during the expedition Arctic Ocean 2016. The depth of the hydrophone was set to 30 m in all deployments.

Station code	Seismic line	Trans-mission channel	Deployment date	Time (UTC)	Longitude	Latitude	Deployment method	Comment
SO-00-00	-	48	11 AUG 2016	09:33:04	6.18754°E	80.14052°N	Stern Oden (rope)	Equipment test
SO-01-01	LSL1601	90	18 AUG 2016	03:42:46	85.32371°W	88.20805°N	Helicopter (landed)	
SO-02-02	LSL1602	83	19 AUG 2016	09:41:22	88.50878°W	87.89414°N	Helicopter (airborne)	
SO-03-02	LSL1602	90	19 AUG 2016	10:14:39	93.76432°W	88.06895°N	Helicopter (airborne)	
SO-04-02	LSL1602	66	19 AUG 2016	16:06:18	96.85189°W	88.14537°N	Helicopter (airborne)	
SO-05-02	LSL1602	58	19 AUG 2016	16:40:13	103.28775°W	88.28786°N	Helicopter (airborne)	
SO-06-02	LSL1602	87	19 AUG 2016	21:59:56	107.42008°W	88.34782°N	Helicopter (airborne)	
SO-07-02	LSL1602	28	19 AUG 2016	22:08:59	115.57632°W	88.43651°N	Helicopter (airborne)	
SO-08-03	LSL1603	58	22 AUG 2016	11:49:40	104.79268°W	89.95670°N	Helicopter (airborne)	
SO-09-03	LSL1603	28	22 AUG 2016	11:57:42	121.56850°W	89.79551°N	Helicopter (airborne)	
SO-10-03	LSL1603	62	22 AUG 2016	22:16:54	124.07438°W	89.42961°N	Helicopter (airborne)	
SO-11-03	LSL1603	83	22 AUG 2016	22:22:52	124.12395°W	89.32005°N	Helicopter (airborne)	
SO-12-03	LSL1603	66	23 AUG 2016	11:56:59	123.31835°W	88.76115°N	Helicopter (airborne)	
SO-13-03	LSL1603	90	23 AUG 2016	12:08:28	123.15656°W	88.53575°N	Helicopter (airborne)	Failed (did not surface)
SO-14-03	LSL1603	87	23 AUG 2016	12:52:57	123.12826°W	88.53766°N	Helicopter (airborne)	
SO-15-04	LSL1604	83	24 AUG 2016	20:17:13	126.71391°W	88.24079°N	Helicopter (airborne)	
SO-16-05	LSL1604	87	24 AUG 2016	20:27:39	129.47318°W	88.03886°N	Helicopter (airborne)	
SO-17-04	LSL1604	90	25 AUG 2016	11:31:52	135.00691°W	87.44739°N	Helicopter (airborne)	
SO-18-04	LSL1604	83	25 AUG 2016	18:52:00	137.47699°W	87.00300°N	Helicopter (airborne)	
SO-19-04	LSL1604	75	25 AUG 2016	21:24:26	138.75337°W	86.75906°N	Helicopter (airborne)	
SO-20-01	OD1601	83	08 SEPT 2016	09:47:48	91.74503°E	88.45950°N	Helicopter (landed)	
SO-21-01	OD1601	90	08 SEPT 2016	10:01:37	96.96410°E	88.49997°N	Helicopter (landed)	
SO-22-02	OD1602	81	09 SEPT 2016	01:21:29	81.80724°E	88.16087°N	Helicopter (airborne)	
SO-23-02	OD1602	75	09 SEPT 2016	01:25:48	82.94177°E	88.22288°N	Helicopter (airborne)	
SO-24-02	OD1602	97	09 SEPT 2016	01:30:53	84.56624°E	88.28618°N	Helicopter (airborne)	
SO-25-03	OD1603	77	09 SEPT 2016	16:09:19	70.30967°E	87.81190°N	Helicopter (airborne)	
SO-26-03	OD1603	83	09 SEPT 2016	16:18:35	72.77267°E	87.89106°N	Helicopter (airborne)	
SO-27-03	OD1603	87	09 SEPT 2016	16:24:02	75.16605°E	87.95560°N	Helicopter (airborne)	
SO-28-03	OD1603	90	09 SEPT 2016	16:28:14	76.87064°E	88.00970°N	Helicopter (airborne)	
SO-29-04	OD1604	77	10 SEPT 2016	15:14:03	60.14431°E	88.43246°N	Aft deck Oden (port)	
SO-30-04	OD1604	83	10 SEPT 2016	16:27:54	61.59443°E	88.49792°N	Aft deck Oden (port)	
SO-31-04	OD1604	87	10 SEPT 2016	17:30:55	63.29145°E	88.55316°N	Stern Oden (rope)	

Table 2.3 Deployment and recovery of Taurus ice stations carried out from Oden during the expedition Arctic Ocean 2016.

Station code	Line	Taurus serial number	Deployment and recovery date	Time (UTC)	Longitude	Latitude	Comments
TO-01-01	LSL1601	0427	18 AUG 2016	03:42:46	85.32371°W	88.20805°N	
			18 AUG 2016	19:15:07	84.11829°W	88.21402°N	
TO-02-02	LSL1602	0544	19 AUG 2016	10:00:00	90.89881°W	87.98800°N	
			19 AUG 2016	17:51:04	90.27274°W	88.02351°N	
TO-03-02	LSL1602	0453	19 AUG 2016	16:30:07	99.88160°W	88.22169°N	
			-	-	-	-	Station not recovered
TO-04-03	LSL1603	0416	22 AUG 2016	22:49:08	123.24917°W	89.22598°N	
			-	-	-	-	Station not recovered
TO-05-04	LSL1604	0544	25 AUG 2016	12:00:29	136.38167°W	87.23333°N	
			25 AUG 2016	20:53:21	135.53067°W	87.26835°N	
TO-06-04	LSL1604	0820	25 AUG 2016	19:18:52	138.27145°W	86.88851°N	
			26 AUG 2016	10:42:55	137.11926°W	86.96297°N	
TO-07-01	OD1601	0544	08 SEPT 2016	09:30:26	87.22632°E	88.42146°N	
			08 SEPT 2016	18:51:33	88.78357°E	88.43946°N	
TO-08-02	OD1602	0427	09 SEPT 2016	01:12:26	80.62755°E	88.09558°N	
			09 SEPT 2016	10:36:10	82.48151°E	88.07406°N	

During the second phase of the program when *Oden* acquired data along lines OD1601 through OD1604 in a single-ship operation, the seismic acquisition started after the ship broke a track along the planned line. For the icebreaking, some corrections to the track line were made to compensate for the assumed ice drift. This was made in an effort to run the seismic line as close as possible to its pre-planned location. Along lines OD1601

through OD1603, Taurus ice stations and sonobuoys were flown out by helicopter ahead of the ship and placed in the vicinity of the track but not directly into it to avoid destruction when the ship is passing by. Poor visibility and a high amount of moisture in the air prevented the use of the helicopter during the acquisition of line OD1604. For this reason, sonobuoys on this line were deployed from *Oden*. The station and line locations are shown in Fig.2.8. Details on the stations are shown in Tables 2.2 and 2.3.

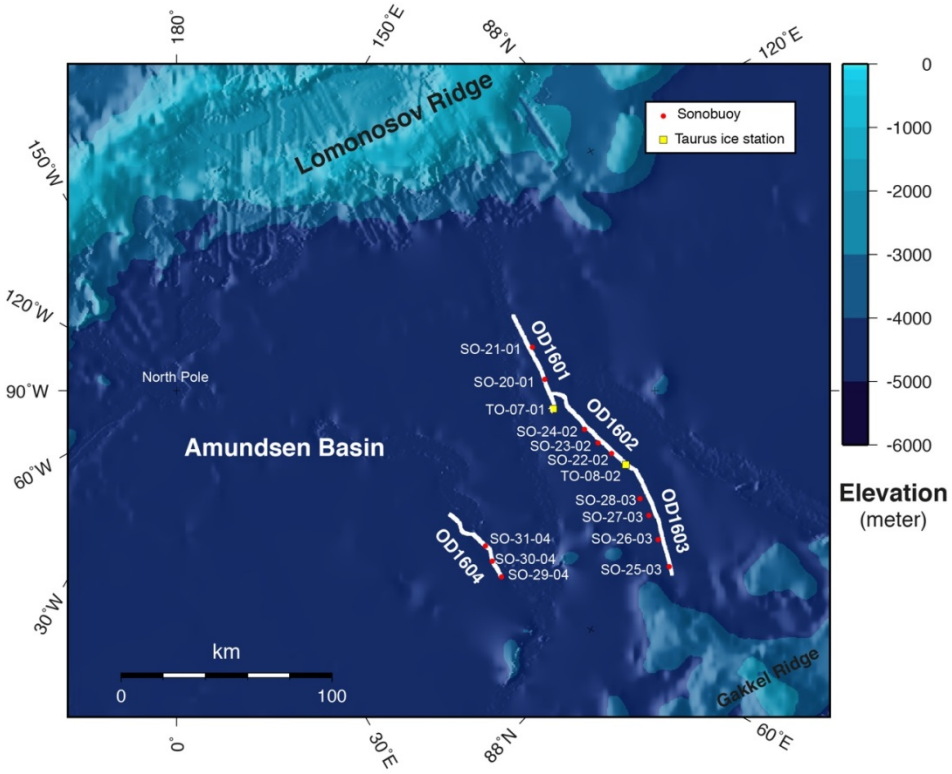

Figure 2.8 Bathymetric map (IBCAO 3.0, Jakobsson et al. 2012) with the location of seismic lines OD1601 through OD1604 (white lines).

2.6 Processing

On board processing of the seismic reflection data along lines OD1601 through OD1604 was carried out on a VMWare Fusion 7.1.1 virtual machine running Linux Centos 4.7 using ProMAX software (version 2003.19.1). The basic processing sequence was as follows:

1. SEG-D read with trace dc bias removal;
2. true amplitude recovery and bandpass filters;
3. spike and noise burst editing;
4. shot gather *f-k* filter and resample to 2 ms.
5. geometry assignment, including gun and cable statics;
6. trace equalization;
7. trace mixing on shot gathers;

8. midpoint sort and stack;
9. seafloor mute
10. post-stack constant velocity migration;
11. SEG-Y output.

The sonobuoy data recorded on the auxiliary channels of the Geometrics system were converted to SEG-Y in ProMAX as well. The recordings on the Taurus seismometers were not processed on board.

2.7 Results

The two-ship operation produced an unprecedented dataset for the region between the Lomonosov and Alpha ridges. High-quality seismic reflection data were acquired along lines with closely spaced seismometers (sonobuoys and ice stations) that provide reversed seismic refraction data. This will allow for the calculation of P-wave velocity models of the upper and lower crust along large sections of lines LSL1601 through 1605. One of the open scientific questions that the dataset will answer includes the nature of the continent-ocean transition zone at the Eurasian side of the Lomonosov Ridge. Brozena et al. (2003) identified Chron C25 as the oldest magnetic seafloor spreading anomaly, an interpretation that is still contentious. Seismic line LSL1603 covers the transition zone between the Lomonosov Ridge and the clearly identifiable Chron C24 with four sonobuoys (two from each vessel) and will provide information on the crustal character in that region. Line LSL1602 will provide information on whether Marvin Spur is of oceanic or continental origin. The crustal character of Makarov Basin and the structural relation to Alpha Ridge are some of the questions lines LSL1604 and LSL1605 will help to answer.

The UNCLOS objectives for lines OD1601 through OD1604 in Amundsen Basin were achieved since the seismic reflection records provide a clear definition of the sedimentary thickness along the lines (Fig.2.9). For the time to depth conversion, 12 sonobuoys and 2 ice stations provide good control on the velocity structure both within the sediments but also within the underlying crust (Fig. 2.10). This may help to distinguish different crustal domains and to identify possible serpentinization processes beneath the generally thin crust. Seismic energy on the seismic receivers can be correlated to offsets exceeding 20 km even without any additional processing.

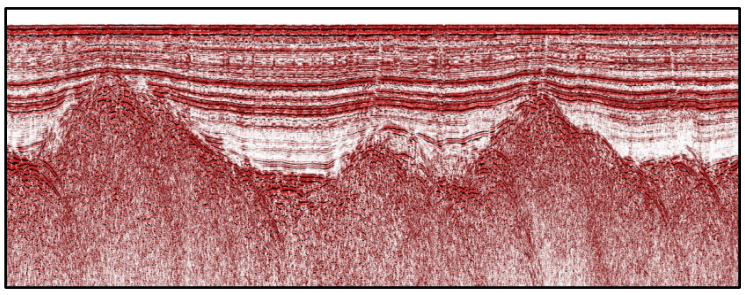

Figure 2.9 Example illustrating the quality of the seismic reflection data collected in Amundsen Basin during the Arctic Ocean 2016 expedition. This is a stacked record section. The sedimentary column is well-imaged down to the basement.

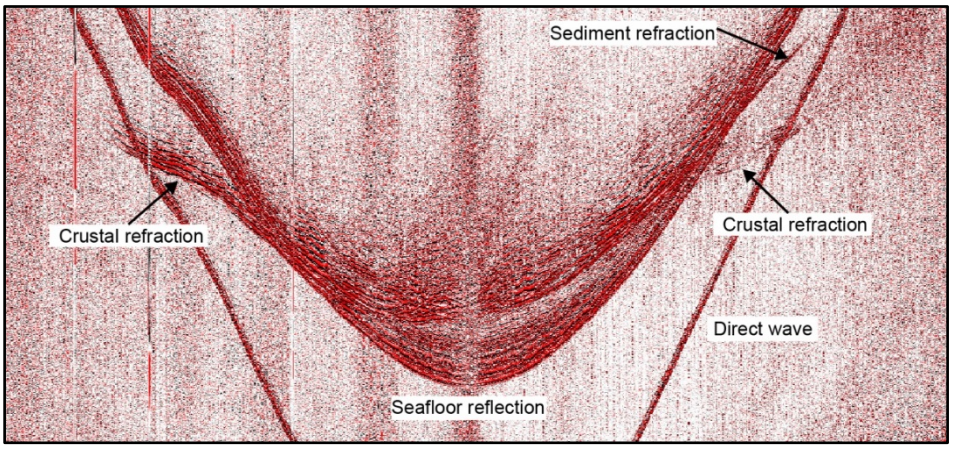

Figure 2.10 Subset of a sonobuoy record of a station in Amundsen Basin. The data are not processed but show efractions both in the sedimentary layers and the crust.

2.8 References

Brozena, J.M., Childers, V.A., Lawver, L.A., Gahagan, L.M., Forsberg, R., Faleide, J.I., Eldholm, O., 2003. New aerogeophysical study of the Eurasia Basin and Lomonosov Ridge: Implications for basin development. Geology 31, 825–828.

Jakobsson, M., Mayer, L., Coakley, B., Dowdeswell, J.A., Forbes, S., Fridman, B., Hodnesdal, H., Noormets, R., Pedersen, R., Rebesco, M., Schenke, H.W., Zarayskaya, Y., Accettella, D., Armstrong, A., Anderson, R.M., Bienhoff, P., Camerlenghi, A., Church, I., Edwards, M., Gardner, J.V., Hall, J.K., Hell, B., Hestvik, O., Kristoffersen, Y., Marcussen, C., Mohammad, R., Mosher, D., Nghiem, S.V., Pedrosa, M.T., Travaglini, P.G., Weatherall, P., 2012. The International Bathymetric Chart of the Arctic Ocean (IBCAO) Version 3.0. Geophysical Research Letters 39, L12609.

Photo: Åsa Lindgren

3. Work Package: Dredge Samples (DS)

Gordon N. Oakey[1], Per Trinhammer[2], Lars Rasmussen[2], Tommy Kessler[2], Anders Dahlin[2], Andreas Madsen[2], Lasse Eriksen[2], Trine Andreasen[2], Thomas Funck[3], John R. Hopper[3]

[1]Geological Survey of Canada (GSC); [2]Department of Geosciences, Aarhus University, Denmark, [3]Geological Survey of Denmark and Greenland (GEUS)

3.1 Introduction

Several potential dredging targets for the Oden Arctic Ocean 2016 expedition were identified by the Canadian science planning team prior to the cruise. Locations were selected based on available multibeam data on the edges of bathymetric ridges and ranked first by largest slope angles, second by expected ice conditions, and finally by distance from Svalbard. In practice, the initial site selections provided only proof-of-concept for the dredging program and none were actually attempted. They did, however, establish specific areas-of-interest (AOIs) that were used in the ship track planning. The three AOIs were the edge of Lomonosov Ridge (adjacent to the Amundsen Basin), Marvin Spur, and Alpha Ridge. In total, five dredging attempts were made (Fig. 3.1); however, the last two sites (#4 and #5) were aborted due to either lack of sea ice (to dock the Oden) or unsuitable ice drift direction. All sites required multibeam mapping to identify slope angles over 25 degrees.

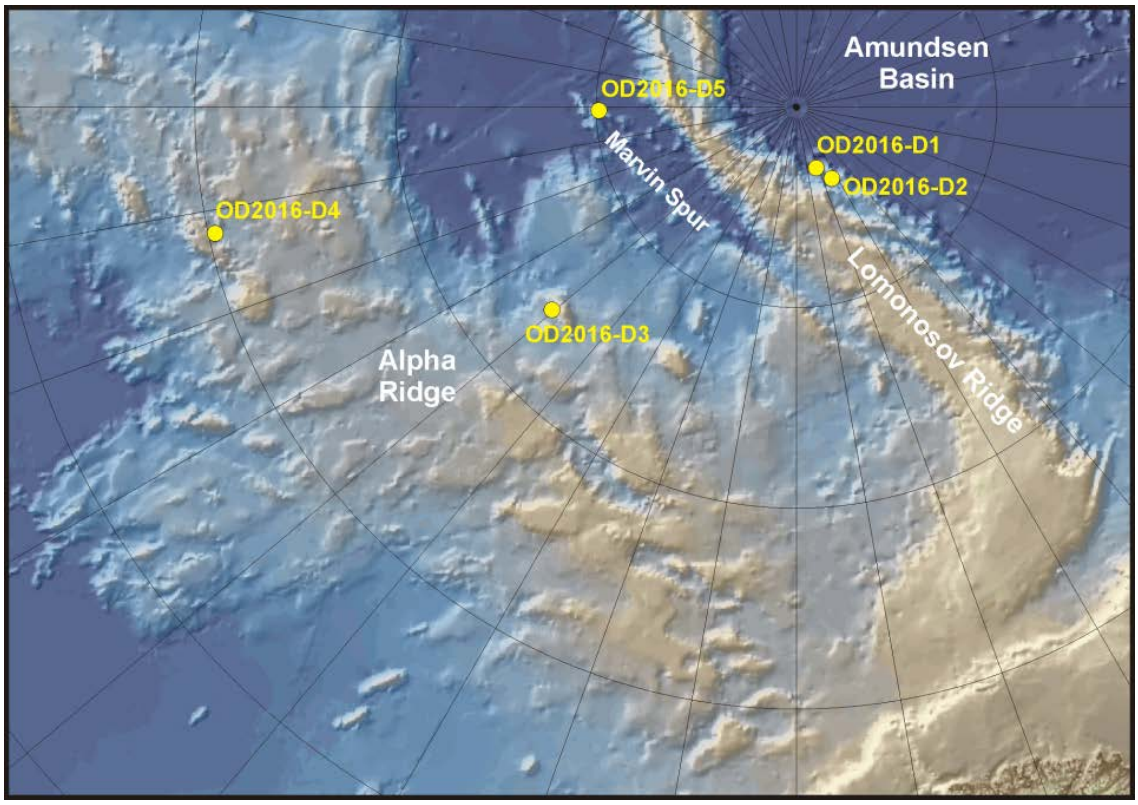

Figure 3.1 Dredge site locations

3.2 Dredging Equipment

The dredging equipment used on the expedition was provided by the Geological Survey of Denmark and Greenland (GEUS) and operated by Aarhus University field technicians. The front of the box dredge (manufactured by Marinetechnik Kawohl, Germany) is attached to a 500 m lead cable at a break linkage. An emergency break cable is attached to the bottom of the dredge cage. This configuration allows the front of the dredge to disconnect from the lead cable if it gets stuck. The dredge will then reverse and dump the contents, but will remain safely secured.

There is a 500 kg "depressor" weight attached to the front of the lead cable by a short (~ 4 m) chain which keeps the lead cable on the seafloor and prevents the dredge from bouncing. The use of the depressor weight was adopted on the GEUS LOMROG III expedition (Marcussen et al., 2012) and has significantly improved recovery success. Additionally, there is a 12 meter steel link wire from the depressor weight point to the Dyneema cable linkage, to keep the Dyneema cable above the sea bottom (Fig. 3.2).

The main Dyneema tow cable and winch were provided by the Swedish Polar Research Secretariat (SPRS). The Dyneema cable is neutrally buoyant in seawater, and the winch load does not increase with increased cable deployment.

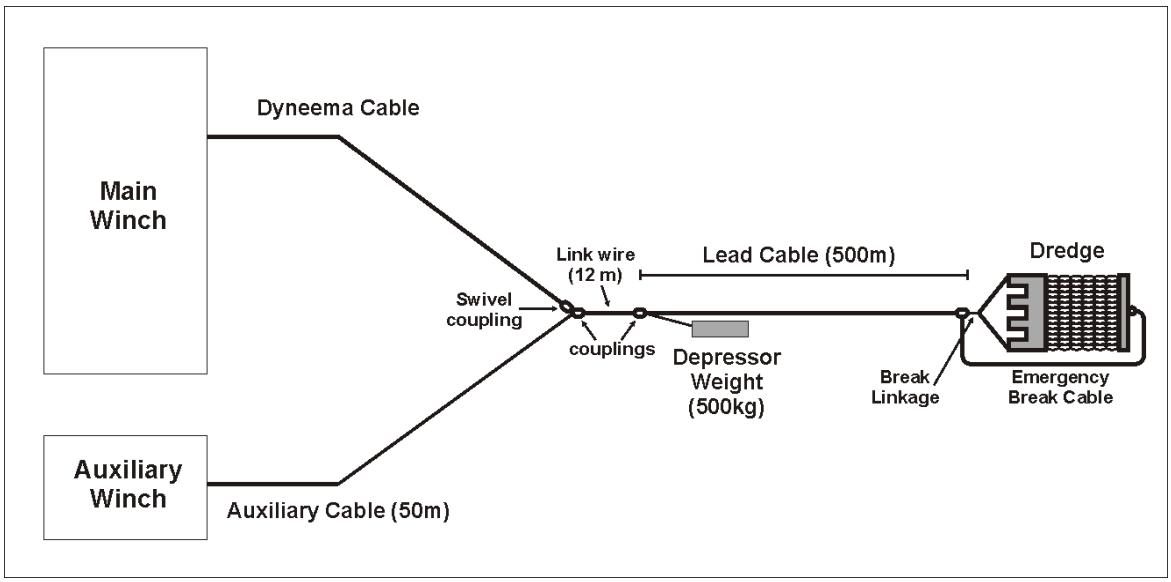

Figure 3.2 Dredge configuration

3.3 Deployment and Recovery

The dredging operations were carried out from the stern “fan-tail” using the main A-frame. The deck crane was used to move the box dredge and depressor weight into position to connect the shackles. First, the box dredge was connected to the lead cable and put over the side. The 500 m lead cable was paid out from the auxiliary winch. The depressor weight was then moved into place and the chain attached to the link wire. The depressor weight was then deployed and the 12 m ling wire paid out. The Dyneema cable was then attached to the 12 m link wire, the auxiliary wire disconnected, and the dredge assembly lowered to the seafloor with the Dyneema cable (Fig. 3.3).

Recovery of the dredging assembly was the reverse order. The auxiliary cable was re-attached to the 12 m link wire and the Dyneema cable was disconnected. Once the depressor weight was recovered and removed, the 500 m lead cable was paid in to bring the dredge onto the deck. The deck crane was then attached to the bottom of the dredge, and the contents dumped onto the deck for washing, sorting, documentation, and storage.

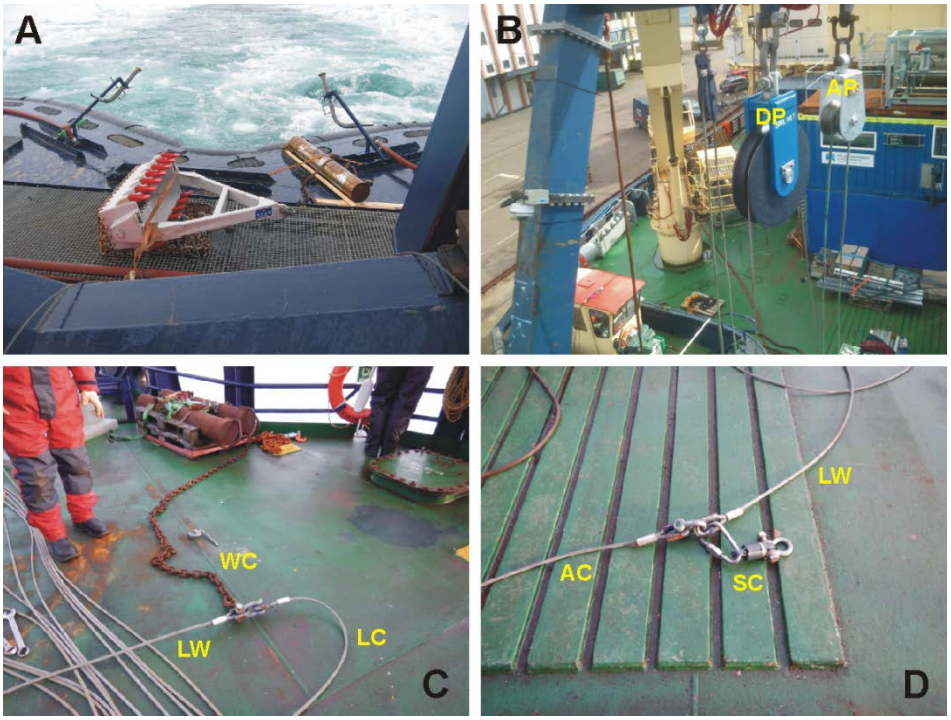

Figure 3.3 Dredge assembly: A) dredge and depressor weight on fan-deck; B) large Dyneema pulley (DP) and small auxiliary pulley (AP); C) depressor weight chain (WC) attached to lead cable (LC) and lea wire (LW) connector; D) lead wire (LW) attached to auxiliary cable (AC), swivel connector (SC) for attaching the Dyneema cable. (Photos by Per Trinhammer; Photo A from LOMROG III Expedition, Marcussen et al., 2012)

3.4 Site Operations

Dredging operations were not possible in open water since the *Oden* will usually turn broadside to the wind. The winching rate of the Dyneema cable is ~ 1 m/s, and with typical water depths of between 3000 and 4000 m, a single station generally takes 4 to 5 hours. It was necessary to dock the Oden into a solid ice pan into the direction of the ice drift in order to keep the Dyneema cable directly astern during the entire operation.

Determination of ice drift direction prior to dredge deployment was a critical element in the recovery success, as it was necessary to drift towards the slope. It was extremely useful to use the helicopter landing and take-off positions from the ice-stations operations (Heavy Metals work package), which provided direct direction and speed of the ice drift. Typically, the wind direction was 30° to ice drift direction, and it was anticipated that with consistent wind speed/direction, the ice drift would remain constant. Unfortunately, it was observed that the ice drift is highly variable (up to 90°) over quite short distances (4 to 6 nm) and in a short amount of time (1 to 2 hours). However, the ice-station drift direction information established whether the pre-planned slope sites for each AOI could be viable dredge targets or whether additional multibeam mapping was required to identify slopes over 25°.

Once a suitable slope was identified, the bridge was provided a way-point to park the *Oden* into the ice. The distance of the way-point to the base of the slope depended on the drift speed, and needed to allow enough time for the dredge to be lowered to ~ 200 m above the seafloor before encountering the slope. When the dredge hit the slope, there was a spike in the tension measured on the Dyneema cable winch. At this point, 500 m of cable was paid out at a rate dependent on the drift speed (see table 1 in the Appendix). Once the suppressor weight was on the seafloor, the *Oden* was allowed to drift for up to 1 hour to ensure a successful drag of the dredge for at least 0.5 nautical mile. During this time, any changes in the cable tension were monitored and recorded in the dredging logs (see logs in Appendix). The Dyneema cable was then slowly recovered, again at the ice drift speed, until the suppressor weight and dredge were clear of the seafloor, followed by full recovery speed. Once the weight and dredge were onboard, the contents were dumped for washing and documentation.

3.5 Safety

In compliance with SPRS safety regulations, a “Toolbox” meeting was completed prior to shipboard operations. The meeting outlined the dredging procedures and the individual tasks and responsibilities of all participants in the dredging operation (including the ship’s crew). Safety issues were identified and mitigation strategies clearly defined. All participants were required to sign the “Toolbox” safety document.

3.6 Overview of Dredge sites 1 & 2

Dredge sites 1 and 2 were on the inner slope of an un-named spur on the Amundsen Basin side of Lomonosov Ridge. These sites are close to the LOMROG-III dredge locations. Although the available multibeam data showed steeper slope angles on the outer edge of the spur, the drift direction defined by the ice stations earlier in the day (160815-1 and 160815-2) was unsuitable. Since a portion of the ridge had not been mapped (see Fig. 3.4 & 3.5), a multibeam transit across the ridge and along the inner trough was carried out prior to dredging. Although the slope angles for site 1 were not as promising as at site 2, it was considered a higher priority because it was coincident with the seismic reflection line collected in 2014 by the Louis S St. Laurent (LSSL14-10) which would have provided geological context of (possible) recovered samples.

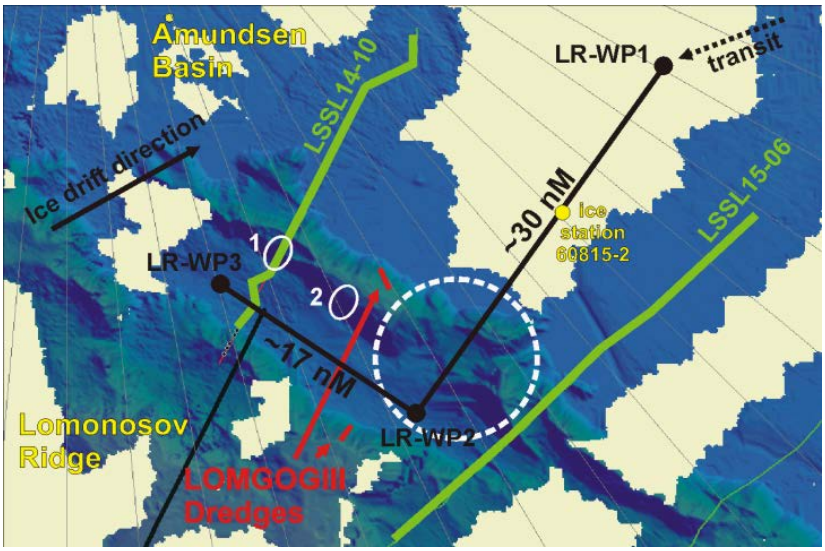

Figure 3.4 Locations of dredge sites *ODEN*2016-D-1 and *ODEN*2016-D-2. Ice drift direction was defined from station 60815-2. Dashed circle shows area requiring new multibeam. Also shown are the locations of the LSSL seismic reflection lines and LOMROG-III dredge sites.

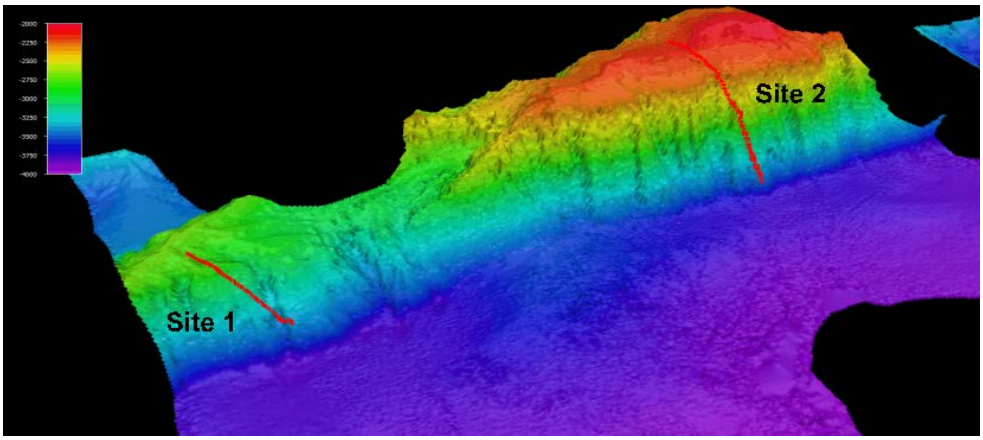

Figure 3.5 Perspective view of dredge sites 1 & 2. Red lines show drift tracks during dredging.

3.7 Dredge Site 1

Dredge site 1 started 15 August 2016 at 22:49 (time in UTC) and lasted for ~ 5 hours. The dredge reached the seafloor in ~ 3415 m water depth and left the seafloor in ~2786 m water depth. Transit distance of the dredge on the seafloor was approximately 1.3 nm. Operations went very smoothly, but only ~1 kg of rock samples were collected in the dredge basket (see Fig. 3.6). At the time the dredge was deployed, it was expected that the ice drift would take the ship to the east over the steep scarp, but because of an unexpected change in the drift direction, the ship transited further north over a less steep part of the ridge, which might partially explain the poor recovery.

Figure 3.6. Recovery of dredge 1. A) Nearly empty basket ; B) recovered samples in bin.

The recovered samples are all soft semi-consolidated laminated mudstones (Fig. 3.7). Clasts are angular, and some contain small voids. There were no rounded clasts recovered and all the samples are believed to have been recovered in situ and not drop stones. Samples were cleaned lightly and stored in individual plastic bags to prevent damage during shipping.

Figure 3.7 Selected samples from dredge 1

3.8 Dredge Site 2

Dredge 2 started 16 August 2016 at 10:11 and lasted for ~ 5.5 hours. The dredge covered a depth range from ~ 3700 m to 2100 m (see Figure 5). Transit distance of the dredge on the seafloor was approximately 2.2 nm. Operations went very smoothly and approximately 700 kg of rock samples were recovered (see Fig. 3.8 & 3.9).

There was only one small rounded drop stone clast recovered and the bulk of the samples are believed to have been recovered in situ. Samples were separated from the seafloor mud and washed for storage in plastic pails for shipping (13 pails in total). Due to the extremely large volume of recovery, only a very preliminary evaluation and sorting could be conducted onboard and will require a significant amount of post-cruise work.

Based on a first visual inspection, the rock samples are believed to be from in situ outcrop on the ridge. Some of the samples were covered by a thin ferromanganese crust and organic tube casts (Polychaeta family) indicating exposure to seawater; however, most had fresh angular faces. The majority of the retrieved samples are well consolidated tan-colored massive siltstones. A few samples did have fine laminations. The largest siltstone sample was ~3.6 kg. Also found were a few angular dark-grey angular clasts with well defined metamorphic fabric (schist?). Several large pieces of manganese crust with well-defined “growth rings” were also recovered, but were not attached to the host-rocks.

Figure 3.8 The dredge is recovered from Dredge 2. A shrimp was included in the catch. Photo: Åsa Lindgren

Figure 3.9 Dredge 2 samples: A) massive siltstone; B) laminated siltstone; C) dark shiest; D) manganese crust. Photo: Lars Lehnert.

3.9 Dredge site 3

Dredge site 3 on Alpha Ridge was on the southern slope of a bathymetric high in the IBCAO bathymetric grid, but had no multibeam coverage. The initial transit crossing (while LSSL collected seismic reflection data on LSSL1604) revealed that the feature was flat-topped with steep edges that warranted targeted mapping to identify a suitable dredging slope. Based on the ice drift direction from ice station 160826-01, the southern slope was considered favorable. Since this area was covered in thick ice and the Oden was operating separately from the LSSL, the mapping team requested a “drift” line up the slope to get the best quality data. Once reaching the plateau, the Oden turned to the western edge of the bathymetric high and then ran a ~ 8 nm line along the slope to finalize a dredging target.

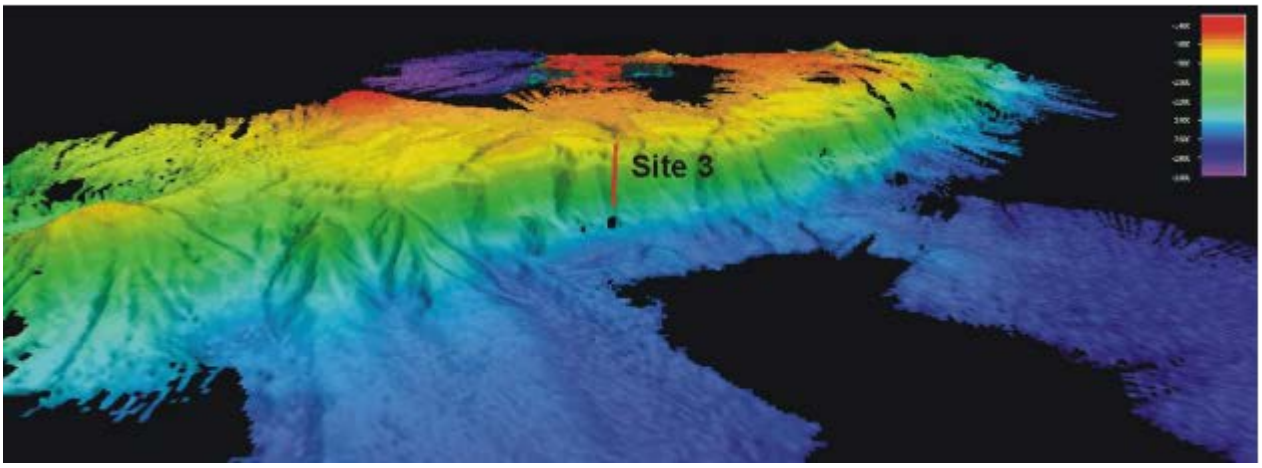

Figure 3.10 Bathymetric 3D image of the dredging site 3 from a southern view. The red line shows the drift path of the dredging operation.

Dredge 3 started 27 August 2016 at 08:07 (UTC) and lasted for ~5.5 hours. The dredge covered a depth range from 2575 m to 1555 m (Fig.3.10). Transit distance of the dredge on the seafloor was approximately 1.0 nm. Operations went smoothly and approximately 100 kg of rock samples (Fig.3.11 & 3.12) and a significant amount of seafloor mud were recovered. The large samples were removed from the mud and washed. The remaining mud was washed in a sieve to collect all remaining smaller stone samples.

The initial on-deck examination of the recovered samples was the identification of two distinct lithologies: a dark-colored conglomerate (?) and a light-colored carbonate (?) crust. Both rock types had minor manganese coating on the outer weathered edges, but most surfaces are unaltered, indicating that these were sampled in situ from outcrop.

After the samples were carefully cleaned and photographed, the “conglomerate” appears to be a volcaniclastic breccia with entrained sedimentary clasts. The fresh broken faces clearly show a vesicular basaltic matrix with angular clasts (both volcanic and sedimentary). The “carbonate” crust was tested with hydrochloric acid, which confirmed that they are limestone. Some of the samples are highly fossiliferous and contain several different (as-yet unidentified) species. Powder from a small sample was examined under a microscope and revealed at least one micro-fossil. These samples should easily be dated from their macrofossil and microfossil assemblages.

Figure 3.11 Recovery from dredge 3. Sea anemones were attached to some samples.

Figure 3.12 Dredge 3 Samples: A) Volcaniclastic breccia (2 pieces); B) Fossiliferous Limestone; C) Zoom-in of fossil details (box in B). Photo: Lars Lehnert

3.10 Dredge Site 4

One of the pre-planned dredge targets was a bathymetric high on Alpha Ridge that was crossed by an LSSL seismic reflection profile in 2011. The coincident multibeam track over this feature (acquired by the USCGS Healy) showed steep slopes on the southern edge, and slightly lower slope angles on the northern face. A brief ship-drift test on the evening of September 3 (~21:00 to 21:15) determined that the north face was a possible target. Additional multibeam data was required to find the best location and a mapping line was run around the western and northern slopes the bathymetric high (Fig.3.13). Although a suitable dredge site was identified, by 07:25 on September 4, a large lead of open water had developed and there were no ice pans to dock the Oden. The dredge station was aborted; however, an addition 15 nm of multibeam data were collected along the north slope before leaving the area and rendezvousing with the LSSL.

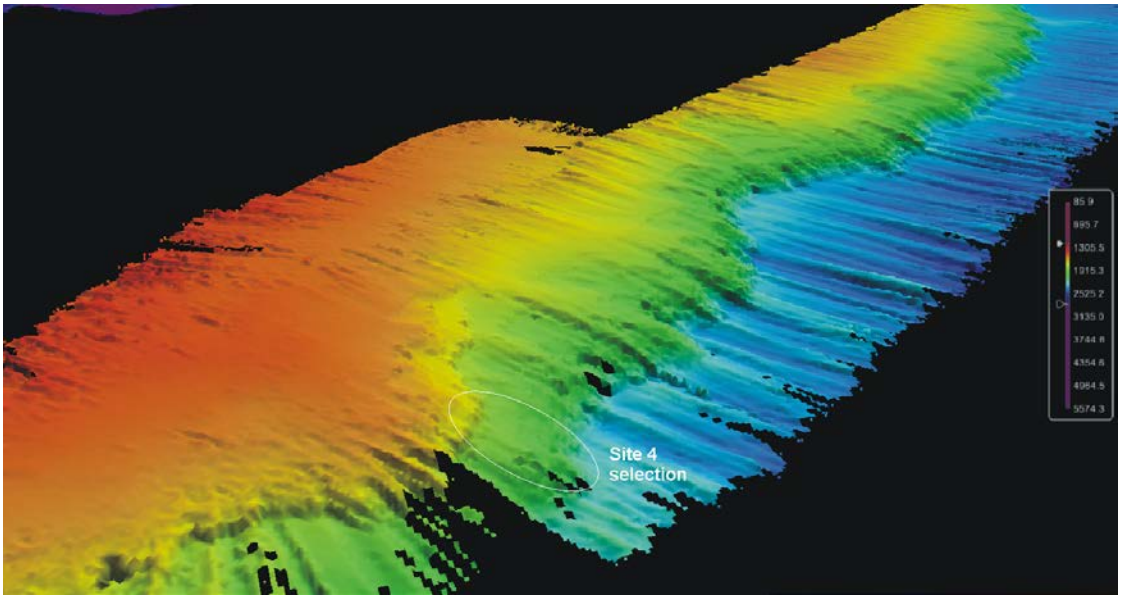

Figure 3.13 3D perspective view of multibeam mapping for dredge site 4. White oval shows selected slope for dredging.

3.11 Dredge Site 5

Another of the pre-planned dredge targets was a north-western end of Marvin Spur. Again, a brief ship drift test (05:45 to 06:35, September 6) was carried out and determined that only the southern face was an option. Since the sparse existing multibeam data over this portion of Marvin Spur, steeper bathymetric gradients are observed on the northern slope (facing Lomonosov Ridge). Additional multibeam mapping was required to identify a suitable location on the southern slope. A 10 nm survey line along this slope did not identify a high quality target. However, during the time it took to review the new data and decide how to proceed (08:15 to 08:40), the ship drift had changed almost 180 degrees from the earlier test. Since this change now made the north slope possible (and because of the scientific importance of the Marvin Spur), the decision was made to continue the mapping and identify a new dredge target. The ridge was crossed and an additional 6 nm of multibeam data were acquired to map the northern slope and identify a dredging location (Fig. 3.14). The *Oden* docked into an ice

pan to drift onto a portion of the slope with maximum dip angles of over 30 degrees. Unfortunately, as the *Oden* drifted, the new direction had changed by 90 degrees and was now moving parallel to the slope with no chance on an intercept. As a result, the dredge target was aborted.

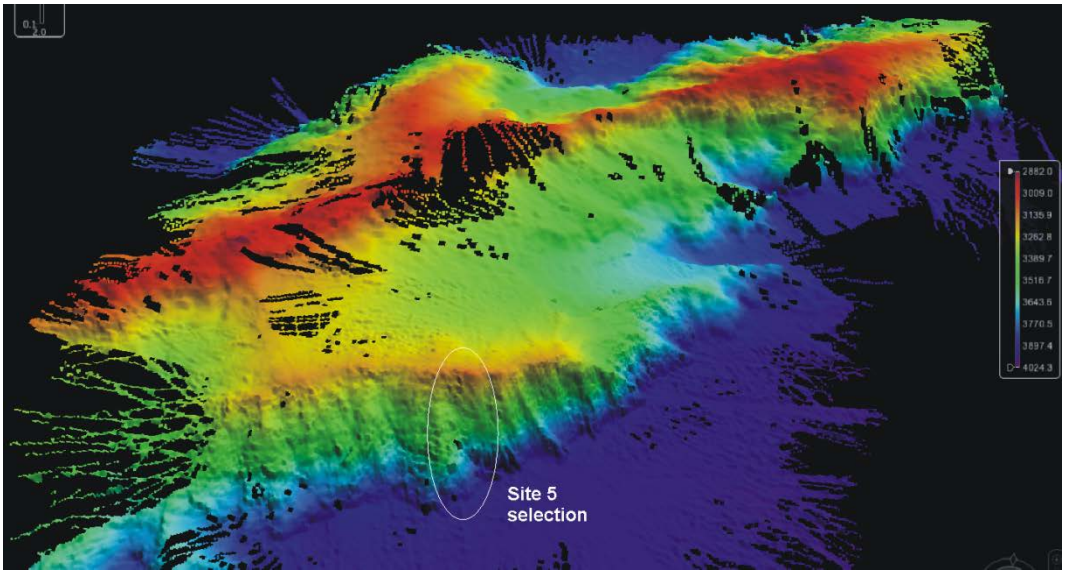

Figure 3.14 3D perspective view of multibeam mapping for dredge site 5. White oval shows selected slope for dredging.

3.12 Acknowledgements

We would like to thanks the multibeam mapping team (Kevin Jerram, Dave Sinnott, Darren Hiltz, Christian Smith, Evgenia Bazhenova, Lara Perez) for their help in planning the dredge site locations and images used in this report.

3.13 References

Marcussen, C. & LOMROG III Scientific Party 2012: Lomonosov Ridge off Greenland 2012 (LOMROG III) - Cruise Report, Danmarks og Grønlands Geologiske Undersøgelse Rapport 2012/119, Geological Survey of Denmark and Greenland, Copenhagen, Denmark

4. Work Package: Gravimeter Data Logging (GDL)

John R. Hopper[1], Rene Forsberg[1], and Gordon N. Oakey[2]

[1]Geological Survey of Canada (GSC); [2]Geological Survey of Denmark and Greenland (GEUS)

4.1 Introduction

Marine gravity data reflect the density distribution of the subsurface. Low gravity values are related to low average densities and high gravity values are related to high average densities. To first order, marine gravity primarily reflects the bathymetry. Over the Amundsen Basin, where the seafloor is flat, the first order gravity signal reflects the basement topography, providing a good indication of sediment thickness. High gravity is expected over basement highs (thin sediment) and low gravity is expected over basement lows (thick sediment).

Gravity increases generally towards the poles due to the flattening and rotation of the earth. After removal of this effect, gravity anomalies can be identified. Variations in gravity anomalies are expressed in mGal (1 mGal = 10^{-5} m/s^2), and a 1mGal change in gravity corresponds roughly to 7 meters bathymetry in a free air anomaly.

4.2 Equipment

An Ultrasys LaCoste and Romberg marine gravimeter, model number S-38, was installed in the pump room near the centre-of-mass of the ship to minimize the effect of the ship's movement (Fig. 4.1). This was the same location as the LOMROG and EAGER cruises. The instrument is a high precision spring balance with a proof mass mounted on a gyro-stabilized platform. Levelling is maintained by a feedback mechanism. The accuracy of the marine gravimeter is about 1 mGal with typically 200-500 m horizontal resolution. However, this is dependent on ice conditions and the speed of the Oden.

4.3 Measurements

The marine gravimeter was operated in "marine mode" and logged data every 10 seconds along Oden's entire track (Fig 4.2). A single survey line was used for the entire trip and the meter worked without problems for the duration of the cruise. Therefore, the meter was never restarted during the cruise. The meter was checked manually at least once per day to verify that everything was functioning normally. Data were logged into single files for each day of operation. Backup copies of the day-files were taken from the data logging computer on a portable hard-drive.

4.4 Ties

The S-38 is a relative gravimeter, meaning that absolute gravity values are not measured but only relative differences between measurement points. In addition, all gravity meters are subject to drift of the measured value, which for the time frame of the cruise is assumed to be linear with time. In order to correct for drift, the readings of the meter need to be tied to known gravity values before and after the cruise. To calculate absolute gravity values from the relative measurements, a tie to the international absolute

reference system is also necessary. Such gravity reference points can be found in Longyearbyen, but unfortunately Oden was not able to dock at the beginning of the cruise and is not expected to do so at the end of the cruise either. Therefore, this has been done by taking a reading at Oden's anchor position at Adventfjorden just off Longyearbyen and comparing this to results of previous cruises, where a proper port tie was possible. This has been proven to give satisfactory results for the LOMROG II and III cruises. As an additional calibration check, the sensor system will remain on board with power during Oden's transit back to Helsingborg, where a final dock-side calibration can be made.

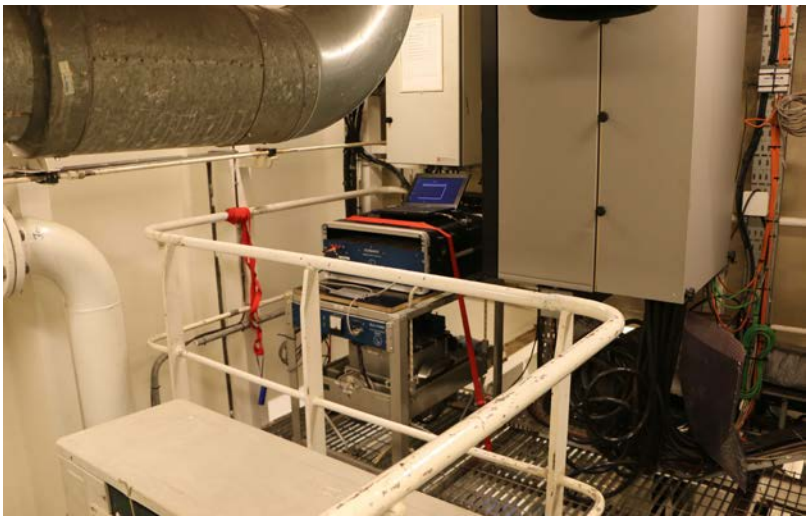

Figure 4.1 Ultrasys S-38 marine gravimeter installed in Oden's pump room.

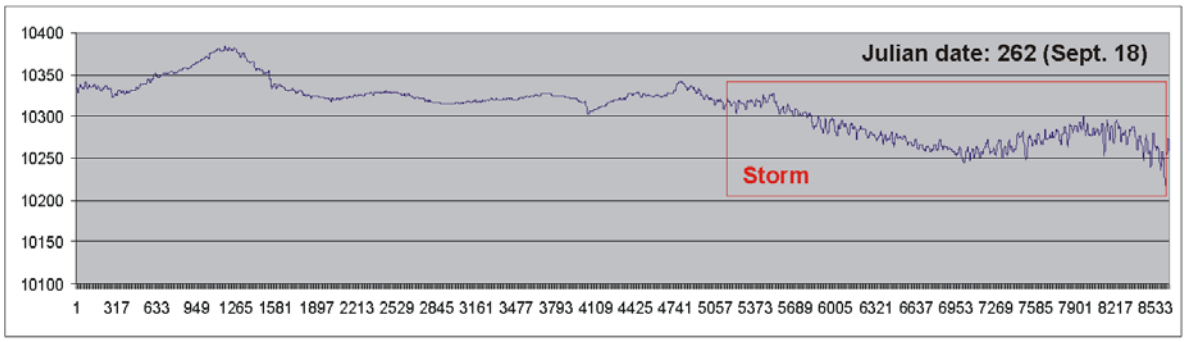

Figure 4.2 Sample of gravity dat recorded on Julian day 262. All data were measure in open water during the transit to Longyearbyen at the end of the expedition. Noise levels during the big storm significantly increased.

4.5 Processing

As there was no GPS navigation logged in the gravity data files, the navigation will be merged using the recorded day and time as part of the post-cruise data processing. All data will be processed after the cruise by the Danish Space Agency (DTU-Space).

5. Work Package: Geophysical Mapping/ Water Column Imaging (GM)

Kevin Jerram[1], Evgenia Bazhenova[1], Darren R. Hiltz[2], Lara F. Perez[3], Dave Sinnott[2], Christian Smith[4], Martin Jakobsson*[4], Christian Stranne*[1,4]

[1] Center for Coastal and Ocean Mapping / Joint Hydrographic Center, University of New Hampshire, USA, [2] Fisheries and Oceans Canada, Canadian Hydrographic Service – Atlantic Region, Canada, [3] Geophysical Department, Geological Survey of Denmark and Greenland (GEUS), Denmark, [4] Department of Geological Sciences, Stockholm University, Sweden

5.1 Summary

The Geophysical Mapping Work Package (GM WP) acquired multibeam echosounder, midwater split-beam echosounder, and subbottom profiler data continuously aboard the Swedish icebreaker Oden along 8728 km of vessel tracks throughout the Arctic Ocean between 8 August and 19 September, 2016. Multibeam echosounder coverage totals over 28864 km^2 (based on a 50-m grid). Multibeam and subbottom data were preliminarily processed on board to create bathymetric grids and images of upper sediment structure to inform selection of sampling sites, including 13 cores and 3 dredges. Post-expedition analysis will focus on bathymetric processing for UNCLOS purposes and contribution to the IBCAO dataset; detailed examination of CTD measurements with simultaneous midwater echosounder data; and examination of subbottom

5.2 Background

The Arctic Ocean is the most sparsely mapped seafloor in the world, owing to the difficulty and expense of acquiring high-resolution acoustic datasets in ice. The Canadian UNCLOS program and SPRS organized the Arctic Ocean 2016 expedition aboard the Oden to collect mapping and sampling data in poorly-mapped areas of interest for both programs, building on recent compilations of all available datasets (e.g., previous UNCLOS work, plus bathymetry derived from satellite, surface vessel, and submarine platforms as compiled in the International Bathymetric Chart of the Arctic Ocean, or IBCAO).

Of particular interest for the GM WP are high-resolution bathymetry and subbottom profiles showing the seafloor shape and structure of the upper sediment layers, respectively. These datasets are critical for identifying the 2500 m isobaths and other parameters for a Canadian UNCLOS submission as well as selecting target sites for coring and dredging efforts. UNCLOS conditions are discussed in the Background section at the beginning of the report. An additional component of the GM WP includes collecting echosounder data in the water column to detect acoustic scatterers, such as plumes of marine gas bubbles and schools of fish, to add to our understanding of their distribution and improve midwater mapping techniques.

5.3 Field sites

The expedition covered Arctic Ocean regions of interest for the Canadian UNCLOS program and SPRS scientific objectives, including mapping and sampling targets over the Gakkel, Lomonosov, and Alpha Ridges; Amundsen, Makarov, and Nautilus Basins; and Nautilus Spur. Figure 30 depicts the cruise track and sampling sites.

5.4 Methods

The Arctic Ocean 2016 Geophysical Mapping work package (GM WP) is divided into three segments:

- Multibeam Mapping and Subbottom Profiling
- Water Column Imaging
- Acoustical Oceanography

In accordance with the objectives for the Arctic Ocean 2016 GM WP outlined in the scope of work, the seafloor and upper sediment layers were mapped continuously along the entire Oden track (outside the 12-nm limit around Svalbard) using the vessel's 12 kHz multibeam echosounder and integrated 2.5-7 kHz chirp subbottom profiler, described below. The majority of the Oden geophysical mapping data were collected during seismic survey lines and transits between regions of particular interest for the Canadian UNCLOS project. More detailed exploratory surveys were conducted for identifying dredging and coring targets in high-priority areas using the subbottom profiles, multibeam bathymetry, and multibeam backscatter information. The areas of interest and transit routes were specified by the Canadian and SPRS teams based on prior planning, then modified throughout the expedition based on ice conditions, equipment state of readiness, and analysis of new bathymetry and subbottom data.

The water column imaging and acoustical oceanography components of the GM WP build on the SWERUS-C3 and Petermann Glacier 2015 expeditions, using newly developed water column imaging techniques to better understand oceanographic processes in the region. The GM team used both the EM122 multibeam echosounder and a specially installed EK80 broadband split-beam echosounder (described in detail in the Appendix) to collect continuous water column backscatter data throughout the expedition. These data were initially reviewed during acquisition to assess interference and will be scrutinized in post-expedition processing to identify various midwater targets such as biological scattering layers, marine gas seeps, and stratified water layers to further understand their spatial and temporal distributions in relation to the geologic context and oceanographic conditions. As in previous years, midwater data quality depended heavily on icebreaking conditions and bubble sweep.

Oden worked in tandem with Canadian Coast Guard icebreaker Louis S. St. Laurent (LSSL) between 11 August and 02 September to break ice and improve survey conditions for seismic, multibeam, and subbottom operations (Fig.5.1). Oden performed the majority of icebreaking duties with LSSL collecting high-quality multibeam and seismic data in the cleared path. This arrangement was changed occasionally when LSSL seismic operations were secured and Oden data quality became a priority, such as during a brief outage of the LSSL multibeam and when subbottom data from the Oden was critical for

core target selection. Mapping work aboard the Oden in support of the SPRS scientific objectives (e.g., surveying core and dredge sites) was taken opportunistically throughout the expedition.

EM122 multibeam echosounder

The hull-mounted multibeam echosounder installed in I/B Oden is a 12-kHz Kongsberg EM122 1° x 1° 'full ocean depth' multibeam echosounder with water column logging capability. The transmitter (TX) array is 8 x 1 m mounted along-ship in the so-called "ice knife", which forms the deepest part of Oden's hull (Fig. 5.2). This array is protected from ice impact by polyurethane plates reinforced by titanium bars. The nominal alongship transmit beamwidth is 1°. Due to the ice protection of the transmitter, the useable angular coverage athwartship is limited to approximately 140° with typical seafloor swath widths of 3-4 times water depth (WD) in low-ice / low-noise conditions.

The receiver (RX) array measures 8 x 1 m and is mounted athwartship with a nominal beamwidth of 1°. This array is protected from ice by a solid titanium plate. The multibeam system receives position, attitude, and attitude velocity data from a Seapath 320 navigation system using NovAtel GLONASS/GPS satellite antennas and a Seatex MRU5 motion sensor. A Seapath 200 is carried on board as a spare unit. The EM122 was operated using Seafloor Information System (SIS) software provided by Kongsberg.

SBP120 subbottom profiler

A Kongsberg SBP120 3° x 3° chirp subbottom profiler is hull-mounted in Oden and integrated with the multibeam system. This system transmits with a frequency range of 2.5-7 kHz from an independent ice-protected transducer and receives using the EM122 multibeam RX array, achieving an approximate range resolution of 0.35 ms (~70 cm). Up to 11 RX beams may be formed. The penetration is typically 50-200 m in clayey ocean sediments, though this also depends heavily on ice and bubble conditions along the hull.

EK80 water column echosounder

As in the SWERUS-C3 Leg 2 and Petermann Glacier 2015, the Simrad EK60 transceiver of the split-beam echosounding system was upgraded to an EK80 to operate in a broadband mode during the Arctic Ocean 2016 expedition. In its original mode, the system on the Oden is capable of transmitting and receiving narrow band (250-1000 Hz) pulses only at the transducer center frequency (18 kHz; see Appendix for details of the EK60 echosounder installation and operation). The ES18-11 transducer on the Oden can be driven over a much broader range of frequencies using the EK80 wideband transceiver (WBT), which was originally designed to achieve a frequency range of approximately an octave when coupled with composite transducers at frequencies of 70 kHz and above. Nonetheless, tests of the WBT in 2014 demonstrated that significant bandwidth could be achieved at lower frequencies with traditional (Tonpilz) transducers like the ES18-11 on the Oden (see Appendix for additional details of these tests).

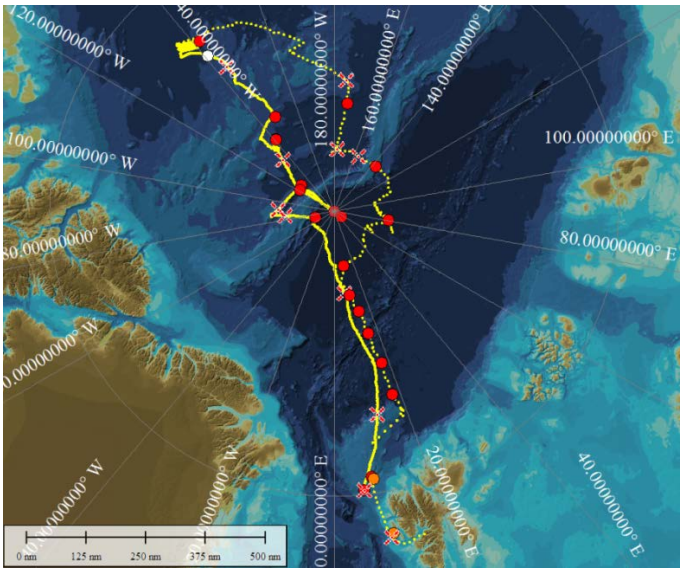

Figure 5.1 Overview of the Arctic Ocean 2016 Oden ship track (dashed yellow line) between 08 August – 19 September, 2016, departing from and returning to Svalbard. Primary geophysical mapping activities included continuous data acquisition with an EM122 multibeam echosounder, SBP120 subbottom profiler, and EK80 scientific split-beam water column echosounder. The Oden ship track is solid yellow while working with Canadian icebreaker Louis S. St. Laurent (LSSL) between 11 August and 02 September. CTD stations (red dots), XBT casts (red crosses), a single XCTD (LSSL, white dot) are also displayed. Background bathymetry is IBCAO v3 in Universal Polar Stereographic projection with the latitude of true scale at 75° N.

Additional technical details of the EM122, SBP120, and EK60/80 are available in the Appendix.

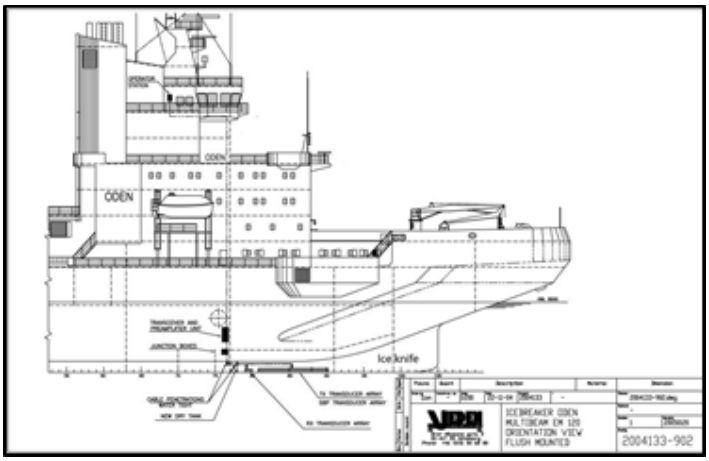

Figure 5.2 Drawing of the EM122/SBP120 system installed on I/B Oden; the EK60/80 transducer (not marked) is installed forward of the EM122 and SBP120 transducers.

Sound speed correction

The EM122 requires accurate sound speed information at the surface of the transducers and throughout the water column to properly perform its beamforming operations and refraction corrections, respectively. Sound speed at the transducer face (or 'surface' sound speed) was provided over the ship data network to SIS by a Valeport sound speed sensor mounted in a sea chest used for engine cooling water intake. Water flowing through the sea chest is expected to closely match that at the transducer face; the surface sound speed varied slowly (e.g., on the order of 0.1 m/s per day) throughout the majority of the expedition, suggesting a very stable upper water column.

Sound speed profiles were generated from multiple sources during the expedition (Fig. 5.3). The preferred source is temperature, salinity, and depth data collected at oceanographic stations using a standard SeaBird911 conductivity-temperature-depth (CTD) sensor suite (see the Physical Oceanography WP section). Sound speed for each sample was calculated using the Chen-Millero formula as implemented by SeaBird. CTD downcasts and upcasts for each station were averaged by the CTD team into CNV files which were then downsampled and reformatted as necessary into ASVP files for SIS using a MATLAB script.

During transits and/or when time limitations prevented CTD stations, sound speed profiles were generated from Sippican T-5 expendable bathythermograph (XBT) probes approximately once per day when ice and wind conditions allowed. XBT probes measure resistance as a proxy for temperature while falling at a factory-determined rate through the water column to estimate a temperature profile. XBT casts were typically collected to 1200-1800 m, depending on software configuration and early termination caused by contact between the probe's copper wire and the hull due to wind (see Appendix for method to address this failure mode).

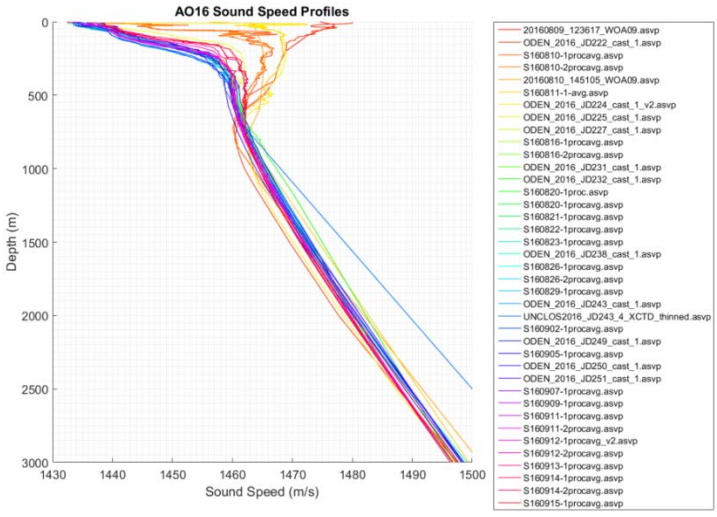

Figure 5.3 Sound speed profiles applied during AO16 from CTD, XBT, XCTD, and World Ocean Atlas 2009 sources. The legend is sorted in chronological order, showing that the greatest sound speed variability occurred in the upper 700 m during the earliest

and latest (and, thus, southernmost) portions of the expedition. Throughout the northern latitudes, the casts revealed a remarkably consistent sound speed environment.

5.5 Operation

Multibeam, subbottom, and water column data acquisition was carried out 24 hours per day by six operators divided into three teams. The decision to operate on eight-hour shifts was made as a group at the start of the expedition. Post-processing for daily bathymetric products was led by David Sinnott and Darren Hiltz, with Lara Perez and Evgenia Bazhenova leading the subbottom data processing and Kevin Jerram providing additional 'floating' coverage for survey planning and other support. Notes on data acquisition parameters, sound speed profiles, data quality issues, etc., were recorded in an Excel spreadsheet for ease of backup and search functionality; this log is an important component of the survey metadata and must accompany the raw datasets.

5.6 Research Activities and Preliminary Results

Multibeam data processing

EM122 data were acquired on board Oden using Kongsberg Maritime Seafloor Information System (SIS) v4.3.0 control and acquisition software. Details of the file storage and backup are provided in the Appendix. The Kongsberg raw .all files were processed onboard using two software packages for different purposes. Throughout the expedition, multibeam bathymetric data were edited and gridded by David Sinnott and Darren Hiltz using Caris HIPS 9.1 software under Canadian Hydrographic Service (CHS) workflows. The Caris projects and grid products are the primary bathymetric products for the expedition and will be delivered to CHS by Sinnott and Hiltz.

In addition to daily and expedition-scale bathymetry processing in Caris for Canadian UNCLOS purposes, QPS Qimera v1.3.2 was used to create a multibeam data project that is readily visualized with Fledermaus v7.6.0. Qimera and Fledermaus were used routinely for on-the-fly data processing during core and dredge site selection (Fig. 5.4 top). Data processing in both Caris and QPS software included checking for refraction artifacts (and correcting, if found, with new sound speed profiles); removing erroneous sounding using the alongtrack swath editor and 3D subset editing tools; and gridding the accepted soundings at resolutions appropriate for the depth range, data quality, and data density. Fledermaus FMGT was used on occasion to examine backscatter amplitude mosaics for drift sites (Fig.5.4 bottom), but data quality and density during transits or in ice were generally not sufficient for useful backscatter imagery.

Daily and site-specific products from Caris and QPS were added to a Global Mapper project used by the GM WP and expedition coordinators for ship tracking, operational planning, and sample target selection. The Global Mapper project included real-time ship position and provided context for the new data using background bathymetric grids such as IBCAO v3 Arctic bathymetry (Jakobsson et al., 2012) and other applicable spatial

datasets (e.g., daily ice imagery provided by the LSSL ice forecaster, historical and desired core locations, and other multibeam datasets used during the planning stage). All data were processed using a Polar Stereographic projection with a true scale at 75°N and horizontal datum of WGS 84 (UPS North / IBCAO convention). A Caris data processing log was maintained by Sinnott and Hiltz using an Excel spreadsheet; this log is a vital component of the survey metadata and must accompany the Caris project.

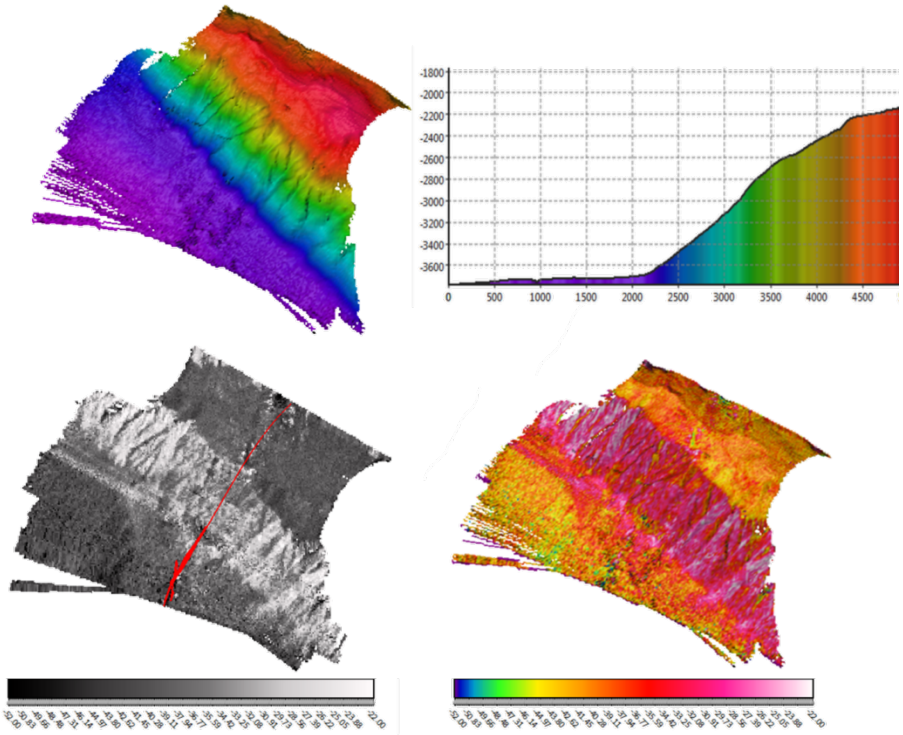

Figure 5.4 Multibeam bathymetry (upper left), elevation profile (upper right), and backscatter amplitude (lower left and right) for one dredge site on the Lomonosov Ridge, processed with QPS Qimera and FMGT. The depth scale the upper two images is approximately 2000 m (red) to 3600 m (purple). Uncalibrated backscatter amplitude (at the 12 kHz frequency of the multibeam) are shown with two color scales in the lower two images. Darker shades in the lower left image represent acoustically soft sediments, with lighter shades corresponding to acoustically harder surfaces. In the lower right image, the yellows and reds represent acoustically softer and harder surfaces, respectively, with whites as the highest backscatter values. These images corroborate the general expectation for accumulation of softer sediments on shallow slopes and exposure of harder surfaces (e.g., rock outcropping with less deposition) on steeper slopes. Data were acquired while drifting, yielding the densest and highest-quality EM122 data during the expedition.

Subbottom profiler data processing

High-resolution sub-bottom profile data were collected along the entire track with the SBP120 sub-bottom system using Kongsberg Maritime's SBP/TOPAS Ver. 1.5.3 system control and acquisition software. The SBP120 2.5-7 kHz chirp subbottom profiler was

run continually throughout the expedition outside of the 12-nm territorial limit around Svalbard. Bottom and sub-bottom reflection patterns obtained with the SBP120 characterize boundaries between layers of differing acoustic properties in the uppermost sediments (Fig. 5.5). These data provided real-time aid to sampling site selection during the expedition and will be used to study depositional patterns and their variation across the Arctic Ocean.

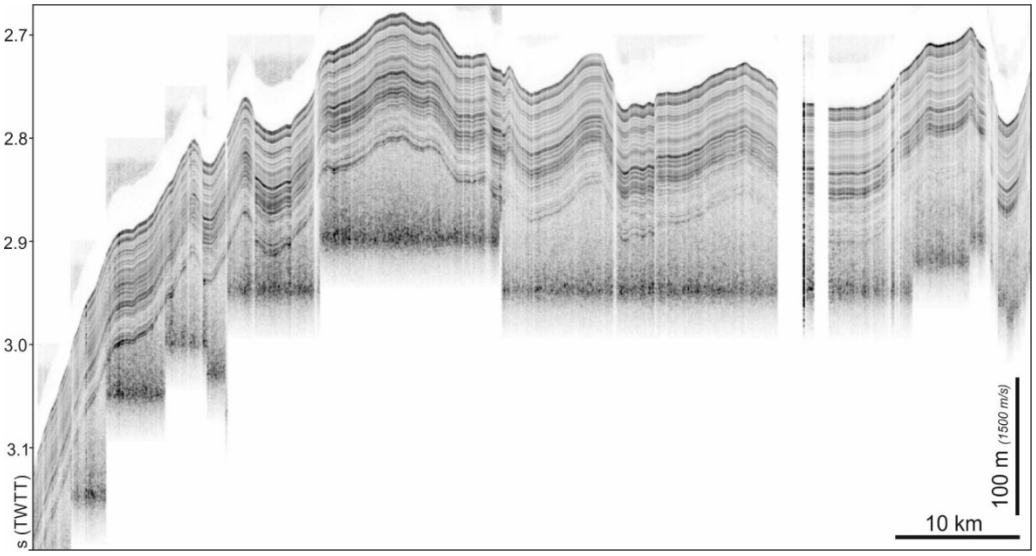

Figure 5.5 Example of stratified sediments over SE part of Alpha Ridge. SBP120 data were acquired in mostly open water conditions on 04 September 2016 and processed in SEGYJP2 software provided by Natural Resources Canada (NRCAN).

Data were logged in .raw and .seg format. In addition to real-time review of the SBP120 operator interface, .seg files were processed for sampling site selection and on a daily basis. The SEG-Y files were imported into the SEGYJP2 software package authored by Bob Courtney of Natural Resources Canada (NRCAN). This software package allows for some gain adjustments during conversion to JPEG2000 (JP2) format, and it allows lines to be combined (or segmented) for ease of interpretation. It also provides a JP2 viewing tool that offers further opportunities to enhance the image produced. The output of this process was then used for core site selection (by correlating these data with the bathymetric surface in Global Mapper) and initial depositional process interpretation.

There were a number of breaks in the acquisition mainly due to heavy ice conditions. Only minor problems were experienced with acquisition or post-processing routines during the cruise (see the Appendix for additional detail). In some cases, files crossing the dateline yielded a navigation error in the SEGYJP2 software when using the speed correction option; these files were reprocessed without speed correction.

Water column data processing

Water column data was acquired using the latest version (v1.8.3) of Simrad EK80 software. The EK80 was run in frequency-modulated (FM) mode with pulse lengths of 1-

8 msec, maximum power of 2000W, start frequency of 15 kHz, stop frequency of 30 kHz, and fast ramping. All pulse length and power setting changes are automatically logged with the data files and were noted in the electronic log kept by the watch standers. The EK80 was initially synchronized with the EM122 and SBP120 to avoid interference, but the total transmission cycles for these systems could extend to nearly 200 ms (depending on mode) and interfere with the EK80 record in the shallow region of interest (0-300 m for water layer stratification). Interference from the EM122 and SBP120 transmission pulses was effectively relocated to a deeper portion of the EK80 recording cycle by introducing a delay (200-500 ms, depending on water depth) to the EK80 transmission after receiving the ping trigger from the EM122. Preliminary processing on-board involved replaying files collected at CTD stations in EK80 software to verify file integrity and begin comparison to the CTD data (Fig.5.6).

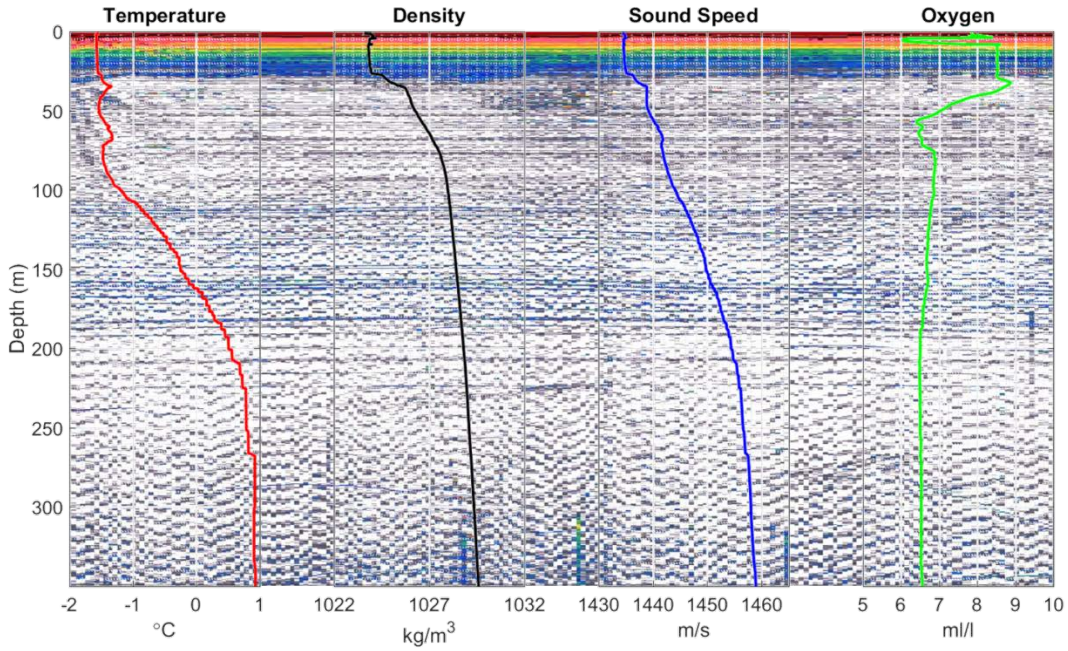

Figure 5.6 EK80 midwater backscattering data collected while drifting for a CTD station (background) with profiles of temperature, density, calculated sound speed, and oxygen measured on board the CTD. Approximately 180 pings over 30 minutes are presented as uncalibrated volumetric scattering strength (S_v) with 20*log(r) gain applied. The echogram color scale is from -77 dB (light blue) to -41 dB (dark red); samples with S_v below -77 dB are white. Additional post-processing will examine the capability to identify and possibly track stratified water layers using the high-resolution EK80 broadband water column acoustic backscatter.

EK80 target strength calibration

One of the primary advantages of the EK60/80 is that the system can be calibrated with a standard procedure to measure the sensitivity of the system throughout its beam pattern. This allows the measured backscatter strengths to be corrected for beam pattern effects, yielding absolute values of acoustic target strength for corroborating the apparent

stratified water layers observed in the EK80 realtime display with 'ground-truth' measurements at CTD stations.

5.7 Discussion and future analyses

Coverage of the Arctic Ocean

Oden's tracklines during Arctic Ocean 2016 were dictated primarily by the Canadian UNCLOS and SPRS priorities for mapping and sampling. The bathymetric and upper sediment structure surveys collected during this expedition were naturally focused on regions with sparse coverage, poor quality, or limited public availability of historical datasets and, thus, make a significant contribution to mapping efforts in the Arctic Ocean. Approximately 8728 line km of multibeam, subbottom, and midwater data were acquired from the departure and arrival at the 12-nm boundary around Svalbard, yielding approximately 28864 km^2 of bathymetric coverage by the Oden EM122 alone (based on a 50-m grid).

The bathymetric dataset includes transects on the Gakkel, Lomonosov, and Alpha Ridges. Transits between these structures were planned to take advantage of open water whenever possible, given the constraints of the expedition schedule and other desired stations (e.g., CTD and coring stations). Coring and dredging sites were mapped with additional scrutiny of subbottom data to assist target selection, and then remapped in extra detail while drifting during the sampling operation. In some cases, the seafloor backscatter amplitude was also of sufficient quality to improve interpretation of the sampling site.

UNCLOS

A more conventional survey plan was run with both the Oden and LSSL acting independently when possible, according to ice conditions, in a region of the Canada Basin important for UNCLOS purposes. Unfortunately, the Oden EM122 suffered from a roll artifact of unknown origin during this survey and these lines will require reprocessing (see Data Quality / Technical Challenges in the Appendix for more detail). A balance was struck on an ongoing basis between data quality and vessel speed through the ice, with expedition leaders providing guidance on time allotment for mapping high-priority sites. During the Oden's seismic operations in heavy ice, multibeam data quality was naturally second in priority to the safety of the seismic gear. Interpretation of the bathymetric surfaces and subbottom data will be carried out by the Canadian UNCLOS program in conjunction with analyses of the seismic profiles and sediment/rock samples.

Water column imaging and acoustical oceanography

Of primary interest for the water column imaging and acoustical oceanography components of the GM WP, the EK80 was run in a variety of modes at CTD stations to collect broadband water column backscatter in areas with water layer stratification. These layers of interest typically occur in the upper 300 m, as confirmed with preliminary processing at several stations during the expedition. The watch team monitored the records for evidence of scattering layers, plumes, gas seeps or other

midwater targets; unfortunately, noise from icebreaking obscured water column data in the real-time display for much of the expedition. This dataset, with the EM122 water column data, will receive much closer scrutiny during post-processing by shore-based GM WP participants.

The calibration process for the EK60/80 is not simple on a vessel the size and shape of Oden and depends heavily on finding suitable conditions; this was not completed during AO16 due to constraints of schedules, ice conditions, and sea states. Calibrations were carried out during the SWERUS-C3 Leg 2 and Petermann Glacier expeditions, providing some history of system response to the same calibration process; these calibrations will be considered for analyses of AO16 EK80 data.

Acoustic data quality

Multibeam, subbottom, and midwater data quality were generally very good in open water, but degraded rapidly when breaking ice, heading into a swell, or transiting at high speed. All acoustic mapping systems were severely affected during icebreaking through increased ambient noise and the effects of ice and bubbles along the transducer faces. These problems are not unique to Oden or the expedition but are described more fully, along with other technical issues, in the Appendix. As in previous years, the two most persistent issues were "punch-through" or over-penetration of beams near nadir and the appearance of "horns" (positive features that parallel the track on either side of the nadir beam) in flat regions of acoustically soft sediments; see the SWERUS-C3 Leg 2 cruise report for detailed examples. The highest quality bathymetry was collected while drifting for winch operations (core, dredge, CTD) with the vessel oriented along the drift direction to provide maximum acrosstrack coverage. The Oden is a remarkably agile vessel and, as in previous years, relied on pirouettes to achieve multibeam coverage over priority areas when ice conditions precluded normal mapping operations.

Photo: Åsa Lindgren

6. Work Package: Sediment coring & properties (SC)

Carina Johansson[1], Draupnir Einarsson[1], Markus Karasti[1], Luz María Mejía Ramirez[2], Grace Shephard[3], Steffen Wiers[4], Martin Jakobsson*[1], Matt O'Regan*[1]

[1] Department of Geological Sciences, Stockholm University, Sweden, [2] Geology Department, University of Oviedo, Spain, [3] Centre for Earth Evolution and Dynamics, University of Oslo, Norway, [4] Department of Earth Sciences, Uppsala University, Sweden, *shorebased

6.1 Summary

The main objective of the sediment coring program was to acquire undisturbed sediment sequences from ridge crests and basins for studies of paleoceanography, paleomagnetics, geochemistry and geology. In addition, outcropping pre-Quaternary sediments were targeted on the Alpha ridge to study the long term Cenozoic geologic and paleoceanographic history of the Arctic Ocean basin. A number of specific sites were planned in preparation for the cruise to meet these objectives. These included coring sites located at the foot of the Lomonosov Ridge to address water exchange history between the Amerasian and Eurasian basins and coring of sediments subjected to erosion of deep-drafting icebergs or ice shelves on the crests of Lomonosov Ridge crest and Marvin Spur, provided that erosion was identified by geophysical mapping. The proposed sites targeting pre-Quaternary outcrops were planned where Late Cretaceous age sediments previously have been cored during the drifting Fletcher's Ice Island, a.k.a. T3, experiment in the 1960s and 1970s and during the Canadian Expedition to Study the Alpha Ridge (CESAR) in early 1980s.

Time allocation for the coring operation and site selection had to fit in the Canadian UNCLOS survey program, which was the main focus of the expedition. In practice this meant that the proposed coring sites in the areas of the Lomonosov Ridge and Marvin Spur had to be abandoned. In the area of the Alpha Ridge, the proposed sites were out of reach due to tough ice conditions. Instead other sites were cored with apparently undisturbed sediment sequences on ridges and in basins. The coring objectives of the Lomonosov Ridge and Amundsen basin were generally met. However, evidence of outcropping pre-Quaternary sediments are so far not found in any of the retrieved cores, neither were ice-eroded areas on the ridge crests identified with the geophysical mapping. However, the coring program must be viewed as successful since several high-quality Alpha/Mendeleev Ridge and Makarov Basin cores were retrieved from previously largely unsampled areas of the Arctic Ocean.

In total, three gravity and eleven piston cores, including seven trigger weight cores, were retrieved at thirteen stations ranging in depth from 855 to 4367 m. At station fourteen, the piston core as well as the trigger weight core came up empty. For unknown reasons the corer had tilted 90^0 on the sea floor. The gravity/piston cores ranged from 3.45 to 10.58 m in length with an average of 3.53 m for the gravity cores and 7.86 m for the piston cores. The retrieved trigger weight cores averaged 1.90 m.

All cores except the smaller diameter trigger weight cores were logged on a multi sensor core logger (MSCL), after which most of them were split. One gravity core and three piston cores were left unopened. After splitting the cores into an archive half and a working half, the archive half was imaged with the MSCL line camera and used for measuring thermal properties. The working half was visually described and used for measuring shear strength. pH was measured in four split cores. All opened cores were sampled for IP25 biomarker analyses and these samples were immediately frozen. Five cores were sampled for paleomagnetics, two of which were also sampled for pore water immediately after coring, prior to logging. Surface sediments were subsampled for microplastics analysis in eleven cores and for mercury incubations in nine cores. In nine cores small subsamples were taken for analysis of mercury isotopes. For the observation of microfossils, smear slides were prepared for most of the cores. In-situ temperature was measured with small temperature probes attached to the core barrel, in all stations except number ten.

After completion of measurements and subsampling, the core halves were wrapped in plastic and placed in plastic rectangular tubes. The cores were then stored at 4°C in a refrigerated container for the rest of the expedition.

6.2 Field sites

Thirteen sites across the central Arctic Ocean were successfully cored. At site fourteen no sediment was recovered. The locations are shown on maps in Fig. 6.1 a & b. Coordinates and depths are given in Table 6.1.

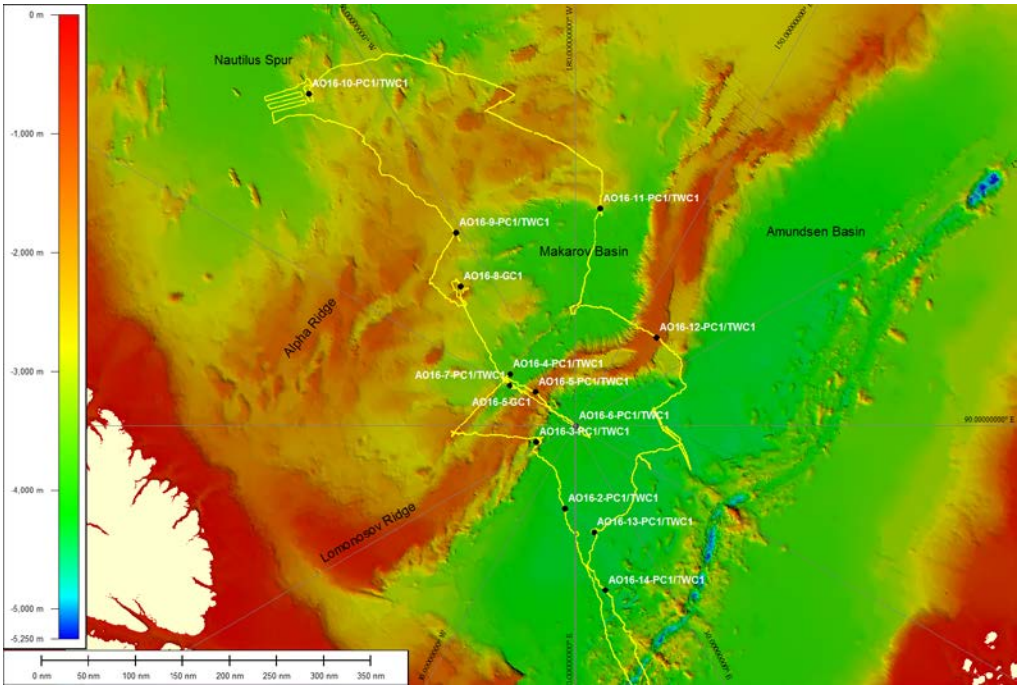

Figure 6.1 a Locations of coring stations AO16-2 to AO16-14 with ship track in yellow.

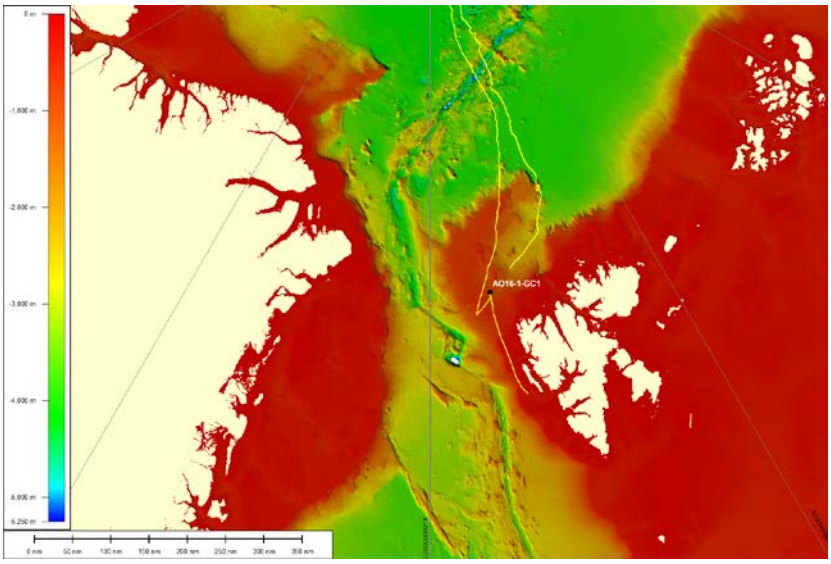

Figure 6.1 b Location of coring station AO16-1 with ship track in yellow.

Table 6.1 Summary of sediment cores retrieved during Arctic Ocean 2016.

Coring Station	Core ID	Latitude (aft deck)	Longitude (aft deck)	WD (m)	Sed. length (m)	Date (UTC)	Time (UTC)
AO16-1	AO16-1-GC1	80.5532	8.0520	855	3.55	160810	19:15
AO16-2	AO16-2-PC1	88.5022	-6.6195	4353	9.45	160815	4:16
AO16-2	AO16-2-TWC1	88.5022	-6.6195	4353	no recovery	160815	4:16
AO16-3	AO16-3-PC1	89.2530	-66.6097	3777	7.74	160817	3:52
AO16-3	AO16-3-TWC1	89.2530	-66.6097	3777	2.85	160817	3:52
AO16-4	AO16-4-PC1	88.5290	-128.5048	3936	7.83	160820	13:09
AO16-4	AO16-4-TWC1	88.5290	-128.5048	3936	2.45	160820	13:09
AO16-5	AO16-5-PC1	89.0780	-130.5470	1253	6.16	160820	22:43
AO16-5	AO16-5-TWC1	89.0780	-130.5470	1253	1.29	160820	22:43
AO16-5	AO16-5-GC1	89.0813	-130.6800	1249	3.45	160820	23:55
AO16-6	AO16-6-PC1	89.9777	71.3810	4233	7.83	160821	17:36
AO16-6	AO16-6-TWC1	89.9777	71.3810	4233	no recovery	160821	17:36
AO16-7	AO16-7-PC1	88.6332	-121.4477	3941	8.31	160824	1:43
AO16-7	AO16-7-TWC1	88.6332	-121.4477	3941	no recovery	160824	1:43
AO16-8	AO16-8-GC1	86.7795	-140.6433	2620	3.59	160826	14:52
AO16-9	AO16-9-PC1	85.9557	-148.3258	2212	7.52	160829	12:36
AO16-9	AO16-9-TWC1	85.9557	-148.3258	2212	1.75	160829	12:36
AO16-10	AO16-10-PC1	82.3980	-141.2450	2872	7.96	160902	15:38
AO16-10	AO16-10-TWC1	82.3980	-141.2450	2872	1.49	160902	15:38
AO16-11	AO16-11-PC1	86.0993	173.1877	3066	7.98	160905	15:34
AO16-11	AO16-11-TWC1	86.0993	173.1877	3066	1.40	160905	15:34
AO16-12	AO16-12-PC1	87.8577	136.9875	1269	5.19	160907	10:26
AO16-12	AO16-12-TWC1	87.8577	136.9875	1269	2.10	160907	10:26
AO16-13	AO16-13-PC1	88.0573	10.1850	4367	10.58	160911	17:44
AO16-13	AO16-13-TWC1	88.0573	10.1850	4367	no recovery	160911	17:44
AO16-14	AO16-14-PC1	86.9982	10.4878	4334	no recovery	160912	11:17
AO16-14	AO16-14-TWC1	86.9982	10.4878	4334	no recovery	160912	11:17

Coordinates, depth and time on bottom were recorded on the aft deck when slackening of the coring winch wire was observed. Coordinates were recorded in degrees and minutes and later converted to decimal degrees, as presented in Table 10. Geographic positions are given with reference to the vertical datum WGS84. Times for sampling stations are provided in UTC.

6.3 Background

General scientific objectives of the Arctic Ocean 2016 expedition were to collect undisturbed sediment records for paleoceanographic studies, sample outcrops for studies of the long term Cenozoic history of the Arctic Ocean, and to collect new heat flow data.

A key paleoceanographic objective was to collect one or more cores from the Lomonosov Ridge to:

- sample for sea ice and productivity proxies (e.g., IP25, microfossils, carbon and oxygen isotopes) to reconstruct history of Arctic sea ice and its impact on other environmental factors. Samples for IP25 and other biomarkers require immediate sampling and freezing.
- perform paleomagnetic studies in order to improve our understanding paleomagnetic variations in Arctic Ocean sediments with the ultimate goal of constraining existing age models. The paleomagnetic program included pore water sampling to investigate ongoing diagenetic processes.
- look for sediment sequences with good carbonate preservation permitting the use of paleoceanographic proxies based on analyses of microfossils with calcium carbonate shells.

Heat flow data are generally sparse in the Arctic and of particular interest was to collect new data from the Amundsen Basin and the Lomonosov ridge west of the North Pole, to fill in prominent data gaps.

In cooperation with the Heavy Metals Work Package a specific objective was to subsample geographically spaced surface sediments for studies of microbially mediated transformations of mercury species and also analysis of plastic microfibers.

6.4 Methods – sampling, observations and shipboard analyses

The Stockholm University piston/gravity coring system was used during the AO16 expedition. This system is capable of taking up to 12 m long sediment cores from the aft deck of IB Oden. The corer itself can be rigged to take longer cores, but because this device is operated across Oden's fantail, the limited space between the winch container placed on the aft deck and the fantail limits the length of the corer that can be deployed. The corer was recently upgraded in preparation for the SWERUS C3 2014 expedition. This recent upgrade makes it possible to switch between two different dimensions of the core barrel/liner system. The change between dimensions requires changing core barrel, couplings, liner, core cutter, core catcher and piston. In addition, the piston stop was redesigned as a part of the upgrade so it could be loosened in order to make it possible to push out the core liner using a metal rod. This feature makes the retrieval of sediment filled liners after each coring much easier. A new method of having threaded liners that

can be pulled out works very well and saves time. Previously, the liners were taped together and the joints got stuck in the barrels when sediments got between the barrel and liner.

The core head, wire, weights and the release mechanism remains the same between the two setups. The original liner dimension has an inner/outer diameter of 80/88 mm while the new wider diameter setup takes a liner dimension with an inner/outer diameter of 100/110 mm. Transparent polycarbonate liners were brought for the smaller diameter while standard dimension PVC pipes were used for the larger during the AO16 expedition. The core head can be loaded with lead weights of up to 1360 kg. The standard release arm is designed so that a trigger weight of 1/10 of the main core head weight is recommended. Hydrostatic safety releases are used to secure the release arm from triggering prematurely. However, in waters shallower than 300 meters a safety pin that is pulled just before the corer is lowered below the water surface is used.

One complete piston corer and one complete gravity corer were brought on IB Oden for the AO16 expedition and two setups of the “old” smaller diameter version as reserve. The piston/gravity coring equipment was stored in a specially made 20’ container placed on the aft deck next to the launching cradle described below (Fig 6.2). Liners were stored in other storage places on IB Oden. The piston corer in its launching cradle is seen in Fig. 6.3. This support “cradle” was built 1996. A rail that launches the cradle was constructed and manufactured for the Lomonosov Ridge of Greenland (LOMROG) expedition 2007 to improve the safety of the coring procedure. The cradle with the corer is moving along the rail on nylon wheels. When the cradle reaches the end of the fantail it pivots and places the corer in a vertical position ready to be launched. The trigger weight corer is always launched before the cradle is brought to the position where it pivots. When the corer is in upright position it is lifted out of the cradle with a wire from the main coring winch that runs through a block in the A-frame. Fig. 6.4 A-F shows the different steps to launch the corer.

In addition to the main coring winch, a small winch is required to launch and recover the corer (Fig. 6.5 a & b). The cradle is usually pushed out until it reaches the slope, then it is lowered to the end of the rails where the corer is pivoted using the main winch.

The main winch is a NorthSea winch placed at the end of the rails on the aft deck of IB Oden. It is built into its own special container and has 6 km of Dyneema synthetic rope. An important component of the coring operations is a reader for the length of wire out and registration of pull out force. A remote display provided these parameters from the NorthSea winch (Fig. 6.6).

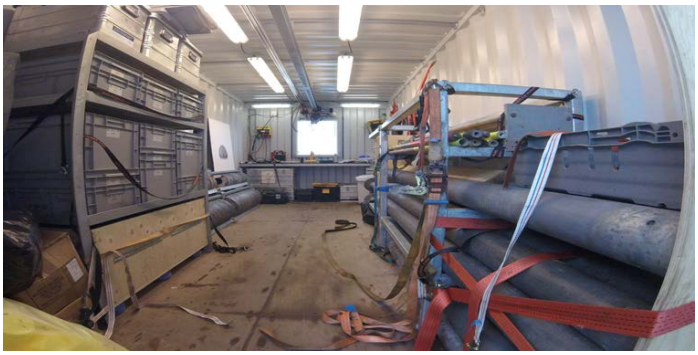

Figure 6.2 Container with the piston/gravity corer stored. Four complete setups were stored in this 20' container. The liners were made in 6.1 m lengths to fit a multiple of 3 m, which is the length of each core barrel. This made the liners slightly too long to fit in a 20' container. The extra 10 cm are for the threads.

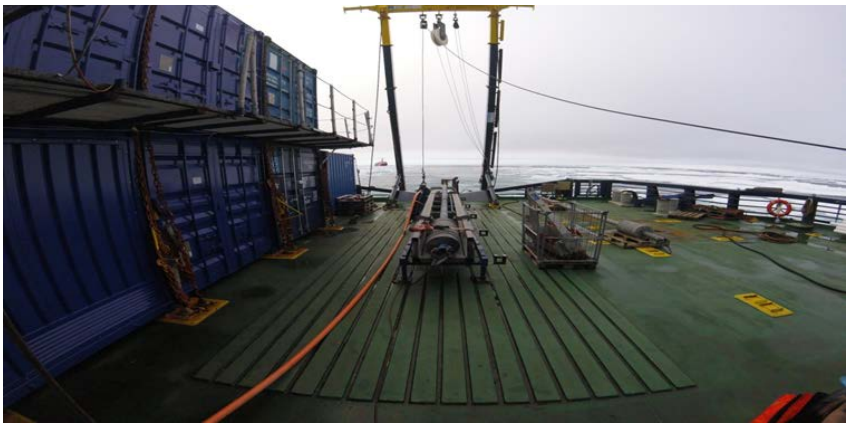

Figure 6.3 Stockholm University large diameter piston corer (center) resting in the deployment cradle. This large diameter corer can also be rigged as a gravity corer, seen to the right on deck. The standard setup during the AO16 cruise was to have both a gravity corer and a piston corer rigged and ready for deployment.

Individual sediment cores are identified using the expedition label Arctic Ocean 2016. This is shortened to AO16 on core and sample labels. The next identifiers are the station number, the type of coring device used, and the number of cores taken at a single station using a specific coring device. Three coring devices were used during AO16, namely Gravity Corer (GC), Piston Corer (PC) and accompanying Trigger Weight Corer (TWC). For example, a single piston core is taken at coring station number eight (8). Its unique identification, or Core ID, hence is: AO16-8-PC1. This translates into Expedition-Station number-Coring device (piston corer in this example). The number 1 after PC (PC1) implies that this was piston core #1 taken at station 8. The trigger weight core that is taken together with this piston core at station 8 is labeled AO16-8-TWC1. If a second piston core would be taken at station 8, this would be labeled AO16-8-PC2, and its trigger weight core AO16-8-TWC2.

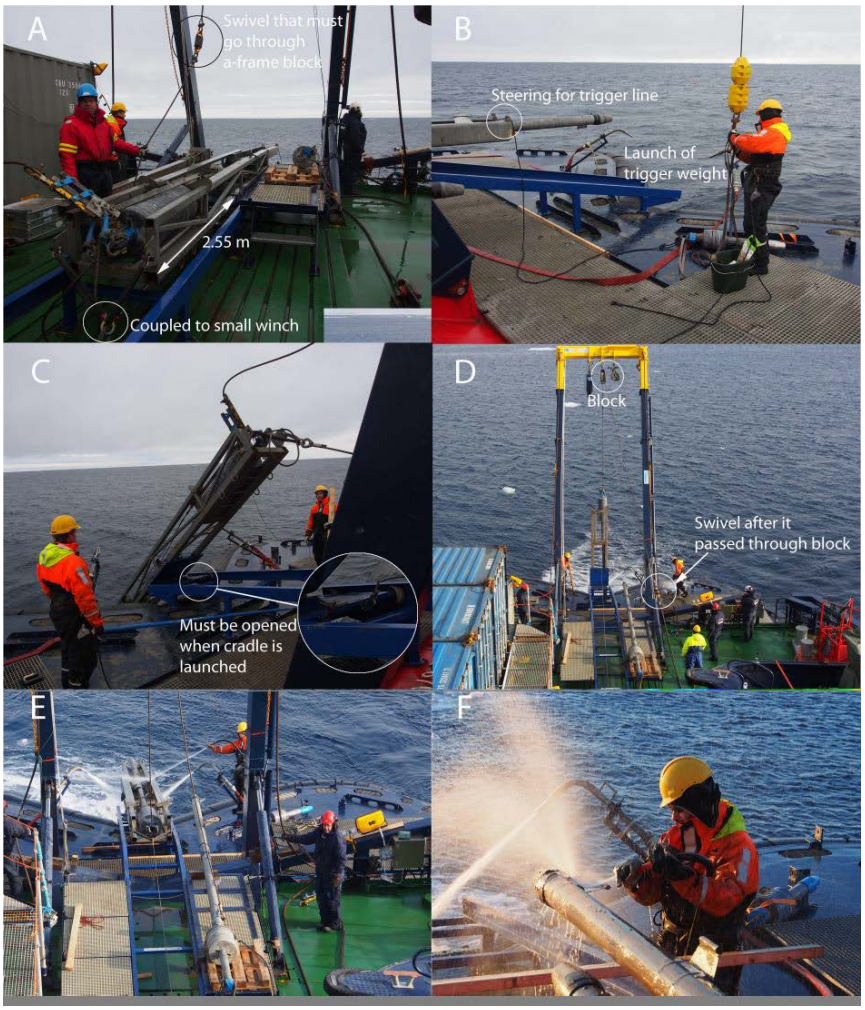

Figure 6.4 A-F shows the main steps of launch and recovery of the piston corer. A) The piston corer fully rigged to be launched using the cradle. The cradle was manually pushed until it reaches the slope of the rails, the winch prevents it from going full speed and since the trigger corer is launched first it assists in dragging out the cradle. The cradle is then pivoted with assistance of the main winch. The balance of the cradle should be adjusted for a soft pivoting. During AO16 the balance was set for maximum weight and optimal for both 9 m and 12 m launches to allow for quicker changes between lengths. The cradle is left in that setting for future expeditions. B) Launch of the trigger weight corer. This is done before the cradle is pushed to the pivot position. A separate lifting rope is used that can be pulled away from the trigger weight corer before launch. Keep in mind to have the winch connected to the cradle before the trigger corer is launched. C) The cradle during pivoting. Note the two screws that must be loosened before the cradle is pushed out to pivot. The screws are only tightened during transit to stabilize the cradle. D) The corer on its way to be docked in the cradle after a core has been taken. Note that the release wire now is longer, which requires that the connection between piston wire and main winch Dyneema must be pulled through the block to lift the corer. No swivel is needed when Dyneema rope is used. E) The corer is pulled up on deck using the small winch shown in Fig. 6.5 b F) The sediment filled liners are retrieved on the fantail of IB Oden. (Image sequence if from SWERUS-C3 Leg 2 cruise report)

Figure 6.5a Small winch mounted in the NorthSea main winch container used to maneuver the cradle.

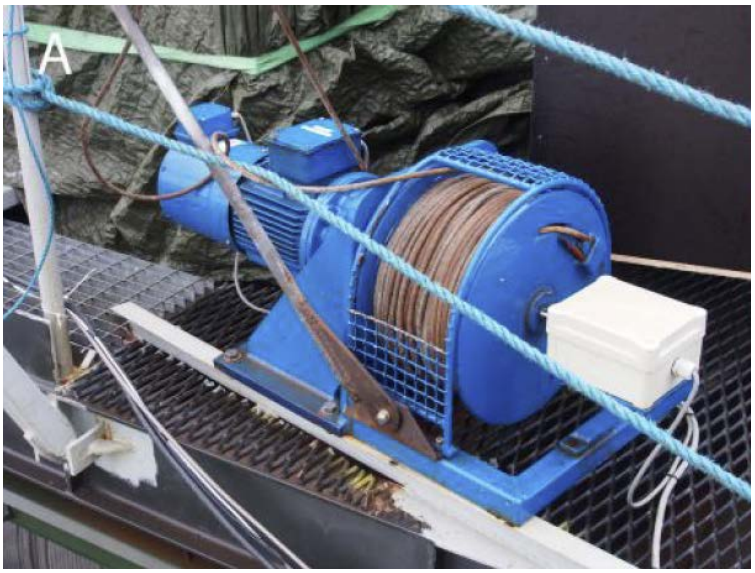

Figure 6.5b Coring winch manufactured by NorthSea.

Retrieved gravity and piston cores are extruded from the base of the corer, that is, from the maximum depth of penetration in the sediment column. The nose cone is often empty but sometimes comes up filled with mud. It holds the Core Catcher (metal finger device) with the core catcher sample, and when mud fills the entire nose cone below this is referred to as the Core Cutter sample, labeled CC. The extruded core liners with their content of sediments are cut into 150 cm long sections. The base of the first section extruded from the corer is labeled A and its top B, the next section C (base) and D (top), etc. Also, all sections are marked with arrows pointing towards the top. Sections are subsequently labeled 1, 2, etc., starting with Section 1 at the top of the core (Fig.6.7), normally at the water-sediment interface.

Figure 6.6 Remote display showing load and wire out of the NorthSea winch.

A full curatorial identifier for a sample consists of the Core ID with the addition of section number and centimeter depth from the top of the section. A sample taken 75-77 cm from the top of Section 4 of the piston core at station 8 (see example above) is labeled: AO16-8-PC1-4, 75-77 cm. This Sample ID is easily converted to absolute core depth with knowledge of the lengths of sections 1, 2 and 3. If sections 1, 2 and 3 each are 150 cm long, the sample is located 525-527 cm (150+150+150+75/77) below the top of the core.

Samples for paleomagnetics were numbered continuously and core, section and total depth were noted on a separate list accordingly. For example, sample 320 was taken from AO16-2-PC1, 101.5-103.5 cm.

When extruding the sediment filled liners from the core barrel after coring, they were cut in 1.5 m long core sections and sealed with end caps fixed with electrical tape. The markings on the pre-labeled liners (A, B, C, etc and arrows pointing towards the top) were checked and filled in when necessary. The core sections were carried to the main lab of Oden where they were stored vertically before being logged on the multi sensor core logger (MSCL). An exception was the two cores from which pore water was extracted. Immediately after coring pore water extraction was started in the lab, prior to logging. Core catcher samples were put in plastic bags and core cutter samples (from the nose cone below the core catcher) were transferred to pre-cut liners. The port side room of

Oden's main laboratory was dedicated to geology, including visual core description, sampling and sediment physical properties analysis. When core sections had acquired room temperature (after several hours or the next day) they were logged on the MSCL. After being logged, the cores were split and divided into an archive half and a working half. To keep the same orientation of archive and working halves in all sections of a core,

they were always split along a line drawn before coring. Placing the sections horizontally, with the line facing you and the bottom to the left and top to the right, the upper half was marked “work” and the lower “archive”. It was also checked that both halves were properly labeled. A separate core splitting facility was placed outside the main laboratory in a weather protected tent.

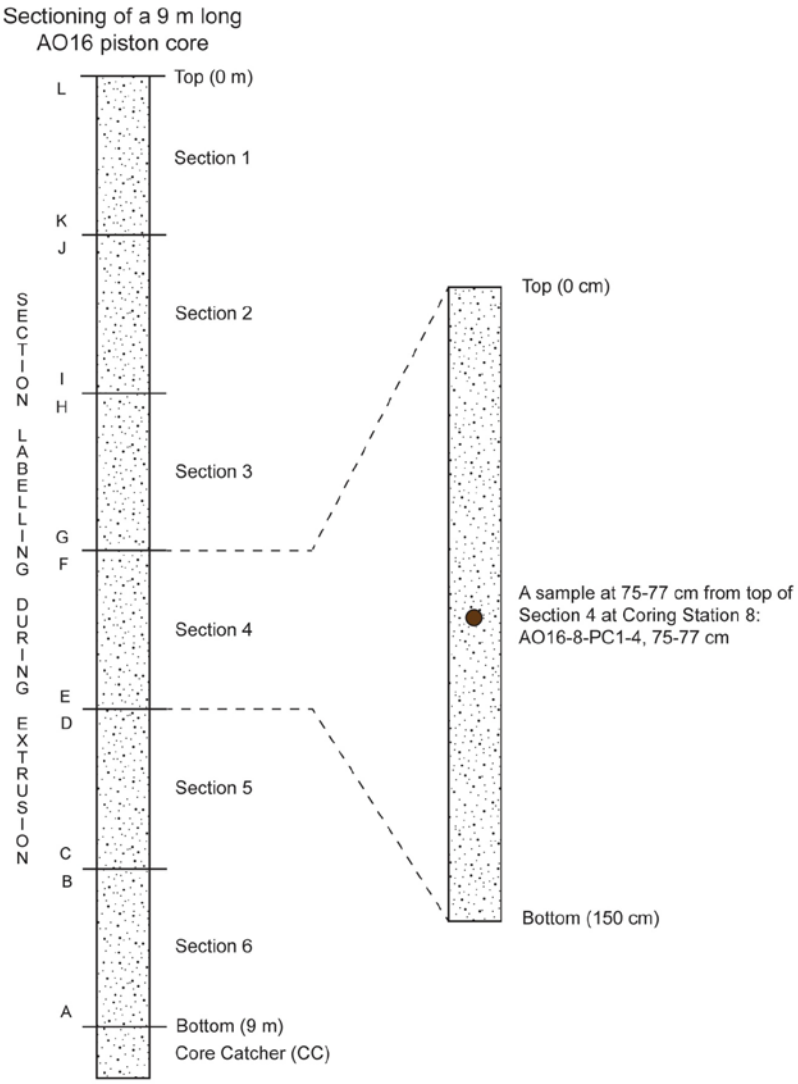

Figure 6.7 Section labeling (left) of a 9 m long piston core. Labeling (right) of a 2 cm thick stratigraphic sample taken 75-77 cm below the top of Section 4 at Coring Station 8: AO16-8-PC1-4, 75-77 cm.

After splitting, both halves were scraped to remove potentially disturbed/moved sediment and create an even surface. The archive half was subsequently imaged with a line scan camera on the multi sensor core logger and used for measurements of thermal properties. The working half was marked with centimeter tape on the liner and described with respect to lithostratigraphic properties. Following description, the working halves were used for shear strength measurements and in a few cores also measurements of sediment pH. When measurements were finished, sub-sampling of the working halves

commenced. Selected cores were sampled for mercury isotopes, mercury incubations and microplastics. Five cores were sampled for paleo- and rockmagnetic measurements before any other samples were taken, to minimize sediment disturbance. Smear-slides were prepared for microfossil assessment of most of the cores. All opened cores were lastly sampled for IP25 biomarkers. After sampling, gaps in the sediment were filled with pieces of foam.

The archive and working halves were wrapped in plastic, placed in labeled rectangular tubes and stored in a refrigerated (+4°C) container on top of the main lab (Fig. 6.8). Whole, unsplit cores were stored horizontally in the same container, as well as core catchers and core cutters not fit to go into liners.

Samples for paleomagnetics and mercury isotopes were stored in the refrigerated container, while samples for mercury incubations and microplastics were taken care of by the Heavy metals WP team. Samples for IP25 biomarkers were for practical reasons stored in a -80°C freezer in the main lab, though a -18°C freezer would have been sufficient.

Figure 6.8 Refrigerated container with stored split and unsplit cores.

The measurement program for shipboard analyses of sediment physical properties was designed to:

1) Provide a basis for making initial stratigraphic interpretations, inter-core correlation and facilitate post-cruise subsampling planning.

2) Collect data on the shear strength at the time of core opening.

3) Collect in-situ temperature, and laboratory measurements of sediment thermal properties, to determine the heat flow at coring sites.

Unsplit sediment cores in PVC liners were logged on the Multi-Sensor Core Logger (MSCL) to obtain measurements of the bulk density, compressional wave velocity and magnetic susceptibility. After opening, the cores were scanned on the MSCL to provide high-resolution digital images.

Shear strength measurements were performed with a hand-held shear vane on most of the split cores. The measurements were made on the working halves of the cores. The sediment thermal properties (thermal conductivity, diffusivity and specific heat capacity) were measured on the archive halves.

In-situ temperature measurements at most coring sites were obtained using miniature temperature probes attached to either the gravity or piston core barrels. Combined with the sediment thermal properties, these measurements will be used to determine heat flow at the coring sites, and investigate the subsurface thermal regime.

Two Star Oddi DST magnetic sensors were attached just below the weight of to either the gravity or piston core barrels. The sensors measured depth, temperature, 3-axis tilt, compass heading, magnetic inclination and magnetic field strength. These measurements will be used to 1) compensate heat flow measurements with a possible tilt and 2) get an absolute orientation of the core from the recorded compass heading.

A summary of all the shipboard physical property measurements conducted during the cruise is presented in Table 6.2.

The chemical properties program on board included pore water sampling using hydrophilic Rhizon samplers on two cores and measurements of sediment pH in the working halves of four cores.

Equipment

The Geotek Multi-Sensor Core Logger (MSCL) from Stockholm University was set-up in the main lab on the foredeck of the Oden (Fig. 6.9). Sensors were oriented in the horizontal direction for whole-core logging. Measurements of the gamma ray derived bulk density, compressional wave velocity (p-wave) and magnetic susceptibility were acquired at a down core resolution of 1 cm. Gamma-ray attenuation was measured using a 137Cs source with a 5 mm collimator and a 5 s count time.

Table 6.2 Physical property and pH measurements performed on cores from AO 2016.

Core ID	Opened	MSCL	Imaging	Shear Vane	Thermal prop.	In-Situ Temp.	pH
AO16-1-GC1	x	x	x	x	x	x	
AO16-2-PC1	x	x	x	x	x	x	
AO16-3-PC1	x	x	x	x	x	x	
AO16-3-TWC1	x						
AO16-4-PC1		x				x	
AO16-4-TWC1	x						
AO16-5-PC1	x	x	x		x	x	x
AO16-5-TWC1	x						
AO16-5-GC1		x				x	
AO16-6-PC1		x				x	
AO16-7-PC1	x	x	x	x	x	x	
AO16-8-GC1	x	x	x	x	x	x	x
AO16-9-PC1	x	x	x		x	x	
AO16-9-TWC1	x						
AO16-10-PC1	x	x	x	x			x
AO16-10-TWC1	x						
AO16-11-PC1	x	x	x	x		x	
AO16-11-TWC1	x						
AO16-12-PC1	x	x	x	x	x	x	x
AO16-12-TWC1	x						
AO16-13-PC1		x				x	

Calibration of the system was done on each day before a core was logged using a machined piece of aluminum that was fit within a section of core liner. The aluminum calibration piece has 5 different thicknesses of aluminum with diameters of 1.8, 2.8, 3.8, 4.8, and 5.8 cm. The liner was then filled with distilled water from the Milli-Q system, and left to equilibrate with room temperature (≈17° C). The liner was then sealed with silicon to prevent the loss of water. For calibration, the liner was placed in front of the 137Cs source. The number of gamma rays passing through each section over a course of 30 s with 5 repetitions, as well as through an interval containing only water, was logged. The relationship between the measured counts per s [ln(cps)] and the known bulk density of the aluminum/water mixture at each step was determined using a 2nd order polynomial. Throughout the expedition the gamma ray source was left open, with the calibration piece used to shield the gamma ray detector from excess radiation while not in use.

Compressional (p-wave) velocity measurements were made on the MSCL by a pair of automated spring loaded rolling transducers. The travel time of the p-wave between the send and receive transducer is logged. Conversion of the travel time into a p-wave velocity requires calibration to account for delays introduced by the electronic circuitry and those associated with the passage of the p-wave through the liner. Calibration was performed by measuring the travel time through the interval of the calibration liner

containing only water at a known temperature. The temperature and thickness of the water is used to calculate a theoretical travel time (TT) through the water inside the core liner. The difference between the logged total travel time (TOT) and theoretical travel time (TT) is the offset time (PTO). A gate of 50 µs and a delay of 75 µs was initially set but later changed to 90 µs gate and 30 µs delay. A digital oscilloscope was run during all core logging to monitor the strength of the p-wave signal and to ensure that it arrived within the defined gate interval. Occasionally, distilled water was sprayed on the outside of the core liner to improve the acoustic coupling between the sensors and the core.

Magnetic susceptibility was acquired with a 125 mm Bartington loop sensor using a 1 s acquisition time. This provided a spatially integrated susceptibility signal that encompasses the entire diameter of the core, with an effective sensor length of generally 4-6 cm. No mass or volume corrections were made to the magnetic susceptibility measurements.

During logging, small variations in core thickness were also measured and logged using the displacement transducers attached to the p-wave housings. Variations in core thickness, usually more pronounced at the taped and capped core ends, were automatically incorporated into the processed calibrated measurements of p-wave velocity and bulk density.

The Undrained Shear Strength (SU) of the sediments was measured using a CONTROLS-group pocket shear vane device. Shear strength was tested at a downcore resolution of approximately 30 cm. For most measurements the big adapter (16-T175/1) for measurements between 0 and 2 N/cm^2 was used, but it some instances the medium adapter for measurements between 0.2 and 10 N/cm^2 was used. No correction was applied to the measured shear strength to account for variations in the liquid limit of sediments.

In-situ temperature measurements were obtained using ANTARES miniature temperature probes attached to the outside of the gravity or piston core barrel. Each stainless steel temperature logger is 16 cm long and 1.5 cm in diameter. They have an operational range of -5 to 50 °C, max 100 MPa, and a resolution of 0.001 °C.

The probes were inserted into stainless steel fins attached to the core barrels using large diameter hose clamps (126-147 mm). The fins protected the temperature probes and kept them 10 cm away from the core barrel. This offset distance reduced the effects of frictional heating from the core barrel as it entered into the sediments.

The probes were programmed and downloaded in the main lab before and after each deployment. A 1-s sampling interval was used for all deployments. Between 3 and 6 temperature probes were used on each deployment to ensure that the thermal gradient in the sediments could be resolved. Spacing was usually between 0.75 and 2 m, but the distance varied slightly between deployments. Details of sensor spacing are found on the individual logs sheets for each deployment. During the temperature measurements, the core barrel was left in the sediments for anywhere between 1.5 to 5 minutes. The amount

of time depended on the water depth and drift speed of the ship, which in some circumstances was >1 knot.

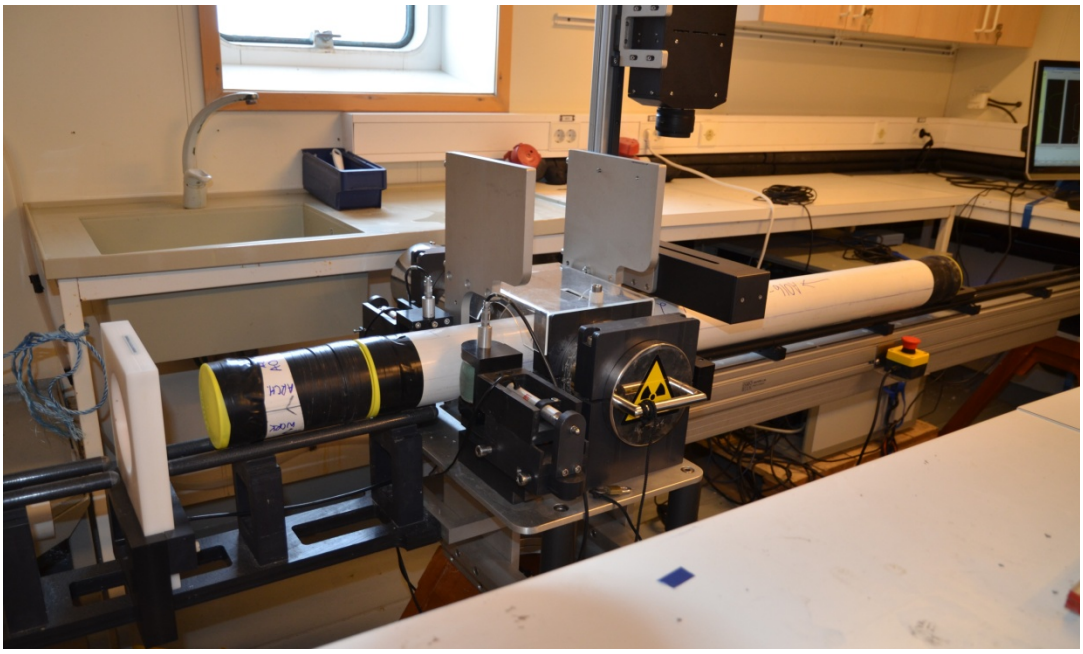

Figure 6.9 The Geotek Multi-Sensor Core Logger (MSCL) in the main lab of Oden.

To monitor the angle of the core barrel and its orientation towards north while embedded in the sediments, two Star Oddi DST magnetic orientation sensors were used. The sensors record the temperature, pressure (depth), ambient magnetic field strength, tilt (in 3 directions), and the azimuth. The DST magnetic was programmed and downloaded in the main lab. A 1 s sampling time was used throughout the expedition. These sensors were attached to the core barrels using hose clamps. They were strapped to the barrels below the weights on the gravity cores and piston core. Since the tilt measurements perform best when the sensor is orientated vertically, whereas the measurements of the ambient magnetic field (intensity and direction) perform best in a horizontal position, one sensor was attached vertically and the other horizontally.

The thermal properties of sediments were measured using a TPS 500 thermal constants analyzer, manufactured by K-analysis in Uppsala, Sweden. The TPS 500 measures the thermal conductivity, thermal diffusivity and specific heat capacity. The HotDisk TPS 500 sensors are made from a thin nickel double spiral that is electrically insulated by two layers of Kapton (polymide). The sensors are mechanically stable and suitable for both transient heating and precise temperature readings. The Kapton material allows isotropic, anisotropic, slab, one-dimensional and structural probe measurements across a large temperature range (from -196 °C up to 300 °C). The measurement range of the HotDisk TPS 500 is 0.03 to 100 W/mK for thermal conductivity, 0.02 to 40 mm^2/s for thermal diffusivity and 0.10 to 4.5 MJ/m^3K for specific heat capacity measurements.

The TPS 500 can be used for 1-sided or 2-sided measurements of sediment thermal properties. During a typical 2-sided test, the sensor is placed between the surfaces of two

pieces of sample. A current passes through the Nickel spiral and creates an increase in temperature. The heat generated dissipates through the sample on either side at a rate dependent on the thermal transport characteristics of the material. By recording the temperature versus time response in the sensor, the samples thermal characteristics are calculated. For shipboard measurements, the 1-sided measurement technique was used, where the sensor was placed on the surface of a split core, and a piece of styrofoam (expanded polystyrene (EPS) form) was used as a backing material. EPS has thermal conductivity values typically ranging from 0.032 to 0.038 W/mK, but it can depend on the density of the EPS itself (the higher the density, the lower the value of the thermal conductivity). The thermal properties of the styrofoam were determined using a 2-sided test at the beginning of the cruise and were 0.0387 W/mK, 0.9017 mm^2/s and 0.0430 MJ/m^3K for thermal conductivity, thermal diffusivity and specific heat capacity, respectively.

A 5 cm diameter, 2 cm tall and 100 g weight was placed on top of the Styrofoam to ensure that the sensor was pressed into the sediment surface and remained in place during the measurement period. Measurements were usually conducted using an 80 s heating period with power of 0.5 watts and repeated at least once.

Sampling of pore water was carried out via rhizon sampling. Rhizon samplers are small hydrophilic polymer tubes which can be used to extract filtered (<0.18 µm) pore water from sediment. The rhizons are inserted into the cores by drilling 3 mm holes in the liner and pushing the tubes into the sediment. The rhizons are then attached to syringes by flexible hoses and pulled to create negative pressure which generally causes water to flow <10 mL/h (Fig. 6.10). Due to the slow rate of collection the syringes are propped open with spacers and allowed to sit up to 12 hours.

The goal of the pore water sampling is to establish the boundaries of current diagenetic zones in arctic sediments. The sample aliquot was set aside for metals and sulfur analysis. These measurements will be performed at Stockholm University following the expedition. Metals of interest include but are not limited to: Mn, Fe, Si and S. These analytes are heavily involved in bacterial mediated reactions as well as precipitation/dissolution reactions with the solid phase sediment. Sulfur, as sulfate (SO_4^{2-}), is one of the primary electron acceptors in the oxidation of organic matter in the sediment. Immediately following pore water extraction, 3 mL were placed in acid washed cryovials for metals and sulfur analyses. The vials were acid washed prior to the expedition. After sampling, 30 µL of ultrapure HNO^3 preservative were pipetted into the cryovials. The vials were placed in refrigerated boxes until the end of the expedition.

pH was measured using two Mettler Toledo SevenGo pro pH meters with InLab Solids Pro IP67 electrodes, intended for measurements in semi-solid materials. Calibration was done using Mettler Toledo buffer solutions (pH 4.01, 7.00 and 9.21) before measurements started. The electrodes were pushed about 2.5 cm into the sediments (the length of the lower, narrow part of the electrode) and were left to equilibrate several minutes until the reading was stable and the pH and temperature of the sediment was recorded (Fig. 6.11). All measurements of individual cores were finished within the same day.

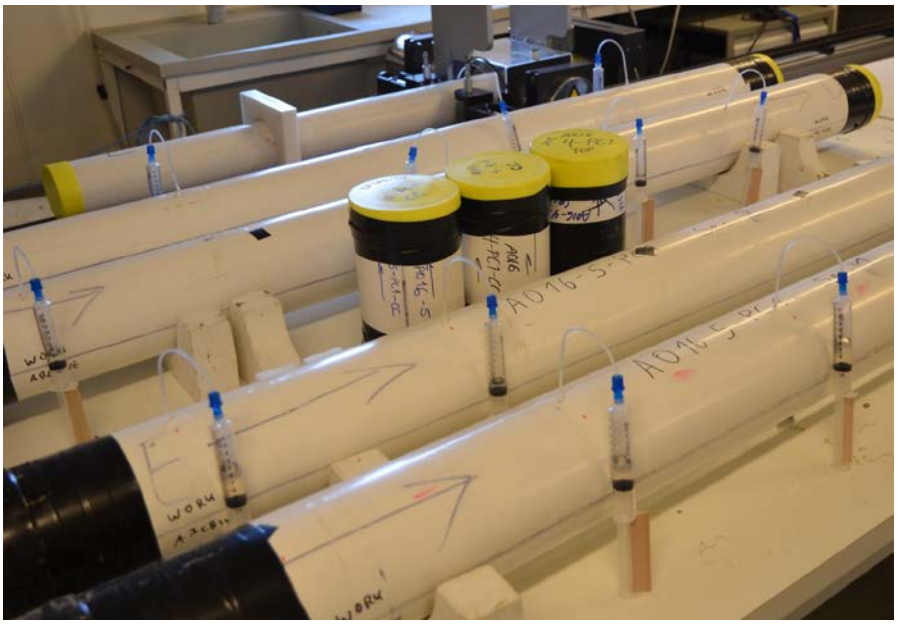

Figure 6.10 Pore water sampling in the piston core from station 5.

Figure 6.11 Measurements of sediment pH.

6.5 Research activities and preliminary results

An overview of all retrieved sediment cores is presented in Table 6.1 (under the heading Field sites). The table shows station number, core identification, latitude and longitude in decimal degrees, water depth, core length, date and time of retrieval. Detailed information about each individual sediment core is summarized in Appendix SC-1. Appendix SC-2 contains sub-bottom profiles for all core sites, and appendix SC-3 multibeam sonar generated maps of the sites.

Three gravity cores, all rigged for 6 m, were retrieved from stations 1, 5 and 8. They ranged in length from 3.45 to 3.59 m, with an average recovery of 59 %. Eleven piston cores were successfully taken, but in station 14 the corer came up empty for unknown reasons. In stations 2 and 13 they were rigged for 12 m, yielding a recovery of 79 and 88 %, respectively. The piston cores from stations 3, 4, 5, 6, 7, 9, 10, 11 and 12 were all rigged for 9 m, ranging between 5.19 m to 8.31 m, with an average recovery of 82 %. The trigger weight cores were all rigged for 3 m. In five stations there was no recovery (2, 6, 7, 13 and 14), only explained in station 2 by a technical mistake. In the other seven stations the trigger weight cores ranged in length from 1.29 m to 2.85 m, with an average recovery of 63 %. Coring details are found in the deck sheets in Appendix SC-1.

During the expedition all gravity and piston cores were logged on the high-resolution MSCL (Appendix-SC-4). The physical properties measurements were used for initial correlation of sediment cores and the first identification of prominent sedimentary boundaries (Fig. 6.12 & 6.13). Cores retrieved in the Amundsen Basin, on the crest of the Lomonosov Ridge and at the foot of Marvin Spur seem all reach at least as far back in time as MIS 6. This interpretation is based on the identification of a high density diamict as been deposited and identified in other cores from this area during MIS 6. The interpretation of cores retrieved from the Alpha Ridge is somewhat more challenging and a comparison with other cores from this region has to be done before a more detailed analysis can be performed.

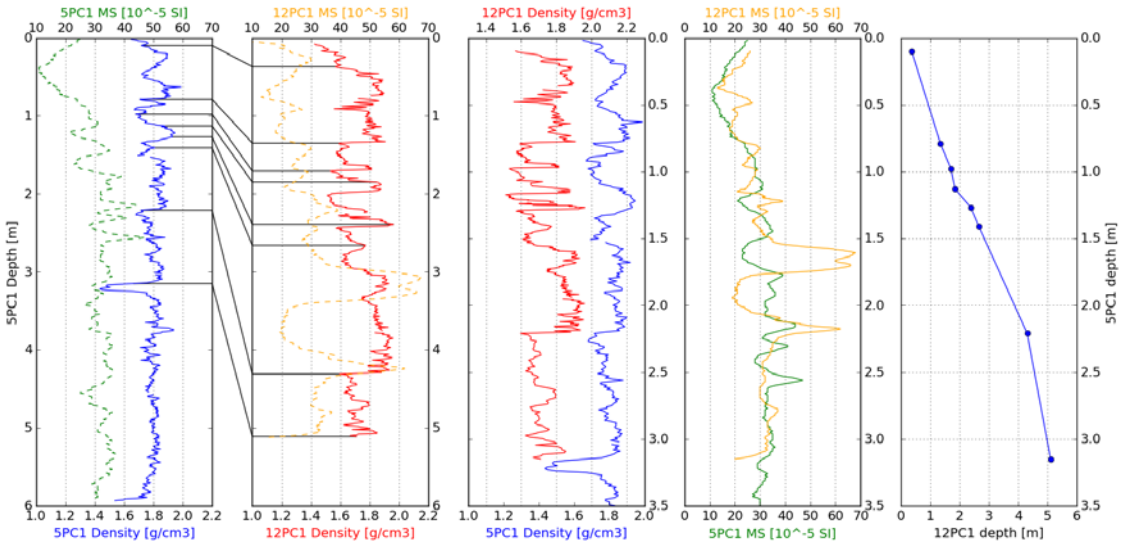

Figure 6.12 Correlation of the two cores retrieved from the crest of the Lomonosov Ridge (AO16-5-PC1 and AO16-12-PC1). The correlation is based on wet-bulk-density and well defined similarities can be seen when both records are put on the same depth scale (here: depth of AO16-5-PC1). Alongside the wet-bulk-density, the magnetic susceptibility of both cores is show, however when put on the same depth scale as defined by the density correlation several discrepancies are observed, suggesting that the wet-bulk-density is a more reliable choice for correlating cores from the central Arctic.

In total, 3 gravity cores, 11 piston cores and 6 core-cutter samples, which were pushed into empty liners, were logged usually 12-24 hours after recovery. A total of 10 cores have been imaged with the MSCL linescan camera. No trigger weight cores were logged during the expedition. The compressional wave velocity measurements caused some problems by 1) causing the logging to stop while waiting for incoming data and 2) recording a travel time of 0 µs. Both problems were narrowed down to the p-wave system but no apparent cause could be found. In case of 1) the measurement was restarted, and in case of 2) logging was repeated with only logging p-wave to get a consistent dataset.

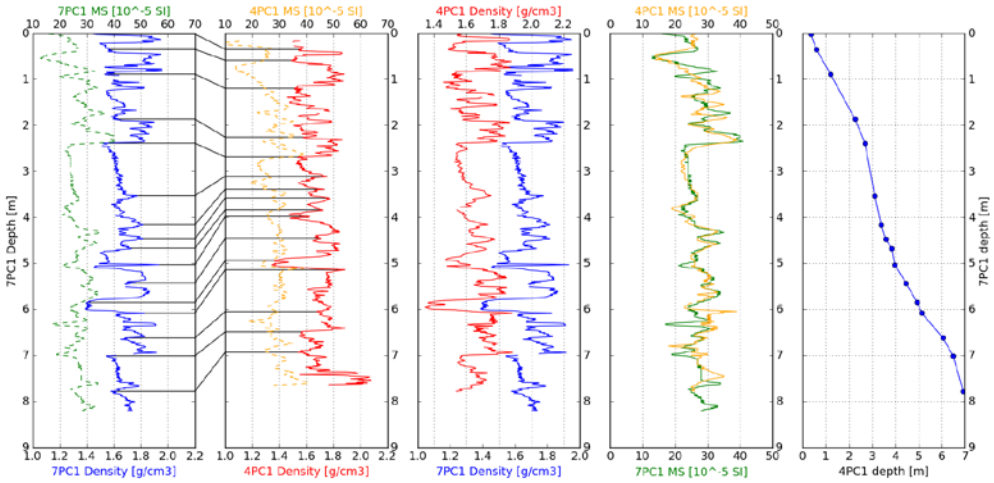

Figure 6.13 Correlation of the two cores retrieved from the foot of Marvin Spur. The two cores show a well defined similarity in wet-bulk-density and magnetic susceptibility. However, a period of moderately increasing density between ca. 2.5 and 3.5 m in AO16-7-PC1 spans over just half the thickness in AO16-4-PC1.

Shear strength measurements were performed on all opened cores except AO16-5-PC1 and AO16-9-PC1. Since beside paleomagnetic and IP25 sampling, measurements of pH were conducted on AO15-5-PC1 it was decided to skip the measurement of shear strength due to limited space in the working half and the possibility of disturbance by the measurements. In case of AO16-9-PC1 the measurement of the shear strength was initially forgotten and only realized after sampling started. To avoid false measurements due to an introduction of instabilities in the sediment due to the sampling it was decided to not perform shear strength measurements. Overall moderate values for shear strength were found in all sediments, with generally higher values in high density layers, as identified by initial logging (Fig. 6.14).

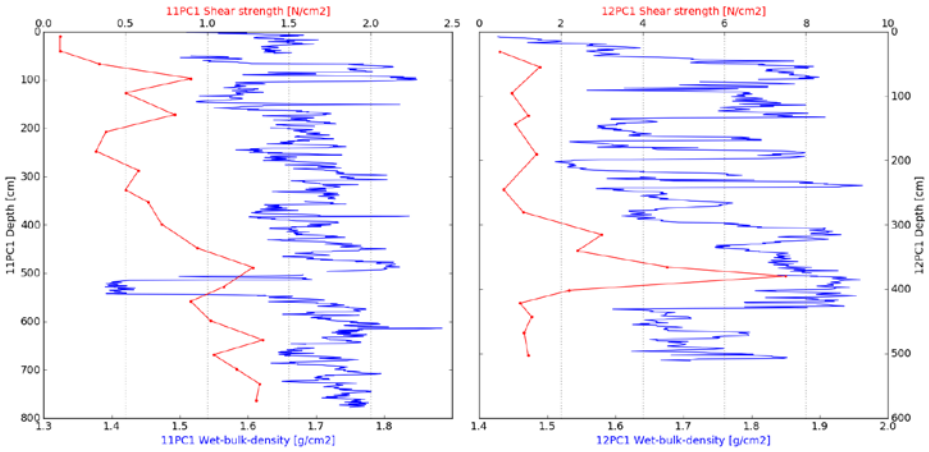

Figure 6.14 Shear strength (red) values alongside wet-bulk-density (blue) for AO16-11-PC1 (A) and AO16-12-PC1 (B). AO16-11-PC1 shows a downcore trend towards higher shear strength values. This increase is attributed to burial depth consolidation of the sediment. AO16-12-PC1 is dominated by high shear strength values around 400 cm and show a general correlation of density and shear strength.

The combination of the DST magnetic and the temperature sensors provided an efficient way to derive in-situ temperatures and track movements of the core barrel through the water column and while embedded in the sediments. The orientation tool data could be downloaded and read within minutes of the core landing on deck, and in a few instances provided important information on establishing whether the core penetrated the sediments or fell horizontally on the seafloor (Fig. 6.15). No depth data could be recorded below the calibration depth of the DST magnetic, which is about 3300 meters water depth.

In-situ temperature measurements were made at 13 gravity and piston coring stations. Further processing and analysis of the data is required to establish how many of these deployments provided reliable in-situ temperature estimates (Fig. 6.15). Possibly due to the cold temperatures on deck and in the water column, the batteries of most loggers failed after the first couple of deployments, recording only a brief period after started in the lab. Additionally three loggers were lost together with the fins. No concluding cause was found for why the fins were lost but a possible explanation is a combination of weak stainless-steel straps, which were used to fasten the fins to the core barrel, and very cohesive clay at the coring site. The sensor of one logger got bend during one cast, but seems to have recorded reliable data in comparison with the other sensors.

The thermal constants measurements were performed as soon as the core sections were split and imaged. A total of 376 1-sided measurements were performed on 8 cores, generally at a 30 cm downcore resolution. Shipboard conditions were not always ideal to perform the measurements and usually better results were obtained when measurements were done while the ship was on station. To reduce the vibration of the liner during measurements, the liner was placed in up to 8 wooden stands and fixated with small foam pieces. Additionally, every measurement was repeated at least once.

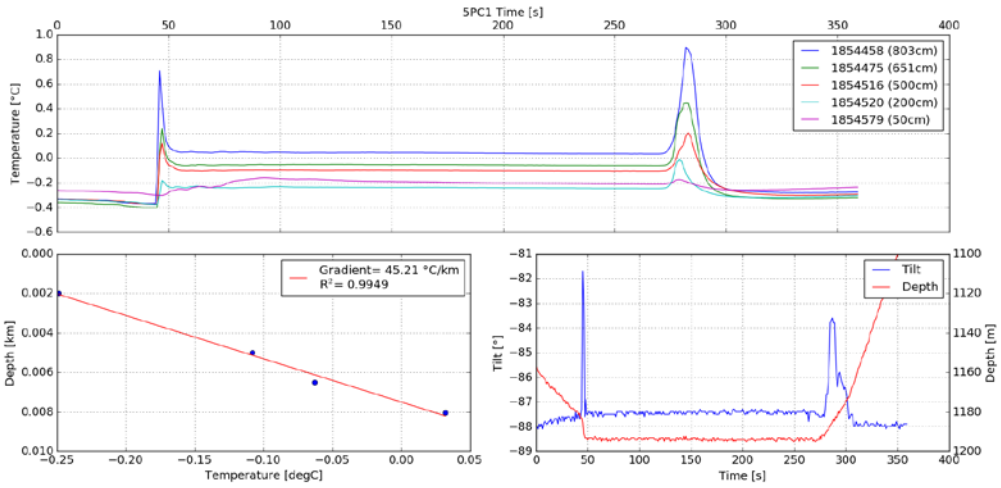

Figure 6.15 Combined temperature and tilt dataset for AO16-5-PC1 from the crest of the Lomonosov Ridge. A: Individual temperature recordings of the probes while in the sediment. The uppermost sensor (1854579) shows an offset in the water column and additionally shows no characteristic frictional heat spike. B: Initial estimate of the geothermal gradient based on the lower four sensors was found to be 45.21 °C/km. C: Depth and tilt recordings from the vertical Star Oddi sensor. An increase in velocity and a tilt spike at 45 s mark the release of the piston core.

The thermal data collected from the 8 cores show a clear relationship between the thermal constants: thermal diffusivity is higher when thermal conductivity increases, while specific heat capacity tends to decrease when thermal conductivity increases (Fig. 6.16). Mean, median and standard deviation for thermal constants measured during the expedition are listed in Table 6.3 (Fig. 6.17).

Table 6.3 Statistics of thermal property measurements.

	Mean	Median	Standard deviation
Th. conductivity	1.175	1.159	0.198
Th. diffusivity	0.365	0.351	0.089
Specific heat	3.287	3.313	0.433

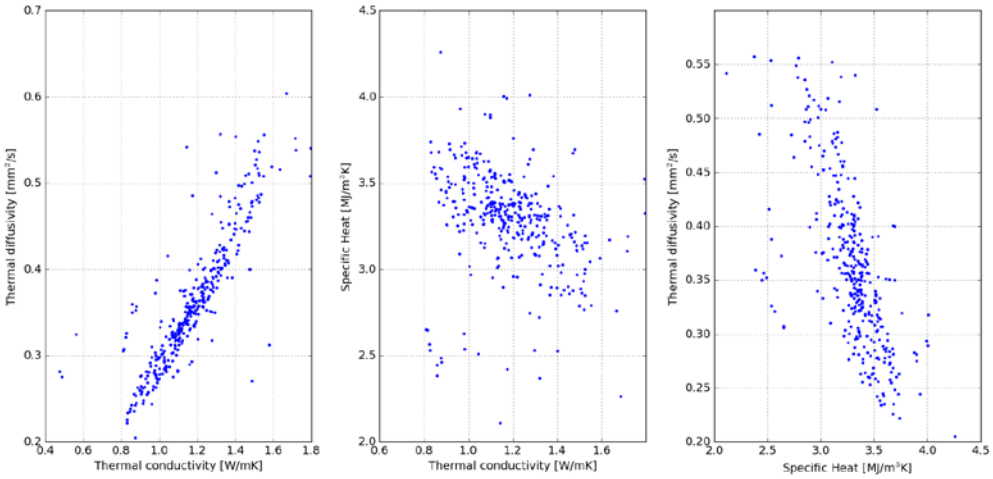

Figure 6.16 Biplots of thermal property measurements. The axes have been scaled to include the bulk of the measurements.

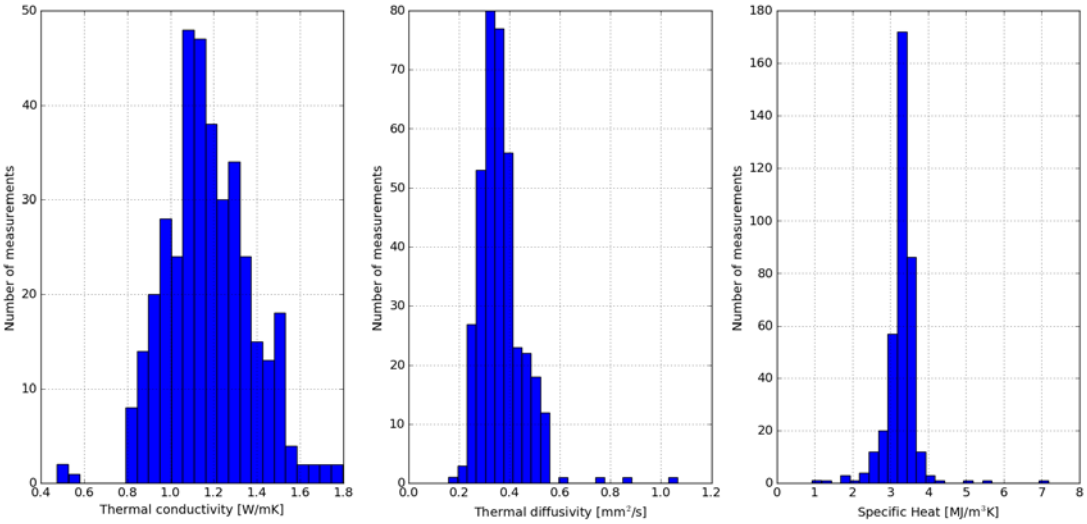

Figure 6.17 Histograms for thermal property measurements.

In some Arctic sediment cores calcareous microfossils have been found to disappear over time. Sequences with abundant foraminifera and ostracods sampled shipboard, have at re-sampling been found scarce in microfossils and it is hypothesized that dissolution of biogenic silica is positively correlated to a decrease in pH. This could severely bias micropaleontological studies conducted on stored cores.

To examine how pH changes over time in Arctic cores, in particular cores from the Lomonosov Ridge, pH was measured in the working halves of four split cores at a downcore resolution of 12 cm in cores from stations 5, 8 and 12 and at a resolution of about 50 cm in the piston core from station 10. The measurements will be repeated at the same depths after some months of storage at Stockholm University. During the expedition smear-slides were prepared for a quick assessment of microfossil abundance,

but no sampling and processing for microfossils was done. An overview of the measurements is presented in Table 6.4.

Table 6.4 Overview of shipboard sediment pH measurements.

Core ID	Core length (m)	Coring date	Measurement date	Number of pH measurements
AO16-5-PC1	6.16	160820	160823	52
AO16-8-GC1	3.59	160826	160828	31
AO16-10-PC1	7.96	160902	160904	17
AO16-12-PC1	5.19	160907	160910	46

After logging in the multi sensor core logger and splitting the cores into archive and working halves, the lithostratigraphy of the working half of each core was described through visual inspection. Core descriptions are presented in Appendix SC-5. Emphasis was placed on sediment color using the standard Munsell color scheme, texture, grain size, structures (laminations, lenses etc.), the nature of contacts between lithologic units (ie., sharp, gradational), and identification of specific features such as ice-rafted dropstones and macro-invertebrate remains (ie., mollusc shells).

Pore water sampling was performed immediately after coring on two cores with a sampling interval of 15 cm where applicable. In total 57 Rhizon samplers were used of which 4 remained empty. Pore water extraction usually took a few hours and was stopped after maximum 12 hours. More than 300 ml was extracted from both cores together but only 251.1 ml was kept for further analysis. The working halves of the split sediment cores were sampled after completion of the visual core description and measurements. In case the core was sampled for paleomagnetic properties this was done first, and all other sampling after that.

The goal of the paleomagnetic sampling was to study the puzzling magnetic directions found in Arctic Ocean sediments. Paleomagnetic sampling was carried out with 7 cm^3 (ca. 2X2x2cm) plastic cubes which were sealed with silicon after sampling to reduce the exposure of the sampled sediment to air (i.e. oxygen). All samples were placed in boxes in the refrigerated container until the end of the expedition. Measurements of the samples will be carried out at Uppsala University and/or at Bremen University and/or Lund University.

Sampling of surface sediment for mercury incubations was done in the upper 2 cm of nine cores. Cores from stations 1 and 2 were sampled on the aft deck immediately after coring using a spoon. In all other sampled stations, samples were taken from the trigger weight cores, using 10 cm^3 plastic scoops. The trigger weight cores were kept cold in the refrigerated container until splitting and sampling them. Sampling of surface sediments for analyses of microplastics was done in eleven cores, using 5 and/or 10 cm^3 plastic scoops. Sampling for analyses of mercury isotopes was done at irregular intervals in nine cores, taking 1-2 cm^2 using a spatula and/or 5 cm^3 plastic scoop.

IP25 sampling was done in all opened cores using 10 cm^3 plastic scoops. All sections were sampled schematically at centimeter depths of 0-2, 4-6, 8-10 etc. In piston and gravity cores two 10 cm^3 scoops were used at each sampling depth, whereas in the trigger weight cores only one scoop was used at each depth. An overview of samples taken shipboard is shown in Table 6.4 & 6.5.

A basic qualitative investigation of the microfossil composition of sediments was conducted. This was performed using smear slides only. No sieving to produce 'sand-fraction' foraminiferal samples was attempted. An Olympus BH-2 transmitted light microscope was used during the expedition. This was revealing various sediment grains and microfossils but not powerful enough to assess nannofossil content.

Smear slides were prepared for most of the coring sites and most of the sections. For coring site AO16-1 (Yermak Plateau) and for sections 1 to 3a of coring site AO16-3 (Foot of Lomonosov Ridge) no smear slides were prepared. Slides were prepared using approximately < 1 head of a match of sediment and Milli-Q water by continuously mixing with a toothpick to disaggregate sediment components, aiming for an even concentration of sediment over the slide. Appropriate sediment density on the slides was checked under a microscope at a magnification of 5X, after which they were left to dry for subsequent microfossil observation. A solid crystalized glue (called AYAC), used routinely elsewhere for nannofossil slide preparation, was used for slide fixing. This required heating of the slides to melt the crystals and fix the sediment smear. A glass cover slip was overlaid and gently pressed in place to spread the glue evenly. Microfossil observation on all slides (except for those between sections 1 and 4 of station AO16-2) was conducted before slide fixing with AYAC glue, since during the preparation of the first slides it was observed that the density of sediment was diluted after applying the glue and also some components were lost. Throughout the process of preparing slides, the technique of applying the glue was improved. It was found that the use of smaller glue crystals limited the formation of bubbles and allowed for better optical results. Therefore, for future studies using AYAC glue, we advise applying the smallest crystals on top of fine grained sediments and do the slide observation after slides are fixed, as re-examination of random slides showed better optical properties of both biogenic and abiogenic sediment particles after slide fixing. Generally, slides were scanned at a magnification of 10X, and higher magnifications were used to better identify specific particles. Digital images of unidentified particles/interesting components were taken, usually at a magnification of 40X, using an Iphone 4S.

For sediments collected with piston cores (PC) from stations 2 and 3 and with trigger weight cores (TWC) from stations 3, 4 and 5, slides were made from a variety of sediment types and colors. For all sediments collected thereafter, smear slides were mainly produced for sediment layers with typical dark brown color, associated with warmer periods, as the possibility of finding microfossils was expected to be higher in these. Sandy textures and increased grain size was avoided (Appendix SC-6).

Table 6.4 Summary of working half sediment samples and pore water samples.

Core	Palaeomagnetics		Pore Water		IP25 etc.		Microplastics		Hg incubation		Hg-isotopes	
	number	size	number	size	number	size	number	size	number	size	number	size
AO16-1-GC1	-	-	-	-	89	2x10 cc	2	5 cc	1	10 cc	24	1 cc
AO16-2-PC1	347	7 cc	-	-	232	2x10 cc	1	50 cc	1	10 cc	19	1 cc
AO16-3-PC1	-	-	-	-	191	2x10 cc	-	-	-	-	-	-
AO16-3-TWC1	-	-	-	-	71	1x10 cc	1	10 cc	1	10 cc	-	-
AO16-4-TWC1	-	-	-	-	61	1x10 cc	1	10 cc	1	10 cc	-	-
AO16-5-PC1	229	7 cc	35	3-6 ml	151	2x10 cc	-	-	-	-	12	1 cc
AO16-5-TWC1	-	-	-	-	31	1x10 cc	1	10 cc	1	10 cc	-	-
AO16-7-PC1	320	7 cc	58	3-6 ml	207	2x10 cc	1	10 cc	-	-	18	1 cc
AO16-8-GC1	138	7 cc	-	-	91	2x10 cc	1	10 cc	-	-	8	1 cc
AO16-9-PC1	-	-	-	-	187	2x10 cc	-	-	-	-	10	1 cc
AO16-9-TWC1	-	-	-	-	43	1x10 cc	1	10 cc	1	10 cc	-	-
AO16-10-PC1	-	-	-	-	200	2x10 cc	-	-	-	-	10	1 cc
AO16-10-TWC1	-	-	-	-	33	1x10 cc	1	10 cc	1	10 cc	-	-
AO16-11-PC1	-	-	-	-	202	2x10 cc	-	-	-	-	13	1 cc
AO16-11-TWC1	-	-	-	-	34	1x10 cc	1	10 cc	1	10 cc	-	-
AO16-12-PC1	202	7 cc	-	-	130	2x10 cc	-	-	-	-	12	1 cc
AO16-12-TWC1	-	-	-	-	52	1x10 cc	1	10 cc	1	10 cc	-	-

Table 6.5 Other samples (core cutters and core catchers, plus features removed from working halves).

Core	Section	cm (top)	cm (base)	Comments
AO16-1-GC1	Core catcher	-	-	Stored in plastic bag. No cutter.
AO16-2-PC1	Core catcher	-	-	Stored in plastic bag. Cutter put in liner.
AO16-3-PC1	Between 2 & 3a	-	-	4 cm piece fell out while cutting the core on aft deck
AO16-3-PC1	3a	44	46	Flat stone, 4 x 3 x 0.5 cm. Against liner, 90^{o} to sediment layers.
AO16-3-PC1	Core catcher	-	-	Stored in plastic bag. Cutter put in liner.
AO16-3-TWC1	Core catcher	-	-	Stored in plastic bag.
AO16-4-PC1	Core catcher	-	-	Stored in plastic bag. Cutter put in liner.
AO16-4-TWC1	Core catcher and cutter	-	-	Stored in plastic bag.
AO16-5-PC1	Core catcher	-	-	Stored in plastic bag. Cutter put in liner.
AO16-5-TWC1	Core catcher	-	-	Stored in plastic bag. No cutter.
AO16-6-PC1	Core catcher	-	-	Stored in plastic bag. No cutter. No TWC.
AO16-8-GC1	Core catcher	-	-	Stored in plastic bag. No cutter.
AO16-9-PC1	2	100	102	Shell, 8x10 mm.
AO16-9-TWC1	Core catcher	-	-	Stored in plastic bag.
AO16-9-TWC1	Core cutter	-	-	Stored in plastic bag.
AO16-10-PC1	1	16	17	2 tubular features, 1 mm diameter, 5 and 13 mm long. CaCO3?
AO16-10-TWC1	Core catcher	-	-	Stored in plastic bag.
AO16-10-TWC1	Core cutter	-	-	Stored in plastic bag.
AO16-11-PC1	2	2	2	Flaky feature. Plastic? (Near top of gap in sediment).
AO16-11-PC1	Core catcher	-	-	Stored in plastic bag. Cutter put in liner.
AO16-11-TWC1	1	88	90	Flat stone, 2.5 mm thick, 2x5cm, one end perfectly rounded (?)
AO16-11-TWC1	Core catcher and cutter	-	-	Stored in plastic bag.
AO16-12-PC1	1	0	0	Piece of shell, 3x5 mm, in top sediment. Removed before capping liner.
AO16-12-PC1	1	10	10	White tube, 2-3 mm diameter, 2 mm long. Shell? Crushed in bag by mistake.
AO16-12-PC1	Core catcher	-	-	Stored in plastic bag. Cutter put in liner.
AO16-12-TWC1	Core catcher and cutter	-	-	Stored in plastic bag.
AO16-13-TWC1	Core catcher and cutter	-	-	Stored in plastic bag.

One of the expedition targets was to core Cretaceous sediments on the Alpha ridge. From previous drilling it is known that these Cretaceous strata are rich in planktonic diatoms (Davies et al. 2009). We hoped to confirm coring of Cretaceous sediments by the presence of diatom oozes in our cores. However, diatoms were never found in high concentrations indicative of the anticipated Cretaceous age in any of the samples investigated and therefore we can imply Cretaceous sediments were not retrieved during this expedition. In fact, diatoms were overall very rare in all sections analyzed. Elongated particles, reminiscent of fragments of diatom frustules or entire pennate diatoms, were found in several samples of different sites and at varying depths (Appendix SC-6). However, due to the lack of polarized light in the microscope brought on board, it was impossible to determine the nature of these particles, as they could also be some sort of mineral. Since at some stations these particles were present irrespective of core depth and didn´t necessarily coincide with other biologically-originated components of sediments (e.g. opal fragments, foraminifera), we infer that most of them were likely non-biogenic minerals rather than frustules. Potential centric diatoms or fragments of centric diatom frustules, which were evidenced by rounded and relatively flat porous particles with prominent outer rings, were rather scarce or completely absent. When present, these were limited to the top of the first section of some cores. Large opal-like fragments from unidentified organisms were more common, especially in the first sections of some cores, though they were also found in second and third sections. These were especially evident in the top of the less disturbed sediments of the Nautilus Basin (station AO16-10) retrieved from the first section of the trigger weight core.

Foraminifera, as observed in the smear slides, were the most abundant microfossil in sediment samples retrieved from the AO16 expedition (Appendix SC-6). In general, they were most abundant in the first sections of the cores, but they were also found down to the third section in some stations (Alpha Ridge: AO16-9; Nautilus Basin: AO16-10; Makarov Basin: AO16-11). At station AO16-11, fragments of foraminifera (potentially altered by diagenesis), were present in the bottom sections (5 and 6). This could imply for instance a different carbonate chemistry in the sediment at this location (e.g. less acidic pH), a deeper location of the carbonate compensation depth (CCD), different environmental settings at the time of foraminifer production compared to the other locations of the Central Arctic, or that sediments from this section could be older (and therefore may have undergone different production, settling and sediment storage conditions) compared to sediments retrieved from other stations during this expedition. This is to be further studied during the shore-based phase of these investigations.

Potentially due to dissolution of calcium carbonate below the relatively shallow Arctic CCD, foraminifera were generally more abundant and apparently more heavily calcified at shallower stations (i.e. stations AO16-8, 9, 10 and 11) (Appendix SC-6). Foraminifera in cores retrieved at greater depths (generally >3000 m) were found to be limited to the first section or completely absent (e.g. Marvin Spur foot: AO16-7). Relatively shallow stations located on the Lomonosov Ridge (i.e. AO16-5 and 12) showed very low abundance of foraminifera, which could be indicative of different production conditions at the surface (e.g. heavier sea ice extension limiting primary production) and/or different sediment properties in this area of the Central Arctic.

Nannofossil analysis has previously been proved to be useful for reconstructing different paleoceanographic parameters in the Arctic Ocean. The presence of foraminifera shells implies suitable conditions for carbonate precipitation, thus sediments should also be checked for nannofossil content in future shore-based studies.

6.6 Discussion and future analyses

The sediment cores retrieved during the Arctic Ocean 2016 expedition carried out jointly with IB Oden and CCGS Louis S. St-Laurent comprise a valuable new cache of material for studies of the Arctic Ocean Quaternary paleoceanography as well the modern ocean environment captured in the uppermost surface sediments. The initial shipboard analyses of the cores from the Alpha Ridge, where outcropping of older pre-Quaternary sediments were targeted, did not reveal any indication of that Early Cretaceous material was recovered as during previous expeditions on drifting ice islands in the 1960s, 1970s and early 1980s. However, while perhaps sediments of Early Cretaceous age can be ruled out by the initial shipboard analyses, the cores may contain pre-Quaternary sediments. This can only be established through further studies. Following an evaluation of all the shipboard measurements carried out on the retrieved sediment cores, additional chemical, micro-paleontological, paleomagnetic and sediment physical analyses awaits all the cores retrieved during the Arctic Ocean 2016 expedition. There is no doubt that this new cache of material will shed new lights on the Arctic Ocean Quaternary history, and we have not given up the hope yet that some new glimpses may be provided also into older periods.

Appendix 1-6 available on request, please contact asa.lindgren@polar.se.

7. Work Package Physical Oceanography

Katarina Gårdfeldt[1], Michelle Nerentorp Matrsomonaco[1], Sofi Johnsson[2], La Daana Kanhai[3]

[1]Department for Chemistry and Chemical Engineering, Chalmers University of Technology, Sweden, [2]Department for Marine Sciences, University of Connecticut, US and Centre for Environment and Sustainability, University of Gothenburg, Sweden
[3] Marine and Freshwater Research Centre, Galway-Mayo Institute of Technology, Ireland

7.1 Summary

The Work Package Physical Oceanography focused on measuring physical parameters, fractions of mercury species and microplastics in depth profiles of the Arctic Ocean. The collected samples were either analysed onboard in the labs or stored and transported to the institutes for analyses in labs after the expedition. Data on vertical profiles of contaminants is useful when trying to discriminate between different possible sources such as atmospheric deposition, oceanic currents and rivers. Such data is also valuable in order to assess future accumulation of mercury (Hg) and micro plastics in Arctic marine waters. Therefore, vertical profile measurements of these and related substances were studied along the AO16 cruise track.

7.2 Background

Mercury is one of the most hazardous compounds on earth. Research on emissions and the environmental behaviour of mercury has shown that biota in remote ecosystems, far from any anthropogenic sources, can be affected. Contamination of aquatic environments with elevated concentrations of methyl mercury in fish has been found to be related to anthropogenic activities in connection with long-range transport of airborne mercury species and subsequent deposition. Since methyl mercury also passes the placenta consumption of contaminated fish during pregnancy may result in exposure of the human foetus to hazardous levels of mercury. This may in turn cause neurological damages and mental retardation of the child. Pregnant women and children are therefore advised not to eat fish which may be suspected to contain elevated concentrations of methyl mercury.

Global warming is changing the ice and snow coverage in the marine polar environment. Climate change also impacts the surface energy budget, biological/ecosystem function and chemical processes in the polar environment. Energy, biology and chemistry systems are coupled, with numerous feedbacks and interactions. For example, changing sea ice regimes in the Arctic (e.g. shifts from multi-year to first year sea ice) will impact biological systems and productivity, which in turn may impact trace gas fluxes. Changing sea ice and snow regimes will also impact contaminant transport and fate of contaminants like POPs, Hg, and other heavy metals.

To date, there have only been two studies to report on the presence of microplastics in Arctic waters (Amelineau et al. 2016; Lusher et al. 2015). The overall findings of the study conducted in surface and sub-surface waters south and south-west of Svalbard, Norway indicated that microplastic abundances in the Arctic were similar to those previously reported in other areas (Lusher et al. 2015). With respect to the study conducted in waters east of Greenland, microplastic abundances were comparable to those reported in other oceans despite the remoteness of the study area (Amelineau et al. 2016).

Due to the paucity of information regarding microplastics in Arctic waters, sub-surface waters were analysed for microplastics during the Arctic Ocean 2016 expedition.

The WP PO had crosscuttings with other WPs during the AO16 expedition:

- WP HM: Data from WP PO will be analysed together with data on e.g. atmospheric deposition and re-emission achieved in WP HM.
- WP TGB: Samples were taken for methane gas in near surface samples (Brett Thornton/Patrick Crill)
- WP GM: CTD data will be used with locations in order to verify possible stair-cased formation of stratified water masses observed via the multi beam technique onboard (To-Yo casts: Christian Stranne)

7.3 Method and Equipment

Two CTD set ups, each with a 24 bottle Rosette with bottle volumes of 7.5 and 12 litres respectively, were used during the AO16 expedition. Both set ups had dual conductivity, temperature and oxygen sensors. CTD data were processed (preliminary processed ASCII data files of all CTD stations) through the sea-bird software and were made available to all expedition participants already during the expedition. Water for chemical analysis was drawn from the Niskin bottles directly after the Rosette was brought into the CTD lab onboard Oden. Gaseous species such as methane (CH_4) dimethylmercury (DMHg) and dissolved gaseous mercury (DGM) were drawn prior other substances and from separate Niskin bottles to avoid loss of gas to headspace.

The depths for closing the Niskin bottles were decided after studying the water column profile obtained when the CTD was descending. The mercury sampling was designed as profile measurements at the CTD stations and the content of mercury species in the samples will be further studied in combination with data on movements of water masses. Moreover, methylated mercury species i.e. DDHg and monomethylmercury (MMHg) might coincide with biological activity, therefore the bottles were mainly closed to follow the changes in the oxygen profile.

The Rosette with the 7.5 litres bottles was used for the Hg speciation, whereas the Rosette with the 12 litre bottles was mainly used for microplastic sampling in order to achieve a higher sampling volume needed to collect enough quantity for analysis. The seawater samples were either analysed in the wet lab on board Oden or stored and transported to the University labs to for analysis after the expedition.

The samples for analysis of dissolved gaseous mercury were carefully poured through a FEP tubing into conditioned glass bottles filled to the rim to avoid headspace. When filled, the glass bottles were transferred from the CTD lab to a dark bucket outside the wet lab. All samples was analysed for Hg(0) within 12h after sampling using a purge-and-trap system, see Fig. 7.1.

Approximately 0.4 L of the water sample was gently transferred from the glass bottle to a clean and conditioned analysis flask. A glass frit of pore size 0 or 1 connected to a Tekran 2537A mercury analyzer was inserted into the analysis flask. A coal canister was installed at the air inlet to create mercury-free air. The pump in the Tekran 2537A analyzer, pumping air with a flow rate of 1 L min^{-1}, was used to suck air through the purging system, creating small gas bubbles purging the sample. Once degassed from the water sample, the mercury gases followed the air stream to the analyzer where the concentrations of dissolved gaseous mercury was detected. The results of the analyses were then divided by the measured sample volume. According to calculations by Gårdfeldt et al. (2002), 9 min purging time is enough to allow DGM in the sample to be depleted. The detection limit was 0.3 pg L^{-1}, calculated as the standard deviation of the total blanks.

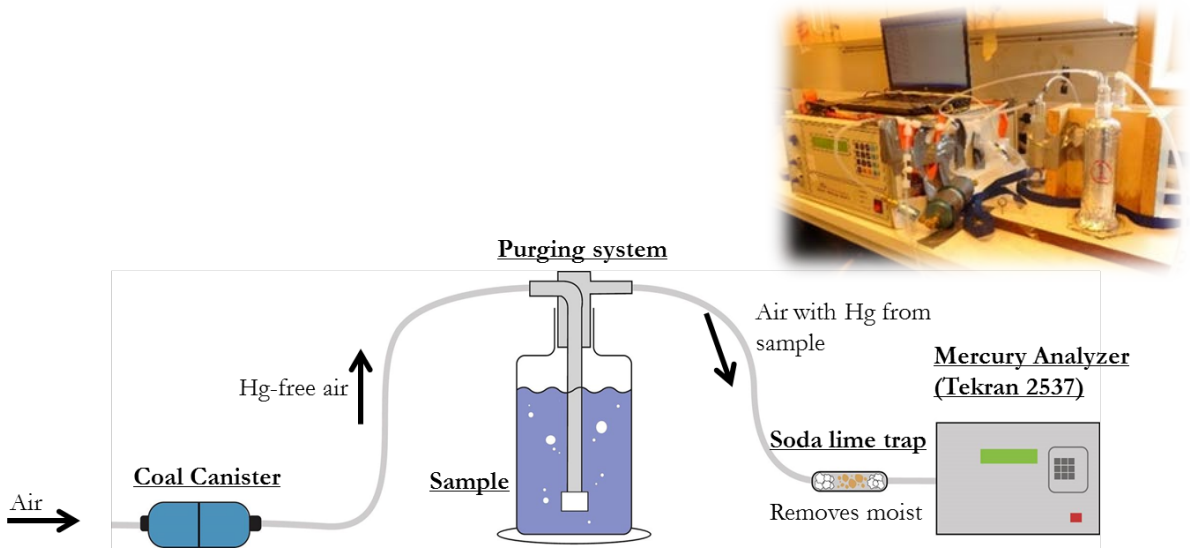

Figure 7.1 Principle of the purge and trap system used to measure elemental mercury in seawater samples and melted ice and snow samples (Nerentorp Mastromonaco, 2016).

The precision measured in field was between 1 to 20%, varying between the campaigns. Wängberg et al. (2001) calculated the statistical reproducibility of the method to be ± 6 % for DGM concentrations between 15 to 20 pg L^{-1}. A soda lime trap was used to protect the Tekran analyzer from humidity.

Dimethylmercury was measured on board Oden during the cruise while samples for determination of monomethylmercury and total mercury concentrations were preserve with trace metal clean sulfuric acid and shipped in precleaned glass bottles to the Department or Marine Sciences (University of Connecticut, USA) for analysis. The equipment to measure dimethylmercury (Fig. 7. 2) was set up in the clean lab available (the air was cleaned with HEPTA filters) on Oden and consisted of a purging setup where the dimethylmercury was extracted from the sampled water using ultrapure argon gas, a thermal desorption unit where the dimethylmercury was desorbed from the analytical trap (consisting of carbotrap®), a packed gas chromatographic (GC) column heated to ca. 70 °C for separation of different chemical forms of mercury that desorbed from the analytical trap, a heated trap with gold coated beads to thermally decompose the different forms of mercury exiting the GC column, and finally a Tekran 2500 mercury analyser for quantification. Based on the vertical profile determined, the flux of dimethylmercury from the polar mixed layer to the atmosphere, and from subsurface waters to the polar mixed layers were calculated following the procedures described by Soerensen et al. 2016 Monomethylmercury and total mercury was determined using a Tekran 2600 mercury analyser and a Tekran 2700 methylmercury analyser.

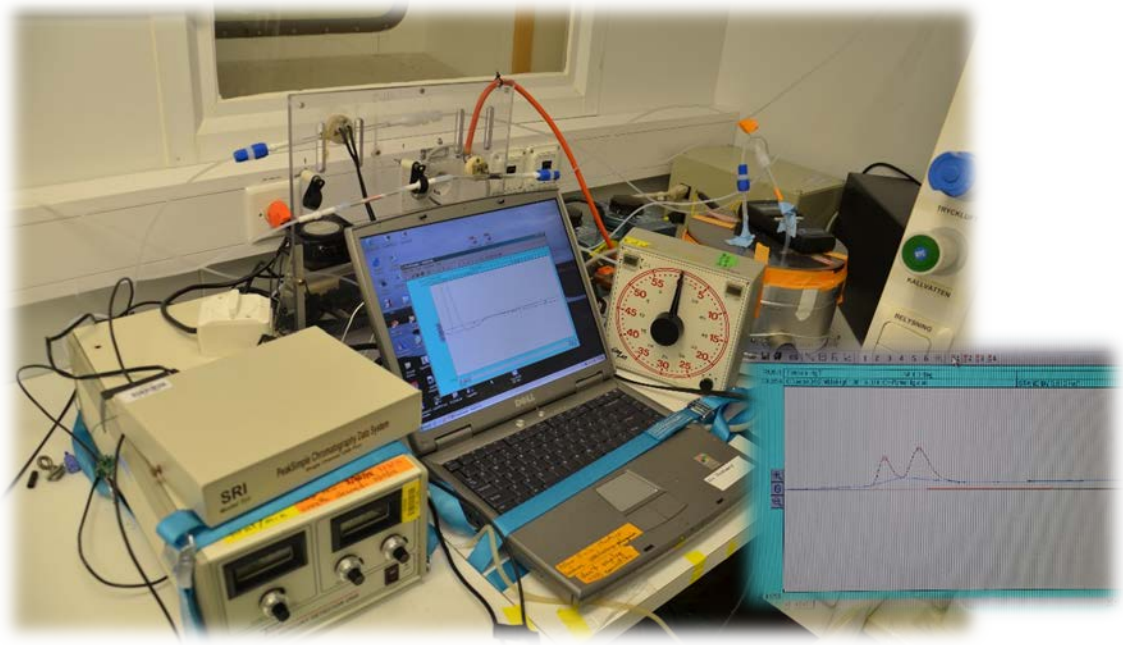

Figure 7.2 Analytical setup for the determination of dimethylmercury in sampled seawater, under ice water, brine, melt pond water and ice samples. The Tekran 2500 analyzer is on the left side of the picture and the thermal desorption unit is seen behind the computer. A chromatogram is shown in the smaller figure to the right where the first peak is elemental mercury and the second peak is dimethylmercury.

Sampling of microplastics in sub-surface waters was conducted using the CTD Rosette (seawater from various depths). Filter papers for each sample were shipped to the laboratory for visual identification of potential microplastics at GMIT followed by FT-IR spectroscopy analyses for identification of polymer type at Plymouth University.

7.4 Results

A total of 25 CTD stations (Fig. 7.3) were sampled of which 16 stations were sampled for DGM (Fig. 7.4), 12 for HgTot, 9 for MeHg and 11 for microplastics. The CTD station name with positions and bottom depth, and number of data per individual constituent and station are given in Table 7.1.

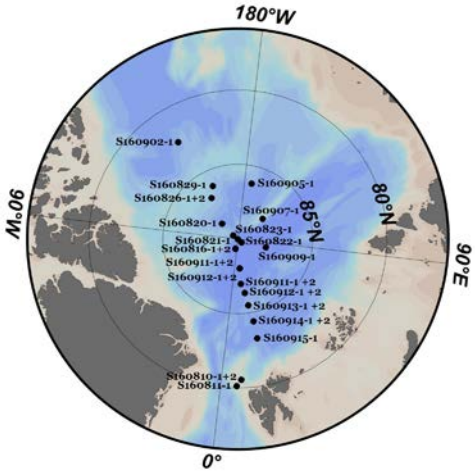

Figure 7.3 All CTD stations sampled for mercury species and microplastics during the AO16 expedition.

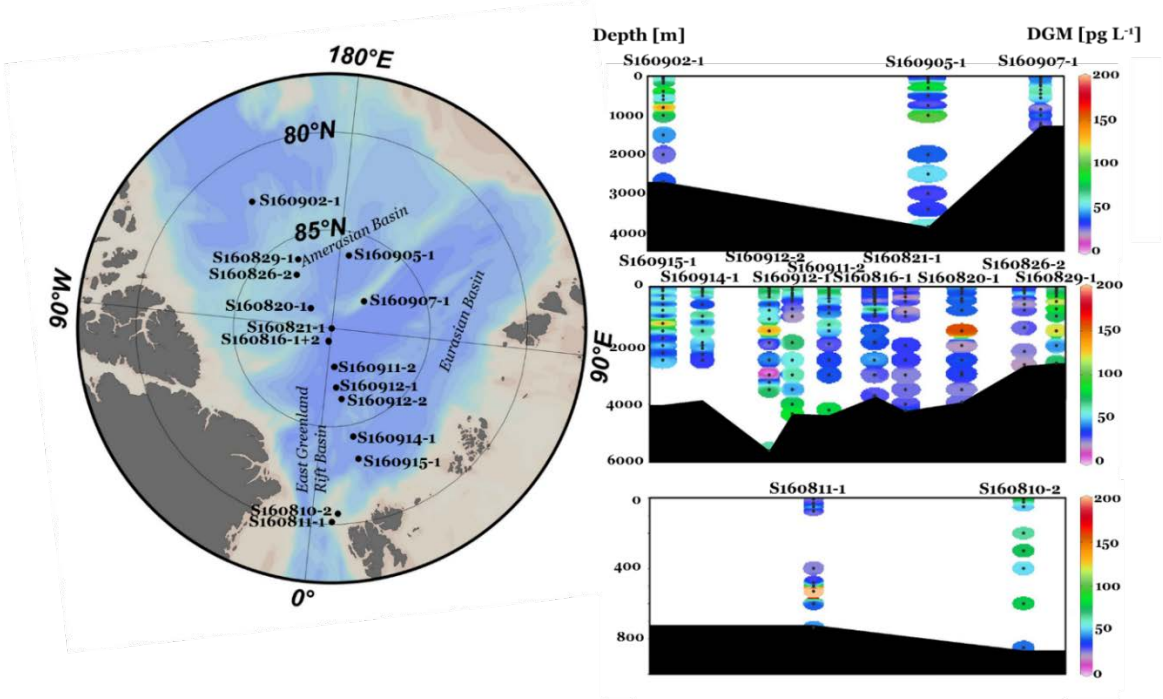

Figure 7.4 CTD stations sampled for dissolved gaseous mercury (DGM) analyses and depth profiles of DGM obtained in analysed samples (Nerentorp Mastromonaco, 2016).

The locations of the CTD stations sampled for DGM and the results of the DGM analyses are presented in Fig. 7.4. The average water column DGM concentration during AO16 was 50 ± 35 pg L^{-1}.

The Arctic Ocean is divided into two basins by the Lomonosov Ridge; the Eurasian Basin and the Amerasian Basin, see Fig. 7.4. The spatial differences were studied, showing no significant variations in water column DGM concentrations between the Eurasion Basin (47 ± 21 pg L^{-1}) and the Amerasian Basin (47 ± 26 pg L^{-1}). However, in the East Greenland Rift Basin the average water column concentration of DGM was found to be significantly higher (68 ± 98 pg L^{-1}). The data will be further investigated in terms of different water masses and the circulation of water in the Arctic Ocean. Results will be presented in future publications.

Concentrations of mono and dimethylmercury and total mercury has so far been evaluated for the 10 stations where the concentations of dimethylmercuy was profiled. Dimethylmercury concentrations ragned from <1.2 fM up to 150 fM in the top 400 m. Interestingly, the concentraion of dimethylmerucy in the in the polar mixed layer (PML) was surprisingly low in comparison to data available from the Canadaian Arctic Artepalagio (Soerernsen et al, 2016, and references therein). The concentrations of dimethylmercury increased in the halocline and were highest between 200 and 500 meter. Based on concentration detected in and below the PML the flux to and from the PML was calculated. The calucted flux to the PML was an order of magnitude higher than the flux of dimethylmercury to the PML, suggesting substantial degradation of dimethylmercuy in the surface. This is in contrary to previous mass budgets made where evation and substantial degradation of dimethylmercury to monomethylmercury in the atmosphere was suggested to be an important source of monomethylmercury in the PML. This model was however constrained as no data on dimethylmercury from the central Arctic Ocean (covering 40 % of the Arctic Ocean) was available. Stability and formation processes of dimethylmercury in marine waters are largly unknown (Jonsson. et al. 2016).

It is therefore difficult to evalute if the dimethylmercury present below the halicline is formed in situ from inorganic mercury or monomethylmercury or if it is transported into the Arctic Ocean with incomming Atlantic waters (seen as the peak in potenital temperature (blue line in left figure in Fig. 7.5). Using degradation rates previously suggested (Mason et al. 1995) and the mean residence time of the upper waters in the central Arctic Ocean we suggest that dimethylmerucry is most likely both formed in situ and being transported into the basin with incomming waters. For samples where both mono- and dimethylmercury was determined, the concentration of the total methylated pool of mercury was caluclated to average at average MeHgT of 140 ± 94 fM. These are similar to the concentraion previously determined in the central Arctic Ocean by Heimburger et al. (2015). The lower concentraion found in both studies in the central basin, in comarison to the Canadaian Arctic Artepalagio, may be explained by an overall lower productivity in the central basin. The concentraion of total mercury was also similar to the levels found by Heimburger et al. (2015). The concetration of total mercury increased in surface waters. This has also previously been observed and could be explained by e.g. river inputs of mercury to the surface waters.

Visual identification of potential microplastics is currently in progress and is estimated to be completed in early 2017. FT-IR analyses will follow.

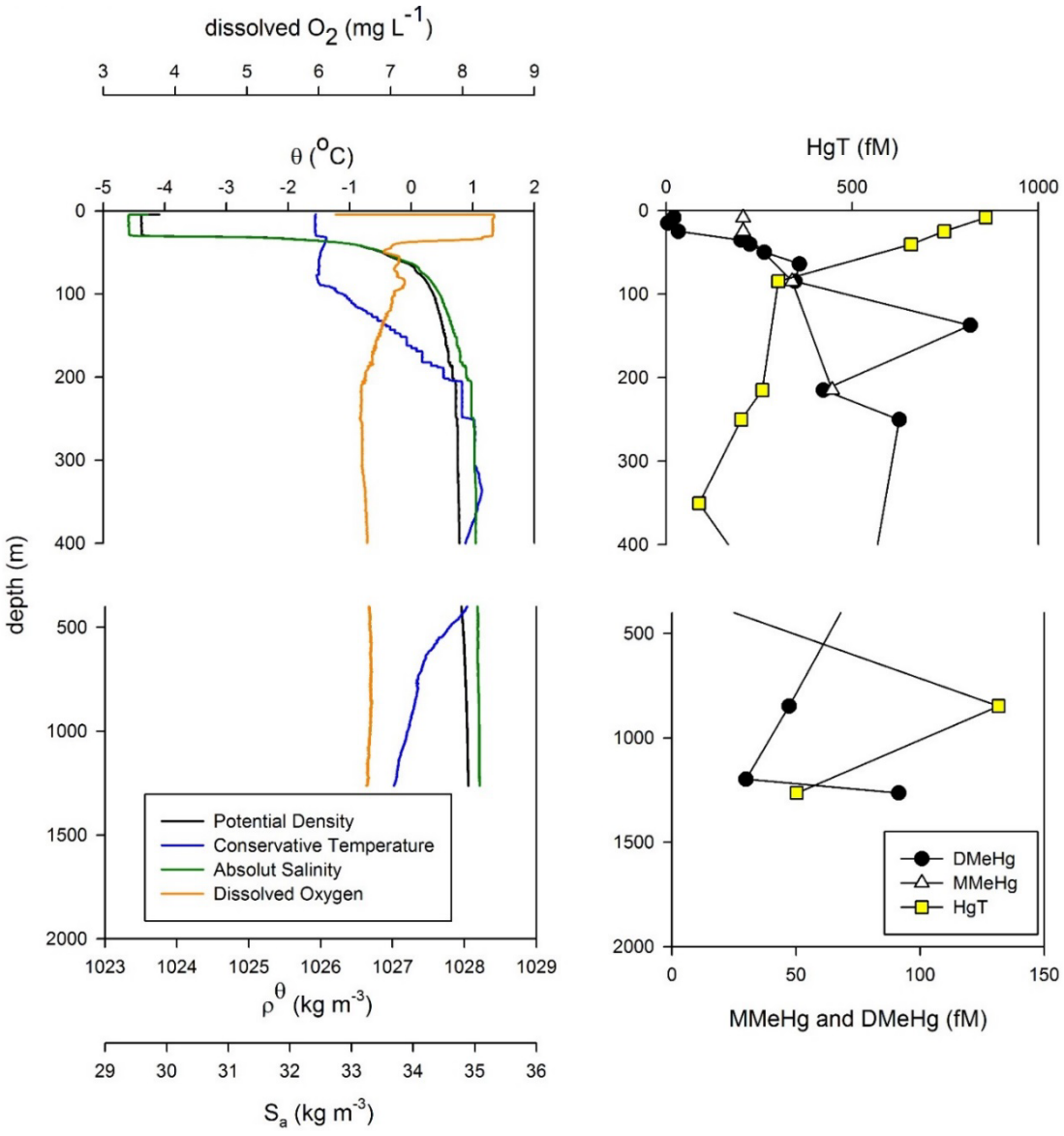

Figure 7.5 Example of profile for mono- dimethylmercury in Left plots show the vertical profile of sea water properties including dissolved oxygen, O_2 (mg L^{-1} orange line), conservative temperature, Θ (°C, blue line), potential density, ρ^{Θ} (kg m^{-3}, black line) and absolut salinity, S_a (kg m^{-3}, green line) at station 1-10. The right plots show concentrations of monomethylmercury (MMeHg, fM, black filled dots), dimethylmercury (DMeHg, fM, white triangles) and total mercury (HgT, fM, yellow squares) at station 1-10.

Table 7.1 CTD stations with positions and bottom depth, number of data per individual constituent and station.

CTD Station	Lat	Long	Bottom Depth	DGM	Hg Tot	DM Hg	MM Hg	CH4	Micro-plastics	Nutr.	Met/ Dem	DOC	Plankt	Bact
S160810-1	80.563	8.035	857						23					
S160810-2	80.563	8.005	862	9					3					
S160811-1	80.136	6.143	730	11					3					
S160816-1	89.340	-7.163	3727	16	9	11	4	1	4	4	4	4	4	4
S160816-2	89.313	-7.284	3757	18	4					4	3	3	3	3
S160820-1	88.537	-127.795	4009	17		3		1					3	
S160821-1	89.989	1.011	4233	2				1					3	
S160822-1	89.661	52.056	4351						23					
S160823-1	88.600	-121.952	3944						24					
S160826-1	86.744	86.744	2708						24					
S160826-2	86.759	-140.798	2695	16	10	10		1		10				
S160829-1	86.105	-148.095	2604	18	13	13								
S160902-1	82.392	-141.713	2700	15	15	15	15	1		15		4	8	
S160905-1	86.203	172.764	3845	18	18	18	18	1		8		2	2	2
S160907-1	87.864	135.931	1264	18	9	15	7	1		8			4	
S160909-1	88.058	80.263	4385						24					
S160911-1	88.038	9.906	4365						24					
S160911-2	88.0422	10.151	4370	18	5	7	7	1		6			3	

S160912-1	86.990	10.303	4333	18	4	12	4							
S160912-2	86.372	13.967	3559	22	3	12	3			4			1	
S160913-1	85.521	15.644	5030											
S160913-2	85.529	15.605	5010						24					
S160914-1	84.405	17.395	3860	23	9	12	6	1		7		4	4	
S160914-2	84.406	17.459	2500						24					
S160915-1	83.244	17.663	4027	18	4	12	3	1					3	

7.4 Data management, deliverables and future (after cruise) plans

Preliminary processed ASCII data files of all CTD station data will be made available. The collected CTD data will be processed by Prof. Göran Björk at University of Gothenburg. Data on water profiles for mercury species will be made open accessible without delays.

Future use of the data: Data will appear in scientific publications, and will be useful for analysis of the origin of methylmercury in subsurface Arctic sea water.

7.5 References

Amelineau, F., Bonnet, D., Heitz, O., Mortreux, V., Harding, A.M.A., Karnovsky, N., Walkusz, W., Fort,J., Gremillet, D., 2016. Microplastic pollution in the Greenland Sea: Background levels and selective contamination of planktivorous diving seabirds. Environmental Pollution 219, 1131-1139.

Gårdfeldt, K. *et al.* Comparison of procedures for measurements of dissolved gaseous mercury in seawater performed on a Mediterranean cruise. *Anal. Bioanal. Chem*. 374, 1002–8 (2002).

Heimbürger, L., Sonke, J. E., Cossa, D., Point, D., Lagane, C., Laffont, L., Galfond, B. T., Nicolaus, M., Rabe, B., van der Loeff, M. R. Shallow methylmercury production in the marginal sea ice zone of the central Arctic Ocean. Sci. Rep. 2015 (5:10318 |), DOI: 10.1038/srep10318.

Lusher, Amy L., Ann Burke, Ian O'Connor, and Rick Officer. 2014. "Microplastic pollution in the Northeast Atlantic Ocean: Validated and opportunistic sampling." *Marine Pollution Bulletin* no. 88:325-333. doi: 10.1016/j.marpolbul.2014.08.023.

Lusher, Amy L., Valentina Tirelli, Ian O'Connor, and Rick Officer. 2015. "Microplastics in Arctic polar waters: the first reported values of particles in surface and sub-surface samples." *Scientific Reports* 5 (14947):1-9.

Mason, R., Rolfhus, K., Fitzgerald, W. Methylated and elemental mercury cycling in surface and deep ocean waters of the North Atlantic. Water. Air. Soil Pollut. 1995, 665–677.

Jonsson, S.; Mazrui, N. M.; Mason, R. P. Dimethylmercury Formation Mediated by Inorganic and Organic Reduced Sulfur Surfaces. *Scientific Reports*. 2016, No. May, 6:27958, DOI: 10.1038/srep27958.

Nerentorp Mastromonaco, M. G., 2016c. Mercury cycling in the global marine environment. *Ph.D Thesis.* ISBN: 978-91-7597-478-1.

Soerensen, A. L., Jacob, D. J., Schartup, A. T., Fisher, J. a., Lehnherr, I., St. Louis, V. L., Heimbürger, L.-E., Sonke, J. E., Krabbenhoft, D. P., Sunderland, E. M. A mass budget for mercury and methylmercury in the Arctic Ocean. *Global Biogeochem. Cycles* 2016, 30, 560–575.

Wängberg, I., Schmolke, S., Schager, P., Munthe, J., Ebinghaus, R., Iverfeldt, I. Estimates of air-sea exchange of mercury in the Baltic Sea. *Atmos. Env.* 35, 5477–5484 (2001).

Photo: Åsa Lindgren

8. Work Package: Trace Gas Biogeochemistry (TGB)

Patrick Crill*[1], Brett Thornton*[1], John Prytherch[2]

[1] Dept. of Geological Sciences, Stockholm university, [2] School of Earth and Environment, University of Leeds, UK

8.1 Summary

Two high resolution cavity ring-down laser spectrometers (Los Gatos Research (LGR) Fast Greenhouse Gas Analyzers) were run throughout the cruise. The first is configured to measure the mean concentrations of CO_2 and CH_4. The second system is configured to measure at 10 Hz, and draws its sample from the top of the foremast, next to the eddy covariance system installed by the meteorology work package. The data from this system was logged synchronously with that from the eddy covariance system in order to make direct eddy covariance estimates of the gas flux. This continues a collaboration with the meteorology group established during the 2014 SWERUS-C3 cruise.

8.2 Background

CO_2 and CH_4 are both important greenhouse gases. Few direct measurements of either gas are available in the Arctic. The measurements made here add greatly to multiyear datasets for the Arctic Ocean. These are needed to understand the variability in concentration on both short and long timescales, and how the air-sea exchange of the gases is changing, and may change in future as sea ice cover decreases over time. A significant gap in understanding of air-sea gas exchange in the Arctic is the impact of sea ice on gas transfer. In order to close this knowledge gap we require direct measurements of the gas flux along with the atmospheric and oceanic forcing conditions (wind speed, air-sea gradients of temperature and gas concentration, ice fraction, floe size distributions, etc) from which to develop and validate parameterizations.

8.3 Methods

The integration of the eddy covariance system installed by the meteorology work package with the LGR in order to make direct gas flux measurements was first undertaken for the 2014 SWERUS cruise as an ad-hoc collaboration initiated during the late stages of cruise planning. The SWERUS results were very noisy, but nevertheless provided good estimates of the gas flux when sufficient averaging was applied. The noise was thought to originate from the small overlap between the water vapour and CO_2 absorption spectra, so that the (fractionally) small contamination from variations in humidity introduces a (fractionally) large high frequency bias into the CO_2 measurement. Although the bias signal is large, it is essentially uncorrelated with the variations in CO_2 and can thus be largely removed by averaging a large number of individual estimates. For AO16 we have attempted to improve the performance of the system by adding a nafion drier to the sample line to remove most of the water vapour before the measurement takes place.

The flux measurements are ultimately combined with measurements of the forcing conditions to estimate the *transfer velocity* as a function of ice fraction.

The measurements are continuous and largely autonomous, with the exception of the need to take daily (sometimes more frequent) water sample from either the underway pumped supply or CTD bottles from which to measure the dissolved gas concentration in the upper part of the ocean mixed layer.

8.4 Instrumentation

2x LGR greenhouse gas analyzers. The first is installed in a container above the foredeck lab, the second in a weatherproof enclosure situated at below the scissor lift behind the foremast. Both systems draw samples from inlets situated on or close to the foremast. The low rate system switches between multiple inlets at different heights in order to estimate near surface gradients in concentration.

8.5 Research activities and preliminary results

Initial estimates of the gas flux have been calculated throughout the cruise. More details on preliminary results from the eddy covariance trace gas fluxes are given in the meteorology work package section. Waterside surface CO2 samples were taken throughout the expedition, typically 2 per day, with a total of 100 samples taken. A combination of samples from near-surface CTD bottles, the ship's underway line (at 8 m depth) and over the side sampling using either Niskin bottle or a custom 'fishing rod'. Gas samples were acquired from the water samples with manual equilibration using nitrogen gas, and stored for later GC analysis post-expedition.

8.6 Discussion and future analysis

A full analysis of the trace gases will take some months work. The intention is to merge the data obtained here with that from the SWERUS-C3 expedition in 2014. The two cruises sampled very different conditions in terms of both sea ice and weather and thus provide complementary. An initial analysis of CO_2 transfer velocities and test of a published gas transfer model for sea ice conditions using SWERUS data is currently in preparation for publication. Further publications are planned looking in more detail at the fluxes and at CH_4 in conjunction with the mean concentration.

Photo: Åsa Lindgren

9. Work Package: Meteorology, atmospheric boundary layer and surface fluxes (MAB)

Ian Brooks[1], John Prytherch[1], Piotr Kupiszewski[2], Anna Fitch[3], Michael Tjernström[2]

[1] School of Earth and Environment, University of Leeds,UK [2]Dept of Meteorology, Stockholm University,Sweden [3] Swedish Meteorological and Hydrological Institute, Sweden

9.1 Summary

The meteorology work package has three distinct objectives:

1) Radiosonde profiling of the thermodynamic structure of the polar atmosphere

2) Measurement of turbulent surface exchange, the surface energy balance, and evaluation of exchange coefficients over sea ice.

3) Measurement of the aerosol particles on which polar clouds and fog form

There are considerable overlaps between these areas, with many of the measurements contributing to more than one objective.

During the first week of the cruise multiple instrumentation problems arose. The most serious was the failure of the Vaisala radiosounding system. Fortunately Axel Meiton and Lars Lehnert managed to improvise a receiving station from an old broad band radio scanner, and some downloaded software developed by radio enthusiasts to pick up radiosonde transmissions (COAA SondeMonitor, http://coaa.co.uk). This system allowed the radiosonde programme to go ahead to collect data for research, although we were unable to process the data to the standard and format required by the World Meteorological Organisation for circulation to the world's weather forecast agencies for initialisation of forecast models. We were thus unable to provide near real-time data to forecast agencies as planned.

The other instrument problems were the failure of the Metek sonic anemometer on the foremast, this was replaced with a Gill sonic anemometer. The latter lacks heated sensing heads and thus suffers data losses when iced up, but otherwise functions well. The licor gas analyser on the foremast also suffered initial problems, but these were solved early on in the cruise. During the second half of the cruise issues arose with failure of the TSI Nanoscan SMPS (measurement of aerosol size distributions) and the pump in the electrostatic precipitator (collection of aerosols on grids for Transmission Electron Microscopy (TEM) analysis).

Apart from the issues above, all systems worked well, and an extensive data set has been collected. This will analysed alongside similar data from the SWERUS-C3 cruise in 2014, where an almost identical set of measurements was made.

9.2 Background

Weather forecast and climate models tend to perform poorly in the Arctic, in large part because the many parameterizations of small scale physical processes within the models are largely developed from measurements at lower latitudes under very different environmental conditions. The difficulty and expense of measurements in the Arctic means that there are few in situ measurements suitable for testing and developing more appropriate parameterizations. Cruises such as AO2016 are invaluable for making the necessary measurements.

The primary aim of the meteorology work package is the study of turbulent exchange processes between the atmosphere and ocean/sea ice under a wide range of ice conditions. Measurement of the surface turbulent fluxes of momentum, heat, water vapour, and CO_2 along with the mean environmental forcing conditions (wind speed, sea ice fraction and conditions, and the gradients in air-surface temperature and gas concentration) allow the calculation of the exchange coefficients (or equivalently the effective 'roughness length') as functions of the forcing conditions, and their parameterization for use in models.

The second area of interest is measurement of the properties of the atmospheric column from the surface, through the boundary layer, and into the upper atmosphere. These vertical profiles are required to initialise weather forecast models, and to evaluate the performance of forecast and climate models. There are very few such measurements in the Arctic Ocean, making any new measurements extremely valuable.

Finally, measurements of aerosol properties are being made to help determine the nature and source of the particles upon which cloud and fog droplets form in the Arctic. The near ubiquitous presence of low cloud or fog, and associated precipitation, effectively cleans the Arctic boundary layer, removing aerosol particles and making it one of the cleanest (lowest aerosol concentration) environments on earth. Since clouds and fog require aerosol particles for droplets to nucleate on, there is an open question as to the source and properties of these aerosols, which must be replenished against losses via precipitation.

9.3 Methods

Most measurements are continuous and autonomous (or semi autonomous) except for the radiosondes which are launched shortly before 0000, 0600, 1200, 1800 UTC.

Turbulent fluxes are measured by the direct eddy covariance technique. The mean covariance between the perturbation from the mean vertical velocity and quantity of interest define individual flux estimates over an averaging period of 20 minutes. All turbulent quantities are measured at 20 Hz (10 Hz for CO_2 concentration). The ship attitude and motion are determined from a combination of a commercial attitude and heading reference system and the ship's navigation data; these are used to correct the raw wind measurements to give true 3-dimensional wind components in the earth frame.

9.4 Instrumentation & measurements

Foremast instrumentation

- Sonic anemometer – 3 dimensional turbulent winds, 'sonic' air temperature
- Licor LI-7500 gas analyzer – water vapour concentration
- Vaisala HMP110 T/RH probe – air temperature and relative humidity
- Inlet to LGR gas analyzer (sited at base of mast) – CO_2 and CH_4 concentration

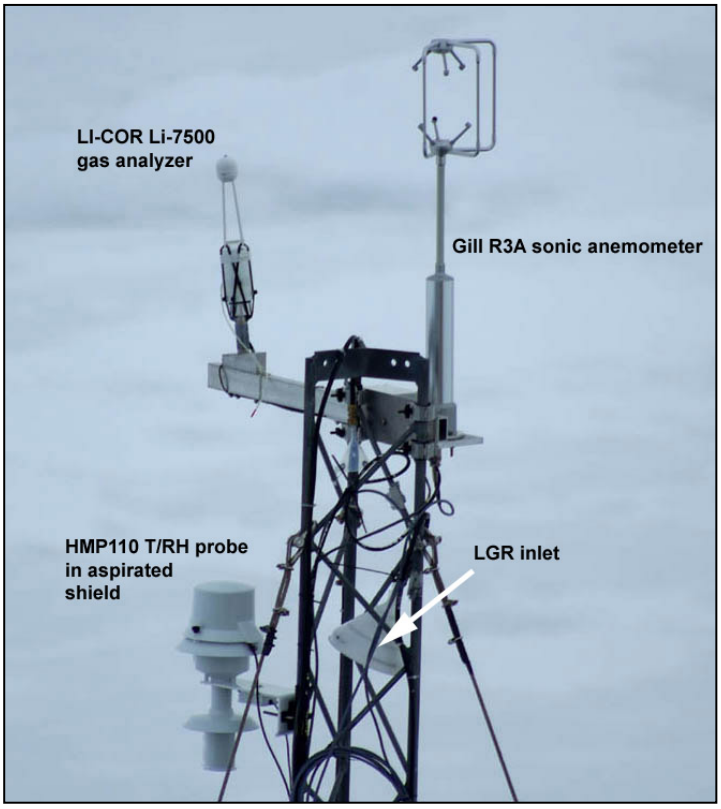

Figure 9.1 Foremast instrumentation

4th deck triple lab

- TSI Model 3910 nano-particle sizer – aerosol size distributions in the size range 10-420 nm electrical mobility diameter
- TSI Model 3330 optical particle size – aerosol size distributions in the size range 0.3 – 10 µm optical diameter
- MISU electrostatic precipitator and two particle impactors (particle collection for Transmission Electron Microscopy)

7th deck

- Radiosounding station
- 2 KT15 infrared surface temperature measurements

- FLIR ACS655sc thermal imaging camera – 10 second timelapse thermal images of the ice off port side
- 3 IP-cameras (port, forward, starboard) – 10 second (port/stb) and 60 second (forward) visible images of the surface to the horizon.
- Vaisala laser ceilometers – overhead cloud base height, cloud fraction statistics, backscatter profiles from aerosol/cloud droplets
- Weather station (air temperature, humidity, wind speed, solar and infra red radiation (downwelling))
- Cloud/fog droplet spectrometers (University of Hertfordshire)
- fog droplet collector (collection of fog water for chemical analysis)

9.5 Research activities and preliminary results

Most of the meteorological research activities require significant work to quality control all the data, merge data sets, and undertake analysis. Only very preliminary 'quick look' results are available at the time of writing.

The radiosonde programme started late, with a test launch at 1800 on 19/08/2016. From this point on, a regular schedule of launches for the standard synoptic reporting times of 0000, 0600, 1200, 1800 every day for the remainder of the cruise. The need to use 3rd party software to receive the data has complicated the data processing – most of the data quality control, filtering and smoothing of profiles carried out by the Vaisala system is not applied by the SondeMonitor software. Preliminary data quality control has been applied in Matlab, but some issues – primarily associated with 'bad' wind estimates resulting from temporary loss of the GPS fix during flight – remain to be dealt with.

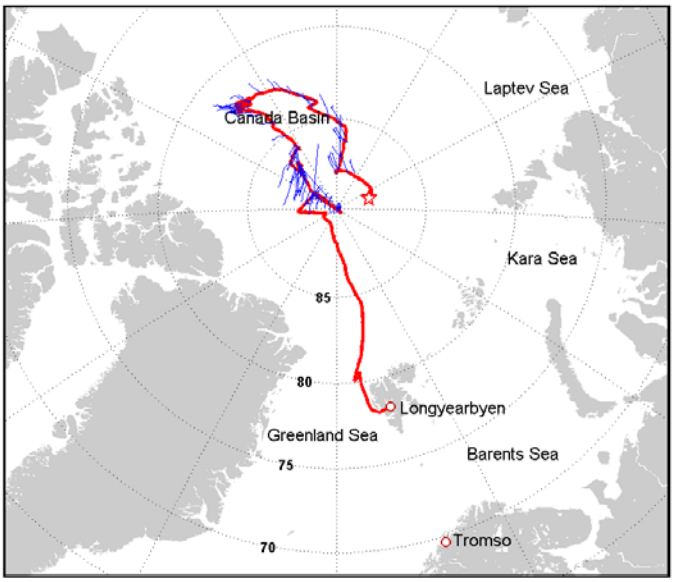

Figure 9.2 Map of cruise track to Sept 6 (red) with radiosonde ground tracks (blue)(some GPS position errors remain in this preliminary data set)

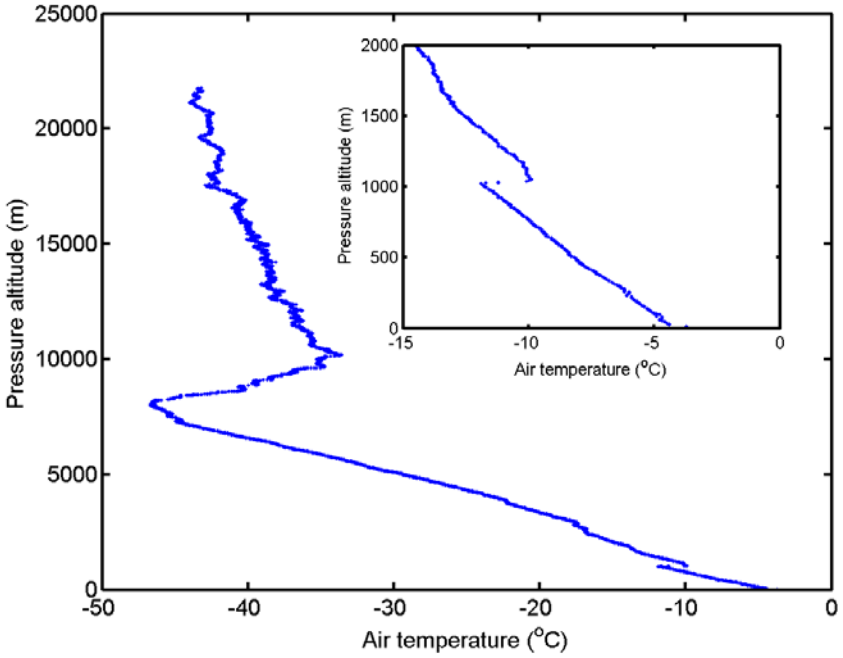

Figure 9.3 Example (preliminary) temperature profile from the radiosonde at 20160822-0600. The tropopause is clearly visible at approximately 8000 m. Inset is the lowest 2000 m, here the top of the boundary layer is visible as the sudden jump in temperature at approximately 1000 m.

Following the replacement of the Metek with the Gill R3 sonic anemometer at around 00:00 on the morning of 16-08-16, foremast measurements of 3D wind and temperature were made at 20Hz. As of the end of 8-09-16, 571 hours of measurements have been made with all required data. Several days worth of measurements have been lost to icing of the instruments, as well as data loss due to winds onto the aft. Following initial quality control, there are 495 20-minute momentum flux and 412 20-minute sensible heat flux measurements available for analysis.

Preliminary analysis of the momentum and sensible heat transfer coefficients show results of the expected magnitude over a broad range of wind speeds. Transfer coefficient dependence on sea ice conditions requires post-cruise processing of in situ and satellite sea ice imagery.

The foremast open path infra red gas analyser was operational from 26-08-16 18:00. Data was lost to icing and to cabling issues. As of the end of 8-09-16 and following initial quality control, 86 20-minute latent heat flux measurements were available for analysis. Initial analysis of the latent heat exchange coefficients shows highly scattered results. This may be due to incomplete removal of periods when the instrument was subject to icing.

The LGR eddy covariance unit has operated from 20-08-16 14:00, obtaining 468 hours of CO_2 and CH_4 flux measurements as of the end 8-09-16. Post-cruise processing of water samples is required before gas transfer velocities can be calculated. Initial examination of CO_2 cospectra from the system show gas flux is being measured. They also appear to show that the use on this expedition of Nafion driers to dry the airstream and reduce the effect of water-vapor induced density fluctuations has reduced the measurement noise level by an order of magnitude compared with a previous expedition on Oden.

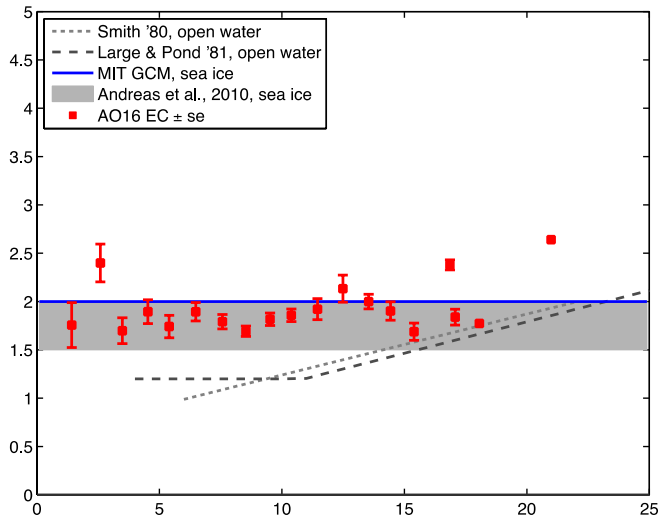

Figure 9.4 Preliminary drag coefficient dependence on wind speed. Individual measurements binned in 1 $m.s^{-1}$ wide wind speed bins. Example wind-speed and sea-ice concentration dependent parameterisations are also shown. Shaded area of the Andreas et al., 2010 parameterisation represents sea ice concentrations from 0 to 100%.

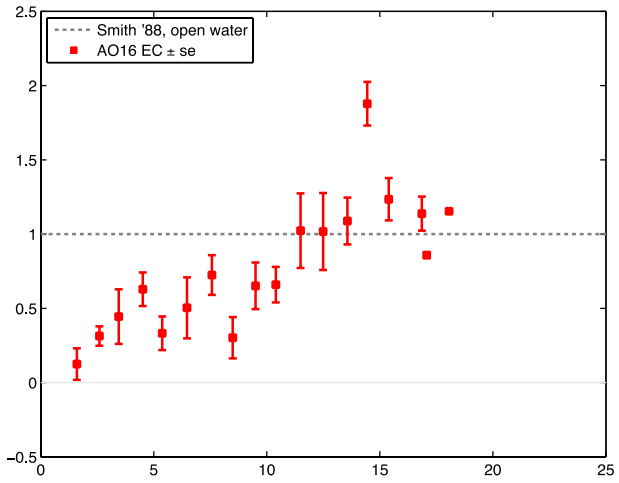

Figure 9.5 Preliminary sensible heat transfer coefficient dependence on wind speed. Individual measurements binned in 1 $m.s^{-1}$ wide wind speed bins.

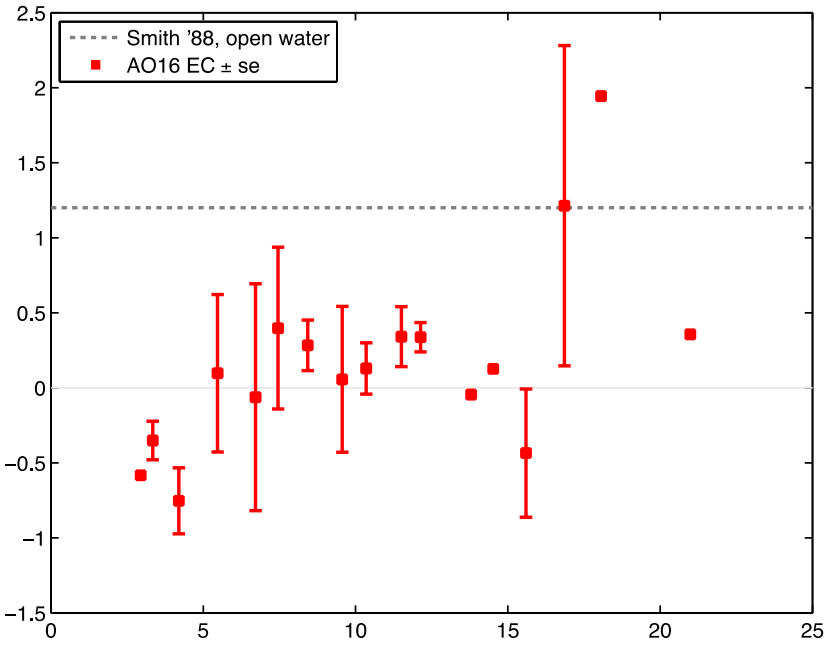

Figure 9.6 Preliminary latent heat transfer coefficient dependence on wind speed. Individual measurements binned in 1 $m.s^{-1}$ wide wind speed bins.

Figure 9.7 Example LGR CO_2 spectra, and corresponding cospectra and ogives (cumulative cospectra) of momentum, sensible heat and LGR CO_2 flux measurements.

Aerosol size distributions in the size range of 10 nm to 10 µm were measured continuously throughout the cruise with one minute time resolution using a setup consisting of a NanoScan SMPS and an Optical Particle Sizer (both produced by TSI). The aerosol particles are sampled using a PM 10 inlet (only particles smaller than 10 µm are sampled) located on the roof of the 4th deck triple lab container. The sample flow is transferred into the lab where it passes through a series of driers before entering the NanoScan SMPS and OPS. Aerosol particles were also collected on grids using an

electrostatic precipitator (built at MISU) and two particle impactors for subsequent analysis using Transmission Electron Microscopy. During a number of ice stations the electrostatic precipitator was deployed on the ice, away from the ship, to ensure sampling in pristine conditions. The TEM grids will be analysed at Stockholm University providing information on the particle morphology and chemical composition.

Concurrent to the aerosol measurements, fog water is collected using the MISU fog sampler located on the railing of the 7th deck. The fog sampler fan is activated when visibility drops below a defined threshold aspirating air through the device. Droplets in the air are thus impacted on Teflon strands within the fog sampler and are subsequently collected in bottles. The samples, each of which takes several days to collect, are stored at -80°C; chemical analysis of the samples is subsequently conducted at MISU.

9.6 Discussion and future analyses

Analysis of the meteorological data will take some time. Much of the analysis of turbulent fluxes will be merged with that of data from the SWERUS cruise. Significant work is required to quality control the many different measurements, and combine raw measurements to produce user-ready final data sets. There are proposals pending for analysis of the turbulent flux data and implementation of parameterizations in the CICE sea ice model (Leeds/University College London) and implementation and testing of surface heat flux parameterizations in the HARMONIE climate model (SMHI).

The measurements of aerosol particles need to be carefully filtered for pollution events, most notably from the ship and helicopter exhausts. This is particularly important in view of the pristine conditions in the Arctic, where any contamination can greatly skew the measured concentrations and size distributions. Filtering for pollution events requires an analysis of the aerosol concentrations (identification of suspect spikes in the data) in conjunction with an analysis of the wind direction, as well as the ship and helicopter operations. The processing of Transmission Electron Microscope samples and fog water samples, which is not possible on board, will be carried out at MISU after the expedition demobilization.

Acknowledgements

The meteorology team would like to thank Axel Meiton and Lars Lehnert for their work improvising a replacement radiosonde receiving system. We would also like to thank Bev Ewen-Smith, developer of the SondeMonitor software, for providing us with a free licence while at sea and for answering questions about the output files and data processing carried out by his software.

10. Work Package: Ice management (IM)

Runa A. Skarbø, Hans-Martin Heyn, Jon Bjørnø, Sveinung Løset* and Roger Skjetne* (* shorebased)

SAMCoT (Sustainable Arctic Marine and Coastal Technology), Norwegian University of Science and Technology, Norway

10.1 Summary

With the recession in sea ice in recent decades, an increase in marine operations in the Arctic is expected. Technologies for safe and sustainable operations are keys in this remote and vulnerable region. This report describes the data collection and work performed by the ice management work package on board Oden on the expedition Arctic Ocean 2016.

The participants of work package Ice Management are a part of SAMCoT (Sustainable Arctic Marine and Coastal Technology), a larger project dedicated to create a better understanding of engineering and physical modelling in the Arctic. The work is a continuation of previous work and data collected on Oden.

We have collected screenshots of the radar operator station at selected locations when the vessel was stationary or drifting and for some transit legs. Four inertial measurement units mounted on different location in the vessel monitored the motions of the icebreaker during icebreaking operations and drifting in sea-ice. A system of 11 cameras continuously monitored the ice conditions around and ahead of the vessel. We have also performed a calibration check on pitch, rpm, power and torque, on the request from SAMCoT partners. Lastly, data from a global navigation satellite system (GNSS) at high latitude has been sampled.

Future analyses will aim at using these data in short-term prediction of short-term local ice drift around the vessel and global ice forces on the vessel. The camera footage will be used to estimate the local ice concentration, floe size distribution and possibly identify ice features such as ridges and melt ponds.

10.2 Background

The Swedish Polar Research Secretariat (SPRS) and the Norwegian University of Science and Technology (NTNU) have previously cooperated on three research cruises, the Oden Arctic Technology Research Cruise 2012 (OATRC2012), OATRC2013 and OATRC2015. Since 2015, SPRS has been a partner of SAMCoT (Sustainable Arctic Marine and Coastal Technology), a Centre for Research-based Innovation funded by partners and the Norwegian Research Council, and hosted by NTNU. SAMCoT has since 2008 been dedicated to do research on technology that makes the exploration of Arctic resources

safe and sustainable. The research activities in WP Ice Management (IM) on Oden on the Arctic Ocean 2016 (AO2016) cruise continue the previous research activities on Oden.

With the recession of Arctic sea ice seen in recent decades, an increase in marine offshore activities in the Arctic is expected. The US Geological Survey has estimated that approximately 25 % of the remaining hydrocarbon resources are located in the Arctic (Gautier et al. 2009). In addition, increase in fisheries in the marginal ice zone, marine transport and logistics to support communities and natural resource exploration and exploitation are expected.

Even with reclining sea ice, the Arctic is not ice-free. The presence of sea ice makes marine operations challenging, and the need for stationkeeping in ice requires ice management. (Eik 2008) has proposed the following definition for ice management:

Ice management is the sum of all activities where the objective is to reduce or avoid actions from any kind of ice features.

The definition of ice management includes actions such as detection, tracking and forecasting sea ice, ice ridges and icebergs, threat evaluation, physical ice management such as ice breaking and iceberg towing and procedures for disconnecting of offshore structures.

The work of WP IM on AO2016 is focused on ice drift detection and forecasting using several different methods and sensors. As a request from a SAMCoT partner, ExxonMobil, they wanted to do a calibration check of pitch and torque. These calibrations would be useful to them for processing the OATRC2015 data.

10.3 Methods

We collected data at different locations depending on the operation status of the vessel. Data has been collected using marine radar images.. Four inertial measurement units mounted on different location in the vessel monitored the motions of the icebreaker during icebreaking operations and drifting in sea-ice. A system of 11 cameras continuously monitored the ice conditions around and ahead of the vessel.

Marine radar image acquisition

Screenshots were collected from the marine radar operator screen on Oden. The port side radar screen of the two radar screens on Oden bridge was selected for capture. The range of the radar screen was set to 3 or 6 nautical miles before logging. The radar operator was asked to remove any rings or other disturbing objects such as the mouse in the PPI image.

The screenshots of the marine radar operator screen were captured using a VGA splitter (ATEN Video Splitter 2P), an Epiphan DVI2USB 3.0 frame grabber with proprietary software installed on a connected laptop running Windows 8. Screenshots were collected with a frequency of 0.2 Hz during drift and 1 Hz during transit. The screenshots images have a resolution of 1920 x 1200 pixels in .png format, on average 3,2 MB in size. Simultaneously to the screenshots, the ship's NMEA data stream of the ship was logged.

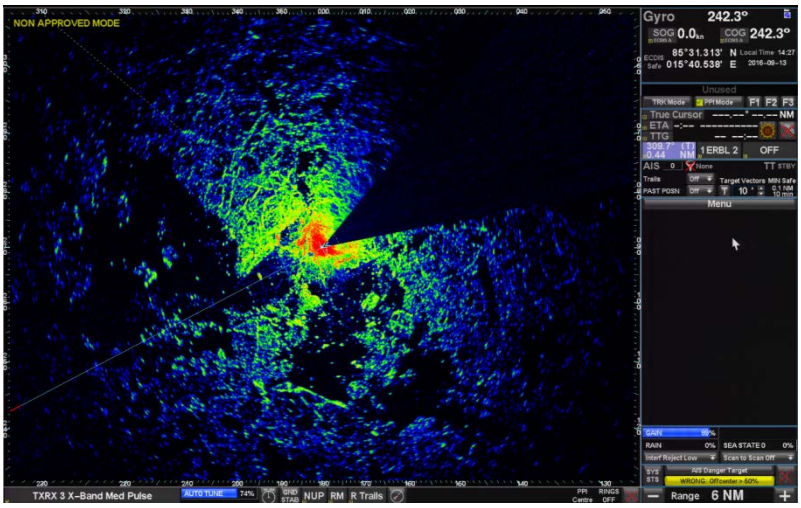

Figure 10.1 Screenshot of radar operator station while the vessel is in ice.

IMU system

Four inertial measurement units (IMUs) mounted on different positions of the vessel record the global motions of the icebreaker. The data is recorded with a frequency of 300 Hz and the sensors are synchronised with the ship's GPS time.

Camera system

Three camera systems with a total of 11 camera lenses record the ice conditions around the vessel. Six camera lenses monitored a 360° field-of-view around Oden. Four camera lenses monitored a 180° field-of-view ahead of Oden towards the horizon. A single lens camera monitored the ice conditions port of Oden. The images were taken at least every second during the entire expedition.

GPS quality measurements

GPS data was collected using a GNSS receiver (a u-Blox EVK-6T-0-001), a GNSS antenna (with cable), a USB cable (USB-A to USB-B) and a computer with python installed.

Calibration check

Manual recordings of the rpm, power and torque values were obtained by filming the gauges and then compared against the SPRS log. The time on the camera and in the log is synchronised, such that data can be compared easily.

The pitch angle was set manually in the engine room, first to full ahead, then in intervals on 5 degrees to full astern. Each position was held for 2 minutes, such that it is easy to extract an average value from the SPRS log. Then the average SPRS log readings were plotted against the pitch angle. This procedure was used for both starboard and port side propellers.

10.4 Research activities and preliminary results

Radar system

A total of 16 data series was collected with radar image screenshots. Eigth data series has been collected while in transit in low speed (or partial transit during logging), while the rest was collected while drifting in the ice.

IMU system

During the expedition, 133 sets of motion data were taken during drifting and transiting in ice. Around 20 reference datasets were taken during operations in open-water. A total of about 300 hours of measurements were taken during the expedition.

Camera system

The camera system operated constantly during the entire operation with at least one image per second. On the 3rd September, the frequency was increased to two images per second for the remaining time of the expedition due to enough available data storage. Time-lapse movies of each day for the 180° camera system were created already during the expedition.

Calibration check

Figure 10.2 and 10.3 shows that the results for both starboard and port side are as expected. They have both a linear trend, and the deviations may be to human error when setting the pitch angle manually. ExxonMobil expected a slightly nonlinear relationship between the log and the pitch, as their data from last expedition showed that.

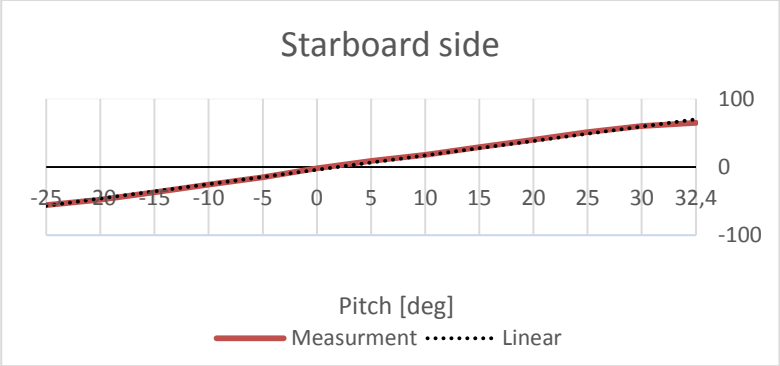

Figure 10.2 Pitch calibration for starboard propeller.

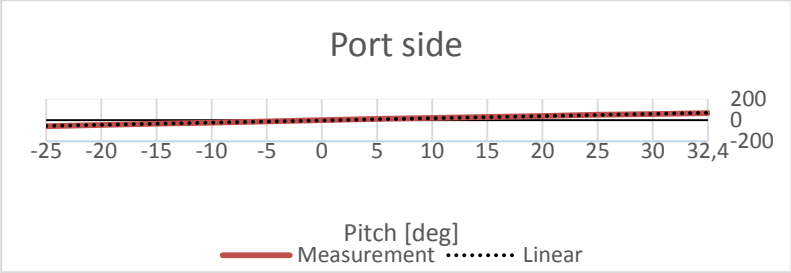

Figure 10.3 Pitch calibration for port propeller.

Figure 10.4 shows that the rpm gauge and the log, for port side, shows the same value, but since the gauge is analogue, it will jump a little. So the values between the log and gauge is expected, but for the starboard side this is not so. RPM calibration for starboard propeller. Figure 10.5 shows the log is off by 11 rpm compared to the gauge. The gauge is the one that is correct, since the propellers had the same settings.

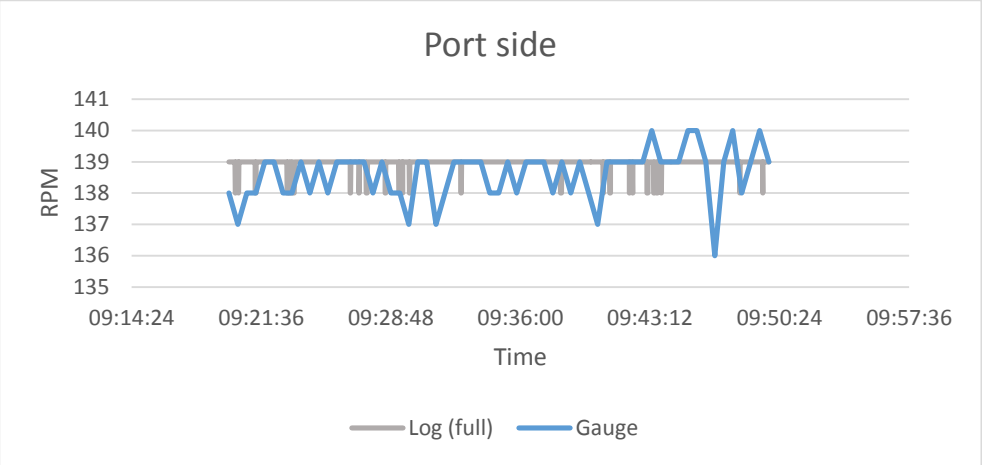

Figure 10.4 RPM calibration fort port propeller.

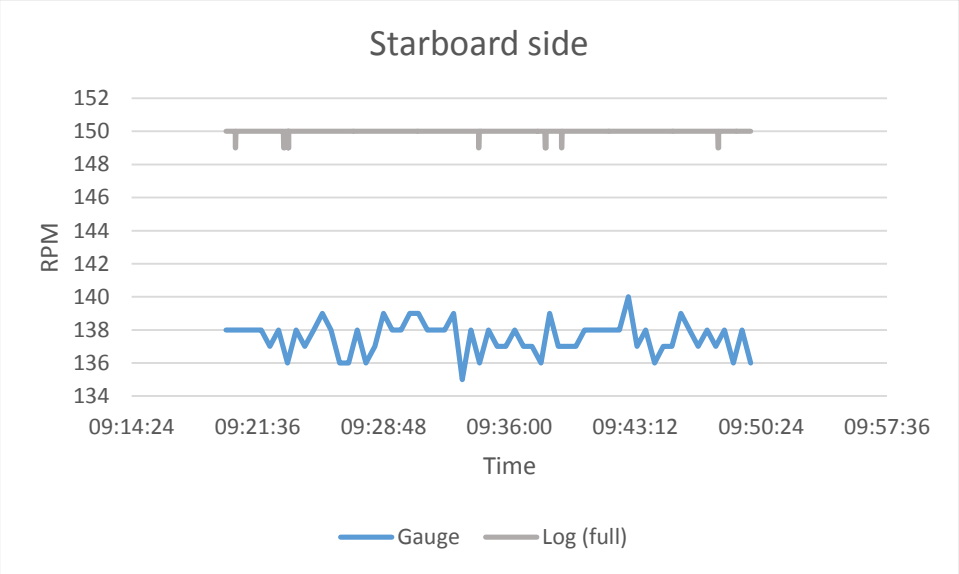

Figure 10.5 RPM calibration for starboard propeller.

When it comes to the torque, there is a time delay between the log and the observed value on the gauges. From Figure 10.6 this offset can be seen, and the shape of the different methods are similar. In Figure 10.7 the log has a little offset from the gauges for the starboard side, and the same time delay.

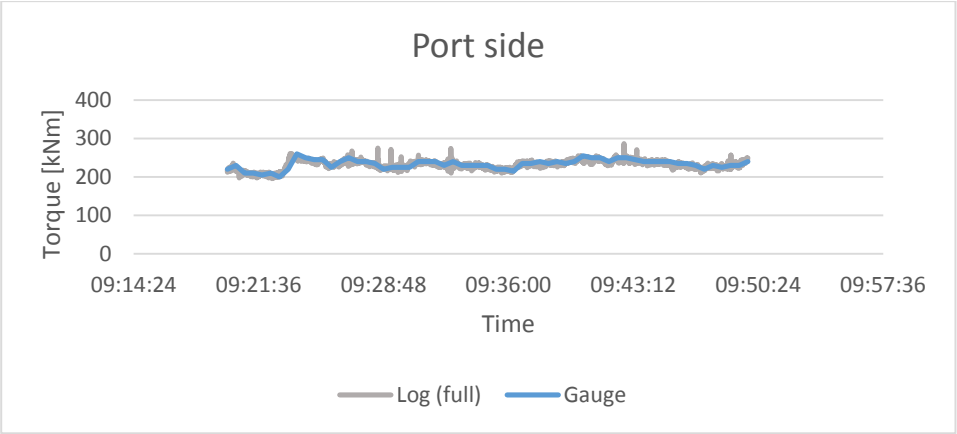

Figure 10.6 Torque calibration for port propeller.

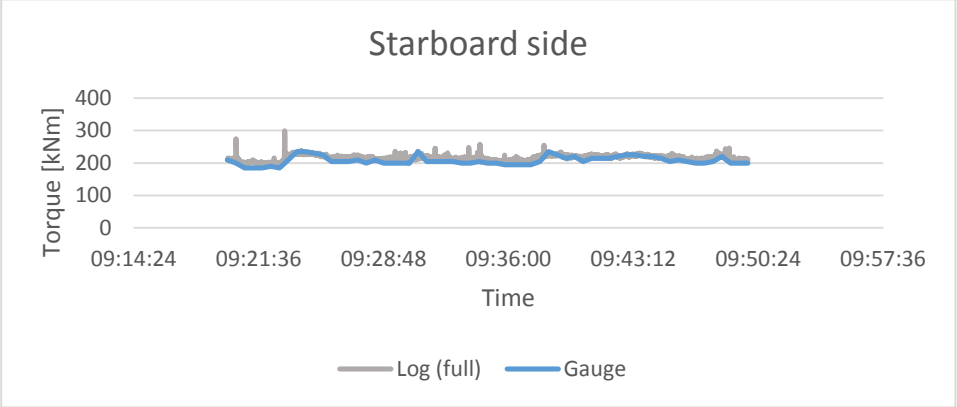

Figure 10.7 Torque calibration for starboard propeller.

From Figure 10.8 and Figure 10.9 it can be seen that the monitor has an offset both with the time delay and the value. The reason for this is unknown, since this should be the same. The monitor updates itself every 10 seconds, so this could contribute to the offset in value, but not in time.

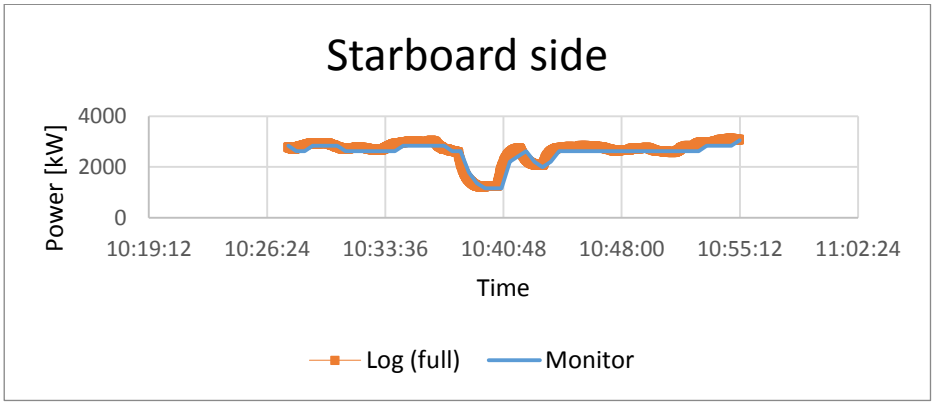

Figure 10.8 Power calibration for starboard propeller.

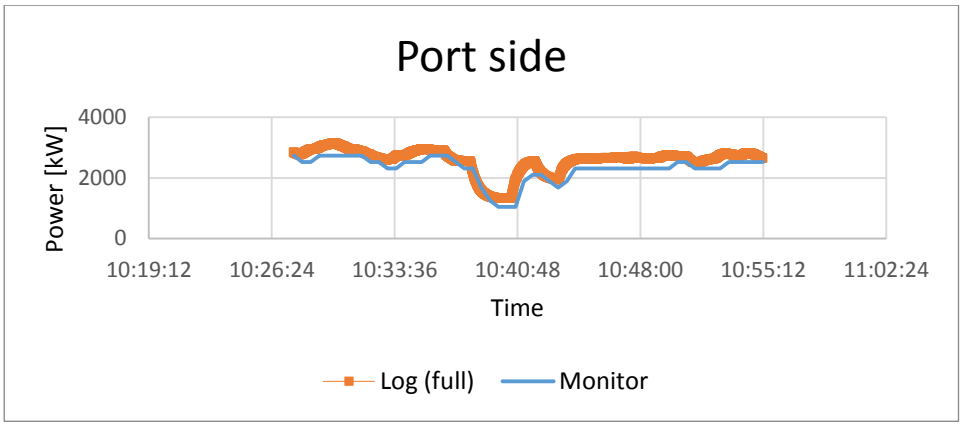

Figure 10.9 Power calibration for port propeller.

GPS system

The GPS system recorded 300 hours of satellite tracking data.

10.5 Discussion and future analyses

The collected data series of radar images will be used as input to a real-time algorithm developed to detect the ice drift around the vessel. The motion data will be used for the estimation of extreme ice accelerations based on signal detection techniques and spatial and frequency sensitive detection of accelerations in ice-infested waters in order to determine e.g. the ice drift around the vessel. The images from the camera system will serve as a reference for the motion data recorded by the inertial measurement units. Furthermore, the images will be used to develop detection algorithms that determine the ice concentration around the vessel, the flow-size distribution and further features of the ice, e.g. colour, thickness and possibly porosity.

We aim to compare the results of ice drift prediction by the three different estimation techniques.The calibration data will be used by ExxonMobil to process their OATRC2015 data, as well as other Oden expeditions could benefit from this information. As a remark, there have been some changes to the control system during the spring of 2016, so the calibration data for rpm, power and torque may deviate from earlier log files from other expeditions. There are also some problems with an uncertain time delay that occurs. For the pitch calibration, this upgrade should not have affected how the angle is measured. So the calibration data collected for the pitch angle is probably the same as the earlier expeditions.

10.6 References

Eik, K. (2008), 'Review of experiences within ice and iceberg management', *Journal of Navigation* 61(04), 557–572.

Gautier, D. L., Bird, K. J., Charpentier, R. R., Grantz, A., Houseknecht, D. W., Klett, T. R., Moore, T. E., Pitman, J. K., Schenk, C. J., Schuenemeyer, J. H., Sørensen, K., Tennyson, M. E., Valin, Z. C. & Wandrey, C. J. (2009), 'Assessment of undiscovered oil and gas in the Arctic', *Science* 324(5931), 1175–1179.

11. Work Package: Heavy metals and Microplastics – Water, Sea-ice & snow and Air (HM)

Katarina Gårdfeldt[1], Michelle Nerentorp Matrsomonaco[1], Sofi Johnsson[2], La Daana Kanhai[3]

[1]Department for Chemistry and Chemical Engineering, Chalmers University of Technology, Sweden, [2]Department for Marine Sciences, University of Connecticut, US and Centre for Environment and Sustainability, University of Gothenburg, Sweden
[3] Marine and Freshwater Research Centre, Galway-Mayo Institute of Technology, Ireland

11.1 Summary

The WP Heavy Metals consisted of six sampling matrixes; water, air, snow, ice, brine and frost flowers. The air sampling program was part of the SPRS Monitoring Test Program. The focus was on measuring inorganic and organic fractions of mercury species and plastic microfibers in the six sampling matrixes, respectively.

During the expedition we conducted process studies in sea-ice and water in order to contribute to the understanding of how sea-ice affects the marine biogeochemistry, with emphasis on heavy metals and their methylation. This is essential to accurately predict past, present, and future climate change responses of marine ecosystems in both the polar and global oceans (Steiner 2016). At selected sea-ice-stations sea-ice cores were sampled and analysed with respect to mercury species and microplastics. Samples was either analysed in lab on board IB Oden or stored and analysed in lab after the expedition. Two helicopters and bear guards were available on IB Oden to assist the ice-coring operations on selected ice-flows along the expedition route.

11.2 Background and aims

Mercury is a well-known global pollutant which impacts human health and the environment all over the globe. The overall aim of this WP was to investigate the importance of sea-ice mediated cycling of mercury and to study the abundance of microplastic particles in the Arctic Ocean environment.

It is generally believed that sea-ice in Polar Regions acts as a cap for dissolved gaseous mercury (DGM) in seawater and therefore prohibits mercury evasion from sea surfaces to the atmosphere. In a recent study, we have seen that DGM is formed within the sea-ice in the presence of sunlight both at Arctic and Antarctic sites (Nerentorp Mastromonaco et al., 2016). We have achieved data that show a diurnal variation of mercury species in sea-ice and water during the polar summer. During the AO16 expedition we performed pioneering studies of mercury species in air, water and sea-ice during polar summer by parallel measurements of inorganic and organic fractions of the metal. The overall goal of the study was to estimate the effects and implications for the transformation pathways of mercury with relevance for the global cycling of the metal, due to future warming and shrinking sea-ice coverage in Polar Regions.

There is currently a paucity of information regarding microplastics in Polar Regions. To date, only two studies (Amelineau et al., 2016; Lusher et al. 2015; Obbard et al. 2014) have reported on microplastics in the Arctic Ocean. In the context of a changing climate, it is important to understand the dynamics of microplastic accumulation in the Arctic Ocean (i.e. their transport to Arctic Ocean, their entrainment in sea-ice, etc). The objectives of the investigations of microplastic particles during AO16 was first to assess microplastic abundance, distribution and composition in sub-surface waters of the Arctic Ocean, and secondly to assess whether sea-ice acts as a sink for microplastics.

Short survey of the field

Mercury

Global warming is changing the sea-ice and snow coverage in the marine polar environment. Global warming has also an impact on the surface energy budget, biological/ecosystem functions and chemical processes in the polar environment. Energy, biology and chemistry systems are coupled, with numerous feedbacks and interactions. For example, changing sea-ice regimes in the Arctic (e.g. shifts from multi-year to first year sea-ice) will impact biological systems and productivity, which in turn may impact trace gas fluxes. Changing sea-ice and snow regimes will also impact transport and fate of contaminants like persistent organic pollutants (POPs) e.g. DDT and PCB, mercury, and other heavy metals. It is known that the role of the surface-ocean and marine boundary layer in global mercury cycling is a function of sunlight and the presence of halocarbons from biological activity in the ocean surface. Oxidation of mercury in the marine boundary layer and in the free marine troposphere is likely to be coupled to photochemistry involving halogens partly originating from halocarbons emitted from the sea surface.

The response time of ecosystems to reduced mercury emissions is long and variable due to the storage of mercury in top soils and in the ocean. The ocean plays a key role in regulating the atmospheric burden of mercury as amounts of mercury are deposited to the world's oceans via dry and wet processes. A large part of this deposited mercury is efficiently re-emitted back to the atmosphere. These fluxes are to a large extent governed by complex chemical and biogeochemical processes where mercury is transformed between different oxidation states with different chemical and physical properties.

Ionic mercury in water is subjected to particle scavenging, transportation, and transformation processes. Andersson et al., (2008b) have shown that sea-ice may act as a barrier for evasion of mercury from the Arctic Ocean and Pirrone et al., (2010) estimated that that emissions from oceans contributed to about 50% of the natural emissions. Preliminary models suggest that emissions from the Arctic Ocean are more dominant in the polar summer (Orderdalen Steen, 2011). The major knowledge gap, however, on mercury loading in Polar environments is the knowledge of trends in mercury concentration patterns, both during Polar night and summer. Moreover, transformation processes of mercury in the sea-ice need to be further investigated in order to assess the influence of climate change on mercury as a global pollutant. These transformation

processes control the availability of mercury to bioaccumulate in marine food webs and thus the risk of mercury pollution for human and wildlife health. The methylated pool of mercury in marine waters exist in two chemical forms, mono- and dimethylmercury. Monomethylmercury is the main form of mercury to accumulate in organism. A large fraction of the methylated mercury pool in marine waters (up to 80 %) however occurs as dimethylmercury (Soerensen et al 2016 and references therein). The role of dimethylmercury for the biogeochemical cycling of mercury in marine systems is largely unknown. However, degradation of dimethylmercury in the atmosphere and in marine waters have previously been hypothesized to be an important source of monomethylmercury (Soerensen et al. 2016). For the Arctic System, a major source of the uncertainties in our understanding of the biogeochemical cycling of mercury comes from lack of data from large parts of the ocean, including the central Arctic Ocean. So far, only the concentration of the total methylated pool has been determined from the central basin from a few stations (Heimbürger, 2015), and no data on dimethylmercury concentrations are available.

Microplastics

Microplastics, i.e. plastic particles < 5 mm in diameter, in the world's oceans are an issue of global importance due to the fact that they are ubiquitous, persistent and a potential threat to marine organisms (Arthur et al. 2009; UNEP 2011). The presence of these particles has been reported in the aquatic, sediment and biotic environmental phases of the marine environment (Lusher 2015). Despite the seeming abundance of information regarding microplastics in the world's oceans, there are many knowledge gaps which remain.

To date, there have only been two studies to report on the presence of microplastics in Arctic waters (Amelineau et al. 2016; Lusher et al. 2015). The overall findings of the study conducted in surface and sub-surface waters south and south-west of Svalbard, Norway indicated that microplastic abundances in the Arctic were similar to those previously reported in other areas (Lusher et al. 2015). With respect to the study conducted in waters east of Greenland, microplastic abundances were comparable to those reported in other oceans despite the remoteness of the study area (Amelineau et al. 2016). Furthermore, Obbard et al. (2014) was the only study to report on the presence of microplastics in sea ice cores (n = 4) in that region. It is important to note that the concentrations of microplastics in the sea ice from the Arctic (38 to 234 particles per cubic meter of ice) were orders of magnitude greater than those that had previously been reported in highly contaminated waters of the world's oceans e.g. the sub-tropical gyres (Obbard et al. 2014). Based on the findings of the study, Obbard et al. (2014) suggested that the Arctic possibly acts as a sink for microplastics and that the particles are entrained in sea ice during its formation.

Due to the paucity of information regarding microplastics in the Arctic Ocean, sub-surface waters and sea ice cores were analysed for microplastics during the Arctic Ocean 2016 expedition.

Overview of measurements during the AO16 expedition

Seawater was continuously sampled using the ship bow water system. Under ice water, sea-ice, brine, frost flowers, melt pond water and snow samples were collected along the expedition route at ice stations reached by mummy chair or helicopter. Continuous air measurements of mercury species in air were performed as part of the air monitoring program onboard the ship. For an adjacent WP (i.e. Physical Oceanography), seawater samples for measurements of mercury species, microplastic and particles in deep subsurface profiles were collected with a device on board measuring oceanographic conductivity, temperature depth (CTD), equipped with 24 bottle Rosette. The analytical methods used are described in Gårdfeldt et al. (2002) and Lamborg et al. (2012).

Samples for analyses of dimethyl- (DMHg) and monomethyl mercury (MMHg) were taken and analyzed during and after the campaign, respectively. Discrete samples for determination of DGM in sea-ice and seawater were taken at various stations using techniques described in Gårdfeldt et al. (2002) and Nerentorp Mastromonaco et al. (2016a). Continuous underway measurements of DGM along the cruise track were obtained with high time resolution (every 5 to 10 min) in seawater using the ship bow water system and a continuous system for DGM determination developed by our team (Andersson et al., 2008a). Continuous measurements of plastic micro particles were performed also using the ship bow-water system. During the expedition we also conducted an air monitoring program for continuous measurements of gaseous elemental mercury (GEM), gaseous oxidized mercury (GOM), and particulate mercury (HgP) in air using a Tekran 2537A and 1130/35 mercury fractionation system. After the expedition, data from the continuous DGM and GEM measurements were used to estimate the net flux of gaseous mercury according to wind models presented by e.g. Wanninkhof (1992) and Johnson (2010).

In summary, the measurements onboard IB Oden and on ice flows reached by helicopter during the expedition, was directed to I) investigate sea-ice and under ice water with respect to variations in concentrations of dissolved gaseous mercury and other species such as divalent and methylated mercury, II) assess mercury speciation during various light conditions as well as the influence of photo reduction of divalent mercury in sea-ice and water as well as DMHg in water, III) assess the influence of diminishing sea-ice on the evasion of gaseous mercury from polar regions, IV) investigate mercury deposition patterns in sea-ice and seawater in relation to environmental parameters, e.g., sea-ice extent, insolation, humidity, temperature, and wind V) investigate sea-ice, under ice water and subsurface seawater profiles with respect to abundance of microplastic particles.

11.3 Methods and equipment

Continuous measurements of mercury species in air

Mercury species in air were measured aboard the IB Oden using the Tekran mercury speciation system which constitutes of the Tekran 1130/1135 sampling modules for oxidized mercury fractions in combination with the Tekran 1130 pump module and the Tekran 2537B CVAFS mercury detector (Lindberg et al., 2002).

The speciation system consist of an outdoor unit (1130 + 1135, Figure 11.1), used for fractionation of gaseous elemental mercury (GEM), gaseous oxidized mercury (GOM) and particulate mercury i.e. oxidized mercury bound to particles (HgP) and an indoor unit for determination of atomic mercury originating from desorption of the three fractions respectively, using Cold Vapour Atomic Fluorecence (CVAFS) (Lindberg et al., 2002). The outdoor equipment was installed on the 4th deck in the fore of the ship to avoid influences from the ship funnel and the indoor equipment was installed in a container on the 4th deck. A schematic presentation of the system is shown in Figure 11.1. The system used is further described in Nerentorp Mastromonaco (2016). The instrument was maintained according to the standard operational procedure developed within the EU project Global Mercury Observation System (GMOS).

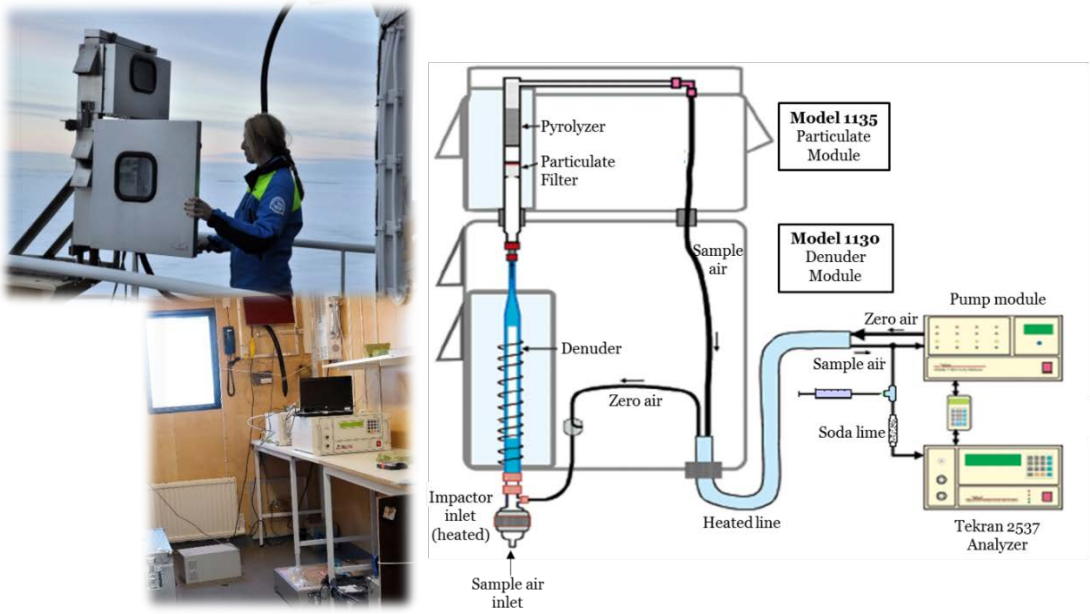

Figure 11.1. The Tekran 1130/35 mercury fractionation unit used onboard IB Oden to measure oxidized mercury species (GOM + HgP) in air.

Continous measurements of dissolved gaseous mercury in seawater

The measurements of dissolved gaseous mercury in seawater (DGM) was performed using the ship bow water system, continuously recorded with 5 min resolution. The method for continuous measurement of DGM is presented in Andersson et al., 2008a and Nerentorp Mastromonaco (2016). The instrumental setup consists of an extractor in which a stream of air is equilibrated with seawater in a constant flow system. During the extraction, mercury in the air stream is brought into equilibrium with DGM in the seawater. The air is then fed to a Tekran 2537A CVAFS mercury detector with which the concentration of mercury is continuously measured with suitable high time resolution. The water to be extracted is provided from the bow water system of the ship. The extractor and the experimental set-up are presented in Figure 11.2.

The principle of this method relies on the fast equilibrium between DGM and air during the extraction, according to:

$$DGM \Leftrightarrow Hg_{(air)} \qquad K_H = \frac{[Hg_{(air)}]}{[DGM]} \qquad \Rightarrow \qquad [DGM] = \frac{[Hg_{(air)}]}{K_H}$$

From determining the mercury concentration in the air stream the true DGM concentration in the water phase can be calculated using the Henry's Law equation. This system has been used on several research expeditions in the Mediterranean Sea as well as in the Arctic and Antarctica (Andersson et al., 2008b; Andersson et al., 2011; Andersson et al., 2007; Nerentorp Mastromonaco et al., 2016b). The DGM instrumental setup will further be equipped with a system for remote monitoring of the measurement performance and data transfer.

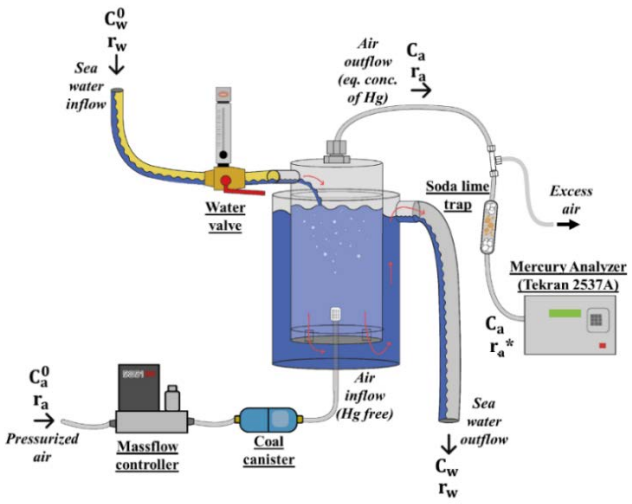

Figure 11.2 Opposite flow DGM extraction system. The seawater from the ship bow water system enters at the top of the extractor while air is introduced at the bottom. The equilibrated air with the mercury concentration C_a and air flow rate r_a is leaving the extractor at the top and is fed to a Tekran 2537A mercury detector (Nerentorp Mastromonaco, 2016).

Methylation and demethylation assays

To measure the rate of formation and degradation of monomethylmercury, methylation and demethylation assays were conducted. Seawater from different stations and depth were sampled in 250 ml glass flasks. The flasks were carefully overfilled with ca 500 ml sample water to limit additional oxygen to be dissolved in the water during the sampling. These were then capped and isotopically enriched mercury standards were added. The water was then incubation dark in 4°C for 0-16 h. Incubations were terminated by adding trace metal clean sulfuric acid to a final concentration of 0.4 %. All samples were stored cold and shipped to the Department of Marine Sciences, University of Connecticut (USA) for analysis using gas chromatography coupled to inductively coupled plasma mass spectrometry. The methylation and demethylation rates (k_m and k_d, d^{-1}) are calculated from the amount of methylmercury formed from added inorganic mercury tracer and the amount of methylmercury degraded from added methylmercury tracer.

Bacterial samples were also collected from the different waters collected by filtrating 600 ml sample onto sterivex filtrations units and stored at -80°C. These samples were then shipped on dry ice to Prof. Stefan Bertilsson's laboratory at Uppsala University to investigate the occurrence of the hgcAB genes that are identified as essential in bacterial strains known to methylated inorganic mercury to monomethylmercury.

Microplastics in sub-surface waters

Sampling of microplastics in sub-surface waters was conducted using the bow water system of Oden (seawater from 8.5 m depth) following Lusher et al. (2014). Filter papers for each sample were shipped to the laboratory for visual identification of potential microplastics followed by FT-IR spectroscopy analyses for identification of polymer type.

Mercury in sea-ice, under ice water, snow and frost flowers

Discrete samples of snow, sea ice, brine, frost flowers and under ice water for determination of elemental mercury at a total of 26 ice stations, see Fig. 11.3. The ice stations were reached by helicopter (21 stations), via gangway or mummy basket (5 stations), see Fig. 11.4a.

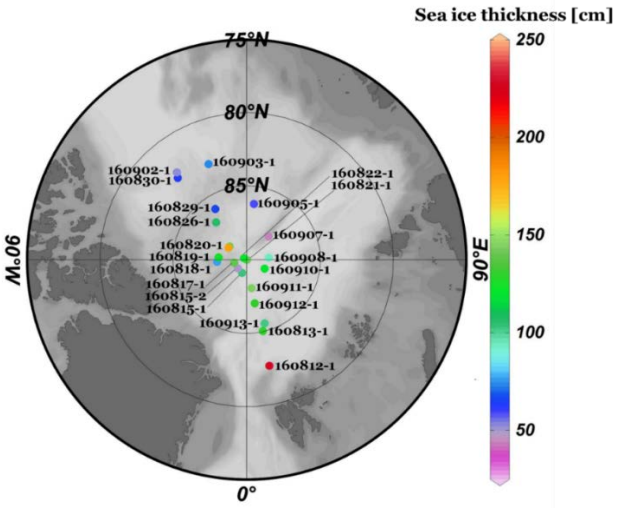

Figure 11.3 Map showing the locations of the 26 ice stations visited for sampling during the AO16 campaign. The colours represent the average sea ice thickness obtained from measuring the length of obtained ice cores (Nerentorp Mastromonaco, 2016).

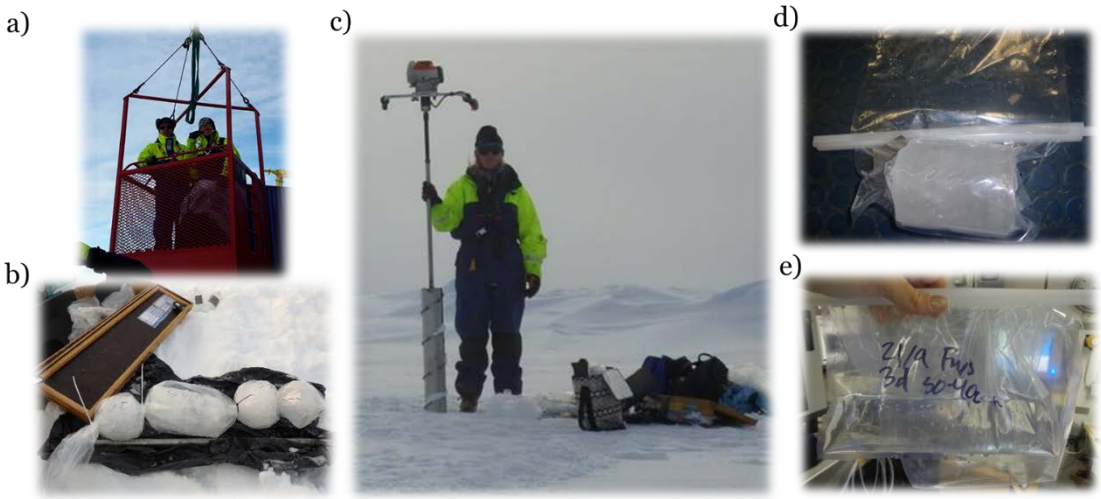

Figure 11.4 a) Mummy basket used for reaching ice stations, b) sampled ice core, c) corer used for sampling ice cores on ice stations, d) cut ice sample and e) melted ice sample ready for analysis. (pictures: Michelle Nerentorp and La Daana Kanhai)

Ice cores were sampled from clean areas that were shovelled from snow just before coring. The corer was made of stainless steel, having a diameter of 12 cm and was powered by a gasoline motor (Fig. 11.4c). The ice core obtained within the corer was often cracked into several pieces that were ordered and aligned in blank tested LD-PE bags that were put in black plastic bags for transportation back to the lab on board, see Figure 11.4b.

In the lab the ice cores were sawed into approximately 10 cm pieces using a stainless steel saw which were put into gas tight blank tested LD-PE bags (Fig 11.4d). The frozen ice samples were let to slowly thaw in room temperature covered by dark bags until totally

melted (Figure 11.4e). The melted ice samples were analysed for elemental mercury using a manual purge and trap method, presented in chapter 7.3 and in Nerentorp Mastromonaco, 2016.

The temperature of the ice was measured in a reference ice core sampled in conjunction to the sample core. Small holes were drilled every 5 to 10 cm and the temperature was measured using a RTD thermometer with a Pt100 element (precision ±0.1° C). Salinity was measured in analysed melted cut sections of the sample core using XS Instruments Cond 70 instrument. The measured temperature and salinity was used to estimate the brine volume of the ice according to equation 11.1;

$$V_{Brine} = S_{Ice}(0.0532 - {}^{4.919}/_{T_{Ice}})$$

(eq 11.1)

Snow samples were collected from clean areas using an acid-cleaned plastic shovel. The samples were put into blank tested LD-PE bags. The samples were let to thaw slowly in the dark in room temperature and the melted samples were analyzed as the described in Fig. 11.5.

Under ice water (UIW) was sampled in the hole of the sampled ice core by inserting a stainless steel bar with an attached glass bottle. When the bottle was filled to the rim it was quickly brought back up. The UIW samples were analysed using the purge and trap method (Fig. 11.5).

Sea ice brine was sampled by drilling partly with the ice corer at varying depths. The brine was sampled directly into glass bottles. The liquid sea ice brine was analysed as the melted ice and snow samples.

Ice, brine, under ice water, water from melt ponds and frost flowers for determination of mono- and dimethylmercury were samples in a similar way as descried above except from that Teflon containers were used when sampling under ice water, brine and water from melt ponds. The same matrixes were also sampled for analysis of total mercury and sampled directly into precleaned glass flasks or acid cleaned gastight plastic bags. Water was also sampled in cubitainers that was used to conduce methylation and demethylation assays and to collect bacterial samples. Incubation experiments and analysis of the samples were done as described above for samples seawater. Towards the end of the cruise, ice browed with ice algae was collected and used for methylation and demethylation assays and to collect bacterial samples (example Figure 11.5).

Figure 11.5 Ice sample collected during the end of the expedition where ice algae were visible. Photo: Lars Lehnert.

Microplastics in sea-ice and under ice water

Sea-ice cores were collected from 25 stations in the Arctic Ocean. Cores were melted, and the melt water was then subject to vacuum filtration. Water from beneath the ice at each station was also pumped and filtered in the field. Filter papers for each sample were shipped to the laboratory for visual identification of potential microplastics followed by FT-IR spectroscopy analyses for identification of polymer type.

Calculations of elemental mercury flux

The transfer of a gas at the air-water interphase is limited by diffusion which is driven by the solubility of the gas and the concentration gradient according to Henry´s law (eq 11.2).

$$H' = \frac{C_a}{C_w} \qquad \text{(eq 11.2)}$$

The kinetics of the gas diffusion is controlled by the gas transfer velocity which is representing the physical turbulence and the diffusivity of the gas. The mercury flux in this study was estimated using the measured GEM and surface DGM concentrations in eq 11.3 (Johnson, 2010);

$$Hg_{flux} = -K_w\left(\frac{GEM}{H'} - DGM\right) \qquad \text{(eq 11.3)}$$

where K_w is the total gas transfer velocity constants expressed on the water side of the interphase [m h^{-1}], GEM is the measured concentration of Hg(0) in air [ng m^{-3}], H′ is the Henry's law constant (eq. 11.2) and DGM is the measured concentration of Hg(0) in seawater [pg L^{-1}]. The calculations are further explained in Nerentorp Mastromonaco (2016).

11.4 Results

Continuous measurements of mercury species in air

The average concentrations for the period 9/8 to 18/9 of measured GEM, HgP and GOM were 1.4 ± 0.2 ng m^{-3}, 2.4 ± 2.0 pg m^{-3}, and 1.6 ± 2.4 pg m^{-3}, respectively. The continuous measurements of the measured mercury species in air are presented in Fig. 11.6. These values are in similar range as what has previously been measured during an oversea campaign in the Arctic in 2004 and estimated by GRAHM modeling for the Arctic Ocean (Aspmo et al., 2006; Dastoor et al., 2015).

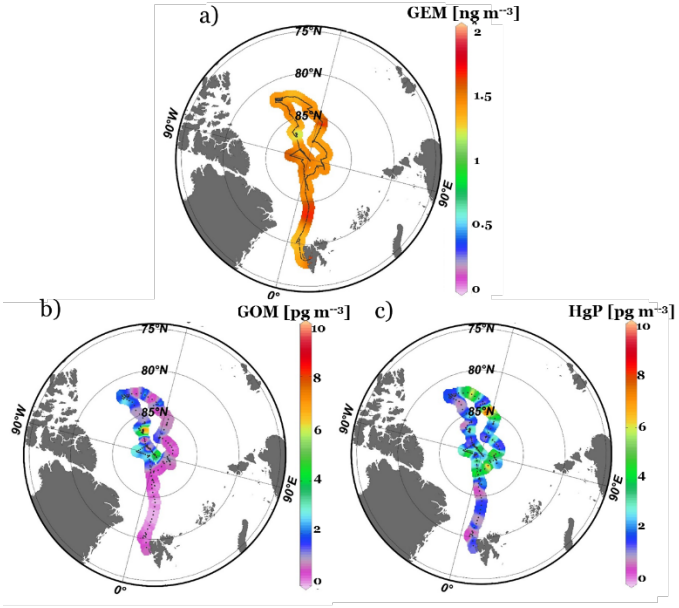

Figure 11.6 Results from the continuous measurements of a) GEM, b) GOM and c) HgP in air using the Tekran 1130/35 system during the AO16 expedition in the Arctic. (Data from 9/8 to 18/9 2016; Nerentorp Mastromonaco, 2016).

Continuous measurements of dissolved gaseous mercury in seawater

The average DGM concentration in surface seawater measured between 8/8 and 28/8 2016 was 40 ± 19 pg L^{-1}. This average is in good agreement with previous DGM measurements performed in the Arctic in 2005 (44 ± 22 pg L^{-1}), using a similar experimental setup (Andersson et al., 2008b). The continuous measurements of DGM in surface water are presented in Fig. 11.7, showing higher concentrations when passing through sea ice (48 ± 15 pg L^{-1}) compared to when operating in open water (19 ± 4 pg L^{-1}). This is due to a capsuling effect of sea ice which hinders evasion of gaseous mercury from the sea surface. This phenomenon was also observed by Andersson et al. (2008b).

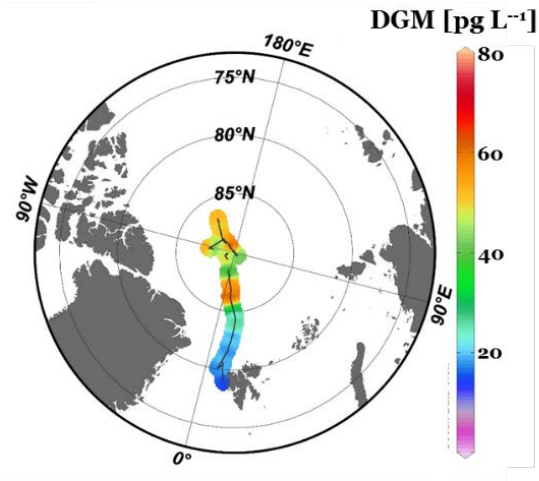

Figure 11.7 Results from the continuous measurements DGM in surface seawater (Data from 8/8 to 28/8 2016; Nerentorp Mastromonaco, 2016).

Calculations of mercury flux rates

Continuous DGM and TGM measurements was used to estimate the net evasion and deposition of gaseous mercury in the arctic marine environment. The average Hg flux calculated for the AO16 campaign was 1.52 ± 2.27 ng m^{-2} h^{-1}, indicating a net evasion of Hg(0) from the surfaces of the Arctic Ocean. Previous calculations of the flux rate in the Arctic Ocean in the literature have shown diverse results ranging from 0.42 ± 0.36 ng m^{-2} h^{-1} to 5.42 ± 5.75 ng m^{-2} h^{-1} (Andersson et al., 2011; Kirk et al., 2008). The calculated flux rates from 8/8 to 28/8 2016 are presented in Fig. 11.8.

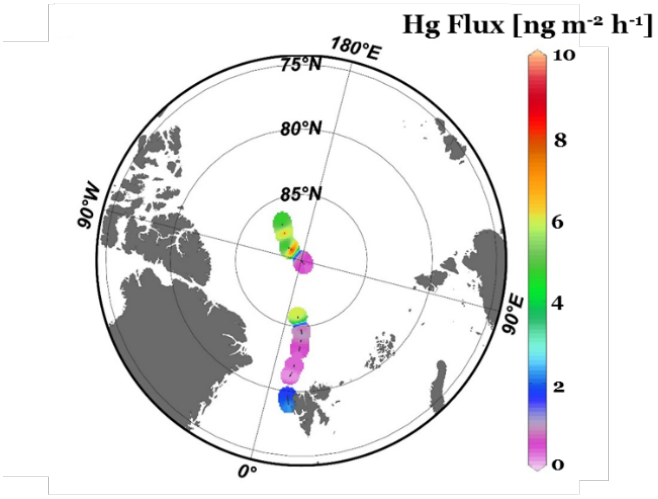

Figure 11.8 Results of the calculated Hg flux rates during AO16 (Data from 8/8 to 28/8 2016; Nerentorp Mastromonaco, 2016).

Mercury in sea-ice, under ice water, snow and frost flowers

Measured Hg(0) in sea ice, snow, under ice water, frost flowers, brine and new ice will be presented in future publications. Examples of results obtained at the AO16 expedition from ice station 160911-1 are presented in Table 11.1.

The highest Hg(0) concentrations were found in sea ice brine. When new sea ice is formed dissolved species within the brine are being rejected during the freezing process forming a crystal matrix, leading to an enrichment in brine pockets. According to Chaulk et al. (2011), mercury is primarily resided within the brine channels in sea ice which could explain the higher Hg(0) concentrations found in brine. Gases within sea ice is according to Crabeck et al. (2014) also likely transported in air bubbles within sea ice cavities (volume fraction in ice around 0.6-2%).

Table 11.1 Measured average Hg(0) concentrations (±StDev) and salinities in the Arctic sea ice environment in samples collected at ice station 160911-1 during the AO16 campaign.

	Hg(0) [pg L^{-1}]	Salinity [ppt]
Brine	358 ± 41	1.75
Frost flowers	86 ± 39	4.40
Under ice water	60 ± 0.2	6.55
Sea ice	24 ± 9	0.56
Snow	9 ± 5	0.04
New ice	38 ± 27	1.9

Mercury, temperature, salinity and brine distribution in sea ice

Hg(0) measured in cut sections of sea ice cores, snow samples (sampled at different sections of the snow profile) and under ice water were used to study the distribution of mercury in the Arctic sea ice environment. Results from ice station 160905-1 are presented in Fig. 11.8a. The profile show enhanced Hg(0) concentrations in the bottom of the ice, in good correlation to the Hg(0) concentration measured in under ice water. This signifies a source of mercury from the underlying seawater, as also explained by Chaulk et al. (2011) and Nerentorp Mastromonaco et al. (2016a).

Measured salinities in the analysed melted cut sections of the ice are presented in Fig 11.8b, showing higher salinity in the top and in the bottom of the ice. The temperature was measured in a reference ice core at the ice station directly after coring and the results

are presented in Fig. 11.9b. The measured salinities and temperatures were used to calculate the brine volume using eq. 11.1. The calculated brine volume is presented in Fig. 11.8, showing similar profile as the Hg(0) profile (Fig. 11.9a). This indicate that a major part of Hg(0) in the ice probably was dissolved within brine pockets in the ice (Chaulk et al., 2011). Results from the remaining ice stations will be presented in future publications.

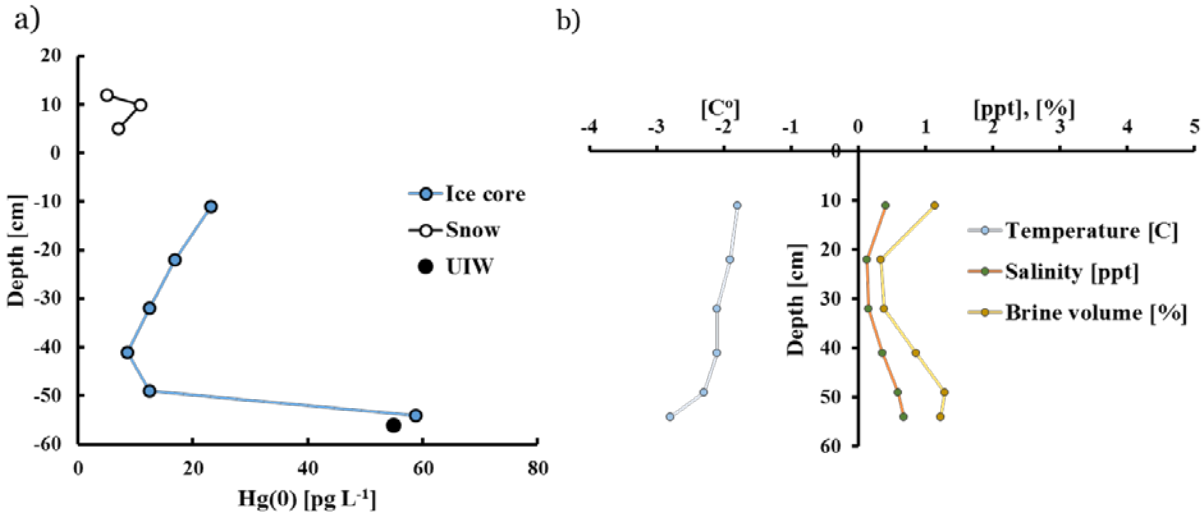

Figure 11.9. a) The distribution of elemental mercury (Hg(0)) in ice, snow and under ice water (UIW) measured at ice station 160905-1, b) measured temperature and salinity and calculated brine volume in the ice core presented in a).

Concentration of total mercury and methylated mercury species from samples collected on ice stations

The concentration of monomethylmercury and total mercury is ice, brine, snow, water from melt ponds and frost flowers are still evaluated. No dimethylmercury was detected in these matrices with the exception from one brine sample where a concentration of 4.3 fM of dimethylmercury was detected. This suggests that the ice sheet is not a source of dimethylmercury to the atmosphere or the surface waters.

Methylation and demethylation assays and bacterial samples

Methylation and demethylation assays are currently being processed at the Department of Marine Sciences (University of Connecticut). Bacteral samples remain to be processed.

Microplastics

Visual identification of potential microplastics will commence during the first quarter of 2017. FT-IR analyses will follow. A picture that was taken from a sample where water was pumped from beneath the ice is presented in Fig. 11.10. On this picture, one can see potential microplastics (i.e. blue fragments, blue fibres). However, this is simply based on visual identification. FT-IR analyses are needed to confirm that these particles are actually synthetic polymers.

At this point, we have no preliminary conclusions as we have to check each sample for the presence of microplastics. This will be done after the expedition and is currently ongoing.

Figure 11.10 Pictures of potential microplastics found in under ice water pumped with the ship's bow water system.

11.5 Discussion and future analyses

Generally lower concentrations of elemental mercury were found in the Arctic sea ice environment than in Antarctica which could be due to geographical differences (Nerentorp Mastromonaco et al., 2016a; Nerentorp Mastromonaco, 2016). However, the data need further processing to support any conclusions. Sea ice is important for the cycling of mercury in Polar Regions since it contains significant amounts of mercury and partly hinders the re-evasion of gaseous mercury from sea surfaces (Andersson et al., 2008b). It also acts as a cap against direct atmospheric deposition (Nerentorp Mastromonaco, 2016). Melting sea ice due to climate change could affect the mercury cycle due to the release of stored mercury within sea ice to the ocean and increased re-evasion from sea surfaces to the atmosphere. Further processing of collected data and future research could help us predict how the cycling of mercury could be affected by climate change and how in turn this could affect the bioaccumulation of mercury in Arctic and Antarctic food chains.

The results from the AO16 expedition will be presented in future publications. A future goal may be to assess whether microplastics which are entrained in sea-ice have pollutants (inorganic e.g. metals and organic e.g. priority pollutants) adsorbed unto them.

11.6 References

Amelineau, F., Bonnet, D., Heitz, O., Mortreux, V., Harding, A.M.A., Karnovsky, N., Walkusz, W., Fort, J., Gremillet, D., 2016. Microplastic pollution in the Greenland Sea: Background levels and selective contamination of planktivorous diving seabirds. Environmental Pollution 219, 1131-1139.

Andersson, M.E., Gårdfedlt, K., Wängberg, I., Sprovieri, F., Pirrone, N., Lindquist, O., 2007. Seasinal and daily variation of mercury evasion at coastal and off shore sites from the Mediterranean Sea. Marine Chemistry. 104, 214-226.

Andersson, M. E., Gårdfeldt, K., Wängberg, I., 2008a. A description of an automatic continous equilibrium system for the measurement of dissolved gaseous mercury. Anal. Bioanal. Chem. 391, 2277-2282.

Andersson, M. E., J. Sommar, K. Gårdfeldt, and O. Lindqvist., 2008b, Enhanced concentrations of dissolved gaseous mercury in the surface waters of the Arctic Ocean, *Marine Chemistry*, *110*, 190–194, doi:10.1016/j.marchem.2008.04.002.

Andersson , M. E., Sommar, J., Gårdfeldt, K., Jutterström, S., 2011. Air-sea exchange of volatile mercury in the North Atlantic Ocean. Marine Chemistry, 125, 1-7.

Arthur, C., Baker, J., Bamford, H., 2009. Proceedings of the International Research Workshop on the Occurrence, Effects and Fate of Microplastic Marine Debris. NOAA, University of Washington Tacoma, WA, USA.

Aspmo, K. *et al.*, 2006. Mercury in the atmosphere, snow and melt water ponds in the North Atlantic Ocean during Arctic summer. Environ. Sci. Technol. 40, 4083–9.

Chaulk, A., Stern, G. a, Armstrong, D., Barber, D. G. & Wang, F., 2011. Mercury distribution and transport across the ocean-sea-ice-atmosphere interface in the Arctic Ocean. Environ. Sci. Technol. 45, 1866–72.

Crabeck, O. *et al.*, 2014. First 'in situ' determination of gas transport coefficients (DO2, DAr, and DN2) from bulk gas concentration measurements (O 2 , N 2 , Ar) in natural sea ice. J. Geophys. Res. Ocean. 119, 6655–6668.

Dastoor, A. *et al., 2015.* Atmospheric mercury in the Canadian Arctic. Part II: Insight from modeling. Sci. Total Environ. 509–510, 16–27.

Heimbürger, L., Sonke, J. E., Cossa, D., Point, D., Lagane, C., Laffont, L., Galfond, B. T., Nicolaus, M.,

Rabe, B., van der Loeff, M. R. Shallow methylmercury production in the marginal sea ice zone of the central Arctic Ocean. Sci. Rep. 2015 (5:10318 |), DOI: 10.1038/srep10318.

Johnson, M. T., 2010. A numerical scheme to calculate temperature and salinity dependent air-water transfer velocities for any gas. Ocean Sci. 6, 913–932.

Kirk, J. L., St. Louis., V. L., Hintelmann, H., Lehnherr, I., Else, B., Poissant., L., 2008. Methylated mercury species in marine waters of the Canadian high and sub-Arctic. Environ. Sci. Technol 42, 8367–8373.

Lusher, A., 2015. Microplastics in the Marine Environment: Distribution, Interactions and Effects, in: Bergmann, M., Gutow, L., Klages, M. (Eds.), Marine Anthropogenic Litter. Springer International Publishing, pp. 245-307.

Lusher, A.L., Hernandez-Milian, G., O'Brien, J., Berrow, S., O'Connor, I., Officer, R., 2015. Microplastic and macroplastic ingestion by a deep diving, oceanic cetacean: The True's beaked whale Mesoplodon mirus. Environmental Pollution 199, 185-191.

Nerentorp Mastromonaco, M. G., Gårdfeldt, K., Langer, S. & Dommergue, A., 2016a. Seasonal Study of Mercury Species in the Antarctic Sea-ice Environment. Environ. Sci. Technol. 50, 12705–12712.

Nerentorp Mastromonaco, M. G., Gårdfeldt, K., Langer, S., 2016b.Mercury flux over West Antarctic Seas during winter, spring and summer. Mar. Chem. http://dx.doi.org/10.1016/j.marchem.2016.08.005

Nerentorp Mastromonaco, M. G., 2016c. Mercury cycling in the global marine environment. *Ph.D Thesis.* ISBN: 978-91-7597-478-1.

Obbard, R.W., Sadri, S., Wong, Y.Q., Khitun, A.A., Baker, I., Thompson, R.C.C.E.F., 2014. Global warming releases microplastic legacy frozen in Arctic Sea ice. Earth's Future 2, 315-320.

Orderdalen Steen, A., 2011. Environmental cycling of atmospheric mercury in the Arctic. *Ph.D Thesis*. ISBN: 978-82-471-3111-4.

Pirrone, N., Cinnirella, S., Feng, X., Finkelman, R. B., Friedli, H. R., Leaner, J., Mason, R., Mukherjee, A. B., Stracher, G., Streets, D. G., and Telmer, K., 2010. Global Mercury Emissions to the Atmosphere from Natural and Anthropogenic Sources, Atmospheric Chemistry and Physics, 10, 5951- 5964.

Soerensen, A. L., Jacob, D. J., Schartup, A. T., Fisher, J. a., Lehnherr, I., St. Louis, V. L., Heimbürger, L.-E., Sonke, J. E., Krabbenhoft, D. P., Sunderland, E. M. A mass budget for mercury and methylmercury in the Arctic Ocean. Global Biogeochem. Cycles 2016, 30, 560–575.

(UNEP), U.N.E.P., 2011. UNEP Year Book: Emerging Issues in our Global Environment. United Nations Environment Programme (UNEP), Nairobi, Kenya.

12 Work Package: Ice Thickness (IT)

Sea Ice thickness measurements using a high frequency radar

The aim is to design a set up with antennae and hard ware installations to allow continuous measurements of sea ice thickness to be observed in real time from an ice breaker. A pilot study was performed during the OATRC 2015 expedition in the Arctic and in October 2016 a follow up study was carried out. Both studies were performed onboard MS Oden.

The basic set up is to mount antennae on a steel frame at the front of the ship and to develop the software making it possible to steer the equipment from the ship bridge. The results from 2015 gave insight into frequency range needed and in 2016 a new pair of antennae was tested. The software development faced severe problems that could not be solved before the expedition launch. So the only improvement that could be made was the antennae test.

The equipment is based on a Hewlett Packard Net Work Analyzer (8753ET). It makes 201 surveys distributed within the determined frequency range at a certain time for each sample. Normally we sample between every half second to every five seconds dependent on the variability in sea ice thickness. The system is controlled by a laptop computer. The cable length plus internal cable in antenna was 2x3.5 m and the height of the antenna over the sea ice was 8 m. The separation of the antennae was 1 m and they were mounted approximately 1.3 m off the ship in its front. The hardware including a computer is placed in an aluminum box on outer deck close to the antennae. The future plan is to keep the Net Work Analyzer in a box but remove the computer indoors.

During the 2016 Oden mission test surveys were carried out between August 20 and August 28. A new set of antennae was tested in the frequency range 200-800 MHz. The antennae and their range was found suitable for the mission. However, the combination of technical problems, shortage of time and poor internet connection did not allow enough sampling for a thorough post data processing of ice thickness, though the frequency range seems promising. The software used is DOS-based making use of Asyst graphics. The program does not allow real time viewing and we are working on a new software suitable for this project.

The present day survey equipment used by staff on ice breakers is very simple and in many sentences poor. It is measuring sticks pointing out of deck allowing estimation of ice thickness of flows rolling aside of the ship. A sufficiently accurate real time survey would give better and quicker signals to the bridge of how to plan the ice breaking and it would also give indications of trend s in ice thickness. A well working equipment would be a very useful tool for the crew of the ships.

The future plan is to make a new test with new software and suitable antennae to make a final statement if this is a future solution on an evident problem in ice

breaking business. The hardware is certainly capable to do the job but there are so many practicalities that may obstacle a good result that a third test run is necessary. An example of a limiting factor is the fact that high frequency radio waves have problems to penetrate liquid water and Oden is flushing water to be able to break the ice. This can probably be overcome by tilting the antennae, but it needs to be tested. And finally the new software needs to be operational.

13 Work Package: SPRS Artist Programme: Polar on Stage/The Big White and Art & Science (PoSta)

Åsa Johannisson

Circus Glass Royale & Department of Circus, Stockholm University of the Arts, Sweden

Other project members: Share Music Sweden

Project partners: Grenna Museum, Svalbard Museum, Iceland Academy of Arts and the University of Gothenburg.

13.1 Summary

Polar on Stage (working title) is an international project with the ambition to bring together cultural heritage, environmental work, research, and education with artistic expressions and performing arts. The project is planned to result in a performance with music, theatre/circus and visual elements – a production for international touring (planned premiere in 2018), an exhibition and additional learning program. The exhibition and the learning program are developed by Grenna Museum and are not the main objective of the WP *Polar on stage* on Oden during the expedition. The expedition Arctic Ocean 2016 and its outcomes will form the content of the performance. Project partners are Grenna Museum, Svalbard Museum, Iceland Academy of Arts and the University of Gothenburg.

Parallel to the development of the performance *Polar on stage* the expedition also offers the possibility to study the interaction in between art and science. The overall aim is to develop methods for interdisciplinary research and collaboration in between art and science raising questions such as: In what ways can art and artistic expression contribute to communicate and express research findings to the public/audience?

12.2Background

Polar on stage (working title)

The initial aim and starting point of the project *Polar on stage* was to actualize issues that origin in Andrée's polar expedition in 1897. Which findings of the expedition are relevant in a contemporary context? The environmental aspects? Today's travel? Current research?

Scientific samples from Andrée's expedition and contemporary research on algae, which can clean the air from carbon dioxide, highlight the need to move towards sustainable development in the Polar Regions. The local perspective is enhanced by the geographical location of Grenna Museum Polar Center in the East Vättern Landscape Biosphere Reserve, recognized by UNESCO. Selecting algae as a starting point with its significance for humankind's survival in the future, the project wants to highlight a glocal – global and local – character of our initiative. Project partners are Grenna Museum, Svalbard Museum, Iceland Academy of Arts and the University of Gothenburg.

Polar on Stage is planned to result in a performance with music, theatre/circus and visual elements – a production for international touring (premiere in 2018), an exhibition and additional learning program. The exhibition and the learning program are developed by Grenna Museum and are not the main objective of the WP *Polar on stage* on Oden.

During the expedition the artistic aim has taken a slightly different course. It has shifted from using Andrée´s expedition as a starting point to focus more on the expedition itself as a frame for the overarching storyline, possibly using André as a historical reference. An archetype of previous researchers and explorers encountering the unknown not knowing what to expect.

Art & Science - Knowledge production and practice based artistic research

Parallel to the development of the performance *Polar on stage* the expedition also offers the possibility to study the interaction in between art and science. The overall aim is to develop methods for interdisciplinary collaboration in between art and science. Questions raised are:

- In what ways can scientific research be transferred, communicated and expressed in performing arts and moving image?
- In what ways can the craft of science, the practice of science, be transferred into a performative context?
- What materials are retrieved and what tools are used in the craft of science and how do these materials and tools correspond to performative and mediated practices?
- What dramaturgical methods and structures are able to emerge from the encounter in between art and science?
- In what ways can art and artistic expression contribute to communicate and express research findings to the public/audience?

12.3 Methods

Story, content and expression

- Observation of activities (craft of science) relating to ongoing research. For example coring.
- Participating in activities (craft of science) relating to ongoing research. For example handling of sediments.

- Interviews/asking questions related to the practical work and to scientific content of the various WPs
- Documentation: sound, photo, moving image, drawing
- Writing a journal giving an account of every day
- Storyboard: creation of various storyboards
- Practical experiments relating to light
- Reflection, reading and writing

Art & Science, Interdisciplinary working methods and knowledge exchange

- Participating in and comparing practices. Example: Rigging of the ship and research equipment in relation to circus rigging.
- Studying the organisation of the ship Oden
- Studying the organisation and process of the expedition
- Lecturing/presenting on the practice of performing arts and fiction film from the perspective of the director and scriptwriter.
- Taking part of WP presentations
- Workshop: Circus acrobatics and juggling. Twice a week during the expedition
- Development of methods. Workshop: Storytelling art and science. 1- 4 times during expedition (not yet executed)

Research activities and preliminary results

As a director and scriptwriter my ambition is to tell the story about the expedition Arctic Ocean 2016. As I was entering the project, the expedition, and a context, travelling on a ship to the Arctic, of which I did not have any previous experience I spent the first 3 weeks absorbing as much information as possible. On Monday 29 August, in the middle of the journey I started to structure the perceived information in various ways and began to make a storyboard. The storyboard was constructed by looking at the expedition from various perspectives.

Perspective and storytelling

The concept of the planned outcome is a live performance with projections, a combination of performing arts and moving image. The moving images consist of graphic material from the expedition. The soundscape is constructed with sound material from the expedition in combination with music.

The overarching storyline stretches from the magma at the centre of the earth (animation) to outer space (satellite images). In between the following perspectives are also present:

- The air, represented by the helicopter and the weather balloons
- The two ships, Oden and Louis
- The surface of the sea and the ice
- The sea – beneath the surface
- The seafloor, its surface and depth all the way down to the magma.

The perspectives listed above also correspond to the research conducted during the expedition. The different work packages/projects can be presented as scenes.

In performing arts and moving image the concept of perspective is also used in a concrete and spatial way referring to the experience of the audience. The audience perspective is what the audience sees or hears in the space where the performance is presented or on the film that is screened. An example is film where the action/scene is filmed through different point of views/perspectives. In other words filmed from various angles and distances. You can also work with a moving camera that is approaching or moving away from the action. As a director and storyteller I try to look at the expedition from as many spatial perspectives as possible.

To be able to tell this story, as research I chose to join the expedition. As well as theoretical aspects and scientific research outcomes, I hoped to also get a practical and spatial experience of what the expedition is about. This experience I obtained through participating in activities, through observation of practice and through dialogue with the other participants in the expedition and the crew of Oden.

Planned activities not yet executed: Workshop Storytelling art and science

12.4 Discussion and future analyses

In what ways can art and artistic expression contribute to communicate and express research findings to the public/audience?

Performance production creation process and preliminary time plan:

- Collecting data from the expedition (2016- spring 2017)
- Scriptwriting (2016- 2017)
- Pre-production, creation and design (spring 2017- spring 2018)
- Rehearsals (summer 2018)
- Opening (late summer 2018)
- Tour (2018-2020)

<u>Performance production organizational process:</u>
Funding, Collaborations, Planning of tour

<u>Research Art and science</u>
Development of joint research project, interdisciplinary collaboration art and science. Questions relating to sustainability. One focus being the development of methods for collaboration. Application to the Swedish Research Council 2017.